Hydrological consequences of proposed interventions in the Tana basin, Kenya

A water balance study

An aerial view of a section of the Tana River delta.

Master's thesis
Kasper Lange
Water Science and Management
Utrecht University
July 2014

Hydrological consequences of proposed interventions in the Tana basin, Kenya
A water balance study

Master's thesis

Author:	Kasper Lange
Student number:	3368181
Study:	Water Science and Management
	Utrecht University
Phone:	+31 6 43 94 34 25
Email:	k.lange89@gmail.com / k.j.lange@students.uu.nl
University supervisors:	Prof. dr. ir. M.F.P. Bierkens / dr. L.P.H. van Beek
Internship organization:	Wetlands International
Internship supervisor:	Frank van Weert
Internship supervisor email:	frank.vanweert@wetlands.org
Internship supervisor phone:	+31 318 66 09 46

Abstract

The Tana River is the largest river in Kenya, with a large part flowing through a (semi-)arid region. The Tana delta is one of Africa's most important wetlands, generating a large variety of ecosystem services. However, the natural system is under pressure from anthropogenic developments. The aim of this study is to provide improved understanding of the hydrological consequences of anthropogenic interventions on the hydrological system in the Tana basin, with specific focus on water supply to the Tana delta. Following the research aim, this master's thesis provides a quantitative scenario-based analysis of the Kenyan Tana Basin water balance using the global hydrological model PCR-GLOBWB. The main research question that is addressed in this thesis is: *How will the river discharge of the Tana River in the Tana delta be affected by climate change and anthropogenic developments in the region?* The interventions are translated into four scenarios: (1) High Grand Falls Dam (HGFD), (2) HGFD plus planned large-scale irrigation schemes, (3) water demand from Nairobi and Lamu Port, and (4) a combination of all scenarios. The results of these interventions are compared to the status quo, i.e. the current land use, with only the climate as changing factor (which is also included in all scenarios). PCR-GLOBWB was not completely successful in predicting the discharge. In Garsen the validation results are: LNSE = -2.96, R^2 = 0.45, RMSE = 123.85 m^3/s. To remove the model bias a normalized correction method has been applied (after calibration). After this correction the validation results in Garsen are: LNSE = -0.10, R^2 = 0.41, RMSE = 34.14 m^3/s. The effects of the scenarios are assessed by determining the change in Q10 and Q90 for the full year and the rainy and dry seasons, respectively for the near, mid- and far future. In conclusion, climate change is expected to lead to an increase in discharge during the rainy season, while there is no strong effect expected in the dry season. With all interventions combined the all-year mean Q10 decreases by 2.60%, 15.16% and 15.65%, in the near, mid- and far future, respectively, while the all-year mean Q90 increases by 10.07% and 3.38% and decreases by 2.85%, respectively.

Index

List of abbreviations

CMIP5:	Coordinated Modeling Intercomparison Project Phase 5
CRU:	Climatic Research Unit
EnKF:	Ensemble Kalman Filter
EA:	Ecosystem Alliance
ESIA:	Environmental and Social Impact Assessment
FDC:	Flow-Duration Curve
GCM:	General Circulation Model or Global Climate Model
GLCC:	Global Land Cover Characteristics
GLWD:	Global Lakes and Wetlands Database 3
HDI:	Human Development Index
HGFD:	High Grand Falls Dam
HGFIP:	High Grand Falls Irrigation Project
IPCC:	Intergovernmental Panel on Climate Change
LAI:	Leaf Area Index
LNSE:	Logarithmic Nash-Sutcliffe Efficiency
LUP:	Land Use Plan
MCM:	Million Cubic Meters
NIB:	National Irrigation Board
LNSE:	Logarithmic Nash-Sutcliffe efficiency
PCR-GLOBWB:	PCRaster Global Water Balance
R^2:	Pearson's coefficient of determination
RCP:	Representative Concentration Pathways
RMSE:	Root Mean Square Error
SEA:	Strategic Environmental Assessment
TARDA:	Tana and Athi River Development Authority
TDIP:	Tana Delta Irrigation Project
TDISP:	Tana Delta Irrigated Sugar Project
TEEB:	The Economics of Ecosystems services and Biodiversity
UNEP:	United Nations Environmental Programme
WRMA:	Water Resources Management Authority

List of Figures

List of Tables

1. Introduction

The Tana River is the largest river in Kenya. Apart from supplying water to more than five million people (Knoop et al., 2012), it sustains one of Africa's most important wetlands: the Tana delta. The Tana delta is an important biodiversity hotspot and generates numerous ecosystem services on which people depend (Ramsar, 2012). The delta is dependent on water supply from the Tana River. However, due to various planned interventions in the Tana basin, the river discharge is expected to be affected, and hence the Tana delta. It is largely unknown what the effects will be on the water availability in the Tana delta. Therefore, this study is conducted to assess the impacts of these interventions on the water availability in the Tana delta.

In the remaining part of the introduction, an area description is given, followed by an overview of the issues in the region that are addressed in this study. Then the relevance of this study is explained, after which an overview of previously conducted studies in the Tana basin is given. Finally the aim and research questions of this study are presented.

1.1 Area description

The Tana River is the largest river in Kenya – roughly 1,000 km in length – with a catchment area of about 126,000 km^2. The river originates from Mount Kenya and the Aberdare Ranges and meanders to the Indian Ocean (Odengo et al., 2012a). The Tana basin can be divided into three sub-basins: upper, middle, and lower (figure 1).

The upper basin is situated at an elevation higher than 1,300 m above sea level and is partly mountainous and hilly. It is characterized by relatively high rainfall, i.e. a yearly average of 1,050 mm with extremes up to 2,600 mm. In the upper basin fast-flowing perennial rivers drain the eastern flanks of the mountains into the Tana River (Knoop et al., 2012; Dickens et al., 2012). The middle basin lies at an altitude between 1,300 m and 500 m above sea level and is characterized by a semi-arid to arid climate with rainfall ranging from 400 mm to 700 mm per year (Knoop et al., 2012). The lower Tana basin is below 500 m altitude and is water scarce. This is mainly due to low rainfall and high temperatures leading to evaporation rates over 2,000 mm per year, far exceeding rainfall in this semi-arid region (Knoop et al., 2012; Dickens et al., 2012). Here, the Tana River is the only perennial stream (IUCN, 2003). Only close to the Indian Ocean, there is relatively high rainfall in the lower basin. In figure 2, it can be observed that a significant part of the Tana flows through a (semi-)arid region. In the lower basin, the Tana River does not gain water from tributaries (except in the rainy season), but continuously loses water through evaporation (Andrews et al., 1975).

The yearly rainfall pattern is bimodal, i.e. there are two rainy seasons. The first rainy season is characterized by long rains from April to June and supplies about 45% of the annual precipitation that falls at Garsen. The second, short-rain, season, from November to December, supplies roughly 25% of annual rainfall (Maingi & Marsh, 2002; Hamerlynck et al., 2010; Leauthaud et al., 2013a). The other seven months have an average rainfall of less than 50 mm (Hamerlynck et al., 2010) providing the remaining 30%.
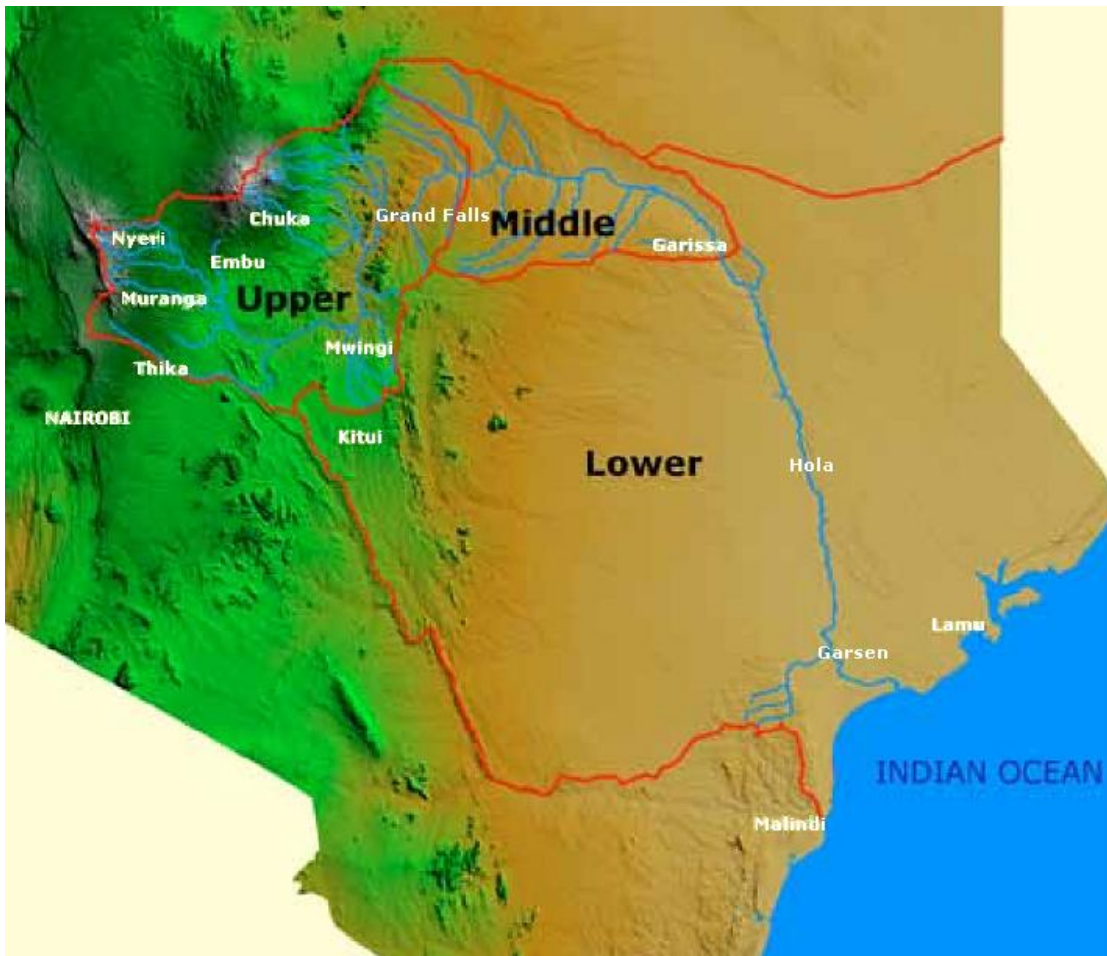
Figure 1: Locations of the upper, middle and lower basins within the Tana basin (after Knoop et al., 2012, p. 9).
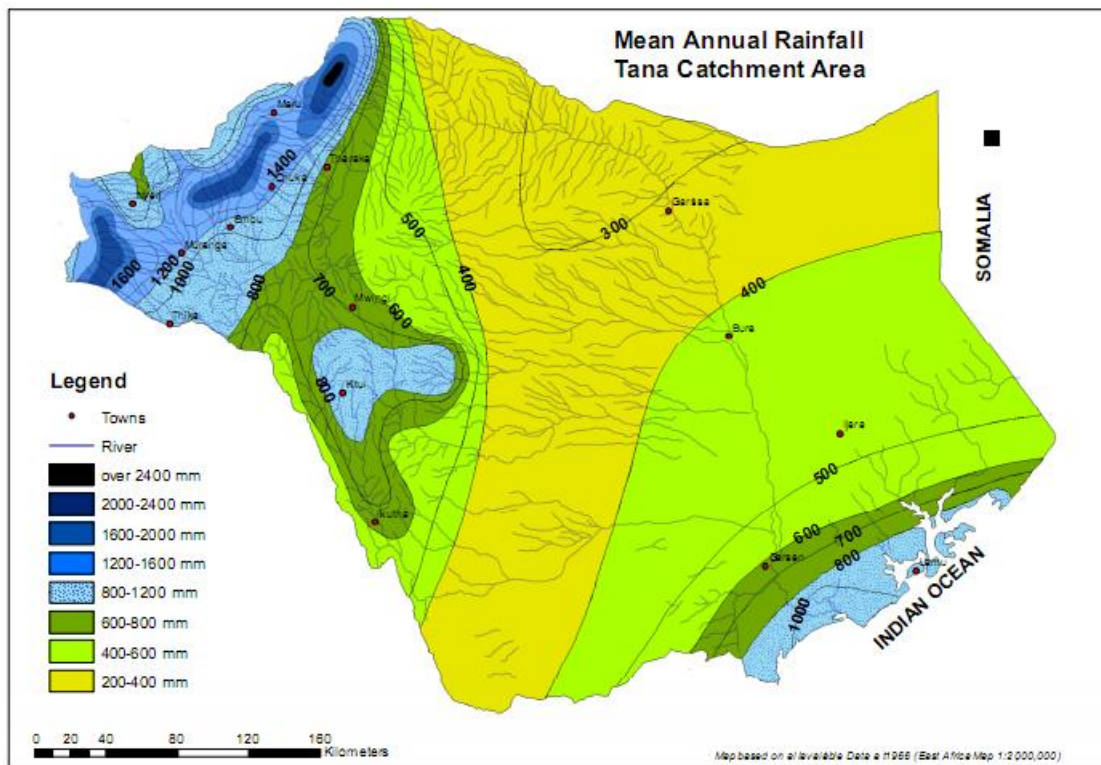
Figure 2: Mean annual rainfall in the Tana basin (Dickens et al., 2012, p. 25).

The focus of this study is mainly on the Tana delta, which is situated south of the town of Garsen (figure 3). The Tana delta – with an area of about 1,300 km^2 – is known for its wetlands and rich biodiversity (Maingi & Marsh, 2002; Samoilys et al., 2011; Duvail et al., 2012; Ramsar, 2012). It receives an annual rainfall of roughly 1,000 mm near the mouth, to about 520 mm at Garsen (Dickens et al., 2012).

The Tana delta is home to more than 650 plant species, with numerous endemic plants. Also, two endemic primate species are found just upstream of the delta (see figure 3). The floodplains function as bird sanctuaries for migratory waterbirds, including red-listed species. Finally, the Tana delta is also home to a number of endemic fish species (Mireri et al., 2008; Duvail et al., 2012). It has been declared a Ramsar site in October 2012 (Ramsar, 2012). The extent of the designated area is given in figure 3.

The delta provides in the livelihoods of a large number (approximately 100,000) of fishermen, farmers and pastoralists. In 2009, the Human Development Index (HDI) of the Tana delta was 0.389, compared to a national HDI of 0.561 (Leauthaud et al., 2013a). This lows HDI suggests that the people in the region strongly depend on the ecosystem services. The ecosystem services that are provided by the delta are manifold (Snoussi et al., 2007; Dickens et al., 2012; Duvail et al., 2012; Knoop et al., 2012; Odhengo et al., 2012a; Leauthaud et al., 2013a). A few important ecosystem services that are generated by the Tana delta are provisioning services, e.g. provision of food (fishing nurseries, wild animals and plant food product), provision of other materials (e.g. timber and roof thatch), deposition of fertile sediments; regulating services, e.g. water supply, waste treatment, peak attenuation; as well as cultural services such as the tourist potential of healthy ecosystems (Duvail et al., 2012). See appendix 1 for a more complete overview of ecosystem services that are provided by the Tana delta (Hamerlynk et al., 2010). The numerous ecosystem services are strongly dependent on regular flooding (Dickens et al., 2012). These floods bring in fresh water for irrigation and extra nutrients (IUCN, 2003), provide groundwater recharge (Hoff et al., 2007), and counter salinization (Royal Haskoning, 1982; Dickens et al., 2012).
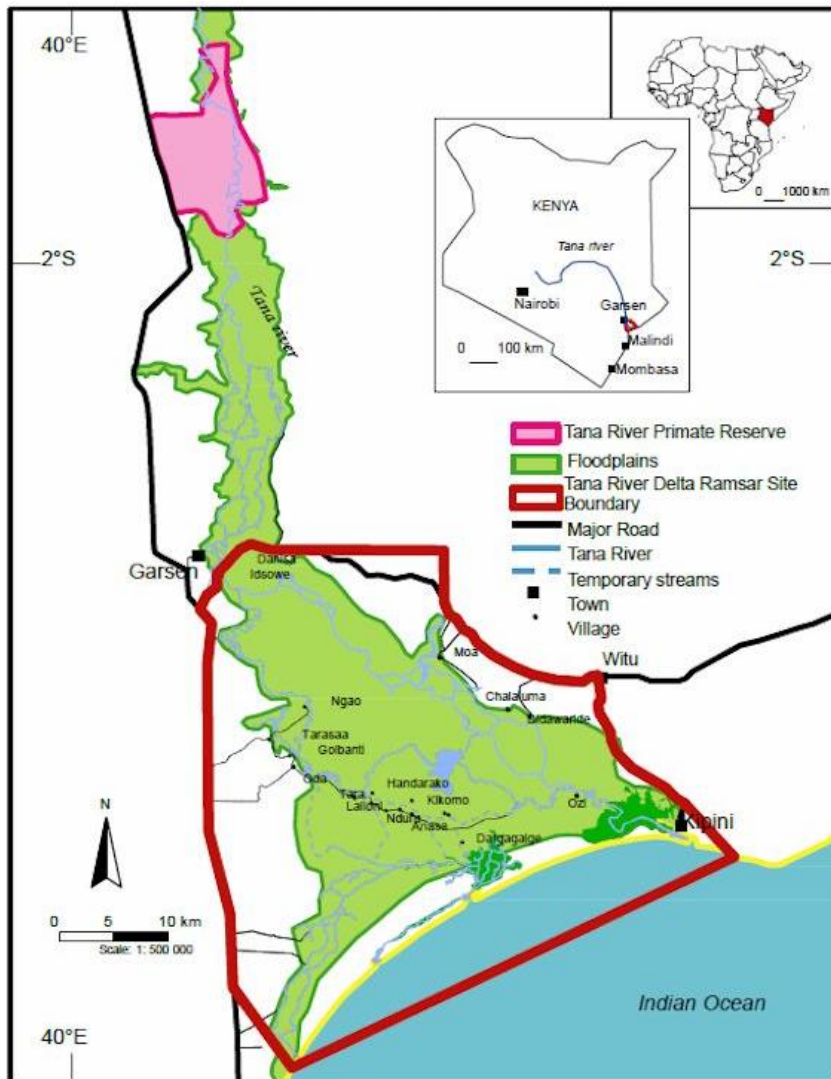
Figure 3: Map of Tana River Delta Ramsar Site (Ramsar, 2012).

1.2 Problem description

In parts of the Tana basin developments are planned, focused on increasing food, energy and water productivity and economic growth. Planned land use, water use, and infrastructural interventions are assumed to provide several benefits, of which the most important are generation of electricity and stable provision of water in (semi-)arid regions (reservoirs) (Nippon Koei, 2013a). However, the interventions also contain the risk of adversely affecting the ecosystems, and in turn people's livelihoods (Hamerlynck et al., 2010). Often, the benefits and disadvantages are not equally distributed in space and time. A classification of the Tana basin in terms of water quantity and quality categorized approximately 43% of its tributaries as alarming, whereas less than 10% was considered to be in a satisfactory condition (Dickens et al., 2012). The potential adverse effects of the planned interventions may therefore result in a degradation of the ecosystem services to a point where it can have direct and indirect adverse effects on people living in the delta (Temper, 2010; Martin, 2012; Duvail et al., 2012). The interventions with the presumed biggest impact are included in this study: (i) damming of the Tana River for energy production and water supply; (ii) construction of irrigation schemes, and; (iii) development of the Lamu Port and provision of water to meet the demand resulting from the urban expansion of Nairobi. These interventions are discussed below in the same order.

1.2.1 Dams

In total five hydropower dams (Masinga, Kamburu, Kindaruma, Gitaru and Kiambere) have been constructed in the Tana River (upper basin), providing almost three quarters of the national energy demand. Additionally, two dams have been constructed in the Chania (Sasumua) and Thika (Thika) rivers, which supply water to Nairobi (Nippon Koei, 2013a). Flooding volume and frequency have greatly decreased since the last dam was constructed in 1989 (Dickens et al., 2012). The five dams have resulted in less variability in discharge, with a 20% decrease in peak flows in May and a roughly 70% increase in low flows in February and March (Maingi & Marsh, 2002).

Additionally, the construction of a new multi-purpose dam is proposed: High Grand Falls Dam (HGFD). The HGFD is a flagship project for the Kenyan government within the National Water Master Plan 2030 (Nippon Koei, 2013a-2013e). The HGFD will be used for – in order of priority – flood management, power generation and supply of irrigation, drinking and industrial water (Republic of Kenya, 2011a). Its hydropower generation capacity will exceed that of the five existing dams combined (Nippon Koei, 2012; Government of Kenya, 2013). A feasibility study has been conducted on the HGFD, which forms the most comprehensive document with respect to the HGFD project (Republic of Kenya, 2011a). However, the downstream impacts of the HGFD on livelihoods and ecosystems (in combination with the other dams) remain uncertain (IUCN, 2003; Dickens et al., 2012; Leauthaud et al., 2013a).

Besides the HGFD, an alternative scheme of the Mutonga and Low Grand Falls dams is under discussion. This scheme consists of two smaller dams which will be used for hydropower. However, the High Grand Falls reservoir will be large enough to cover both the Mutonga and Low Grand Falls dams (Nippon Koei, 2012). In a study by IUCN (2003) it is stated that after finalization of the Mutonga-Low Grand Falls dams, only extreme events occurring every 5 and 10 years are expected to add to the Tana River's flow. This may result in cessation of regular biannual floods, which will have severe environmental and societal consequences (IUCN, 2003). In this study, it is assumed that only the HGFD will be constructed, because the Mutonga and Low Grand Falls plans will most likely be replaced by the HGFD project (Nippon Koei, 2013a) and because the government of Kenya has designated the HGFD to be a flagship project (Government of Kenya, 2013; Nippon Koei, 2013a). Details about the HGFD are presented in chapter 3.2.

1.2.2 Irrigation

Within the Kenya Vision 2030 agriculture has been identified as one of the key sectors to help reach the envisaged annual economic growth rate of 10%. In order to increase the agricultural productivity, irrigation has to be further developed (Government of Kenya, 2007). Irrigation is by far the biggest consumer of water in Kenya. It is expected to contribute to roughly 91% of the total water demand in 2030, of which 94% will be extracted from surface water (Nippon Koei, 2012). With irrigation being the largest water consumer, its effect on the water balance is expected to be significant. Along the entire Tana River there are plans for new irrigation schemes. There is a multitude of plans but only the large-scale irrigation schemes are included in this study. Details about the included irrigation schemes are given in chapter 3.3.

1.2.3 Development of the Lamu Port and expansion of Nairobi

Like the HGFD, construction of the Lamu Port (and corresponding expansion of urban area of Lamu Metropolis (JPC & BAC/GKA JV, 2011) (the Lamu Port plus Metropolis are hereafter referred to as

Lamu Port)) is a flagship project for the Kenyan government, aimed at economic growth and development (Ministry of Transport, 2013). The Lamu Port is linked to the large-scale LAPSSET Corridor (Lamu-Southern Sudan-Ethiopia Transport) project (see appendix 2). The aim of the LAPSSET Corridor[1] is to improve economic development through transnational trade (JPC & BAC/GKA JV, 2011). Part of this project is to build the infrastructure to transport oil from South Sudan to the Lamu Port, where it will be processed and shipped. The transport capacity of the oil pipeline is roughly 500,000 barrels per day, of which 417,600 barrels per day will be exported from the Lamu Port. The LAPSSET Corridor is expected to generate jobs and wealth, mainly in the northern regions of Kenya (JPC & BAC/GKA JV, 2011).

The Lamu Port is expected to require a daily supply of up to almost 300,000 m^3 water in 2050 for industrial and domestic purposes. This water will most likely be supplied by diverting water from the Nanigi barrage (which is part of the HGFD project) after which the water will be transported to the Lamu Port (JPC & BAC/GKA JV, 2011; Republic of Kenya, 2011a). The effect of this water demand on the river discharge is assessed in this study by subtracting the water demand from the channel storage at Nanigi (see chapter 3.4.1).

Besides high water demand, the development of the Lamu Port (figure 4) may have other environmental consequences (Samoilys et al., 2011; Ministry of Transport, 2013), of which most will affect the Tana delta and coast. Adverse effects on water quality are expected, e.g. turbidity due to dredging, emission of pollutants, and possibilities for oil spills. Secondly, the port will need a lot of physical space for which large sections of mangrove forests, and other ecological hotspots in the estuary, may need to be removed. Several mitigation measures are planned to try to limit the adverse effects. A list of expected impacts and suggested mitigation measures can be found in the Environmental and Social Impact Assessment (ESIA) study for part of the Lamu Port development by the Ministry of Transport (2013). These environmental aspects, however, are not the focus of this study. Here, the focus is on the effect on the water balance.

Furthermore, the capital city of Nairobi is expected to grow rapidly, which will lead to higher water requirements. In 2006 Nairobi had the highest annual growth rate in Africa (UN-Habitat, 2006). Although Nairobi is situated in the Athi basin, which borders the Tana basin, part of the city's water demand is extracted from the Tana basin. The way in which the expansion of Nairobi and Lamu is included in this study is further explained in chapter 3.4.

These interventions have in common that it is largely unknown what their respective, and combined, impacts on the river discharge will be and what effect this, in turn, will have on the ecosystems (mainly wetlands, which are found in the Tana delta) and the services they provide. Therefore, in this study the individual effects of the planned interventions as well as their combined impacts on the river discharge are assessed.

---

[1] The LAPSSET Corridor consists of a railway, highway, pipeline, airport, resort cities and oil refinery. They are all designed to connect major centers and sub regions of economic significance in several countries (appendix 2). (JPC & BAC/GKA JV, 2011).

Figure 4: Lamu Port development Plan (RVI Nairobi Forum, 2013, p. 1).

1.3 Scientific and societal relevance

Recent quantitative studies on changes in the hydrology of the Tana basin are few, and there is limited reliable, up-to-date information on water quantity (Dickens et al., 2012). Therefore, this thesis will directly add to the scientific knowledge about the basin, especially on expected hydrological effects of land and water use changes in the Tana basin. However, having scientific relevance – i.e. the pursuit of knowledge for its own sake – is not the only goal of this research.

This thesis will also be important from a societal point of view. The (combined) impacts of all proposed plans can potentially have adverse effects on downstream livelihoods and ecosystems. If possible, the results of this thesis will be used by Wetlands International to inform decision- and policy-making of several large-scale projects: a Land Use Plan (LUP) for the Tana delta and the Strategic Environmental Assessment (SEA) by the Kenyan Ministry of Lands; the Ecosystem Alliance Kenya project in the Tana delta, and; a joint TEEB-study initiative in partnership with the Dutch Ministry of Economic Affairs, UNEP and the Water Resources Management Authority of Kenya (WRMA). These projects are briefly explained below.

Currently, the Kenyan government is working on a LUP for the Tana delta to provide certainty about land use changes in order to minimize conflicts between various groups benefitting from the delta's ecosystem services and to promote green development and conservation of biodiversity. To include sustainable development in this LUP, a SEA is undertaken (Odhengo et al., 2012a; 2012b) for the entire Tana River basin. If finished in time, this thesis could provide valuable insights that could be included in the SEA and LUP.

Additionally, this thesis could be helpful for the Ecosystem Alliance (EA), which is a collaboration between IUCN National Committee of the Netherlands, Both ENDS and Wetlands International. The aim of the EA in Kenya is to improve people's livelihoods in the Tana delta by protecting ecosystems (IUCN NL, 2013). Sound (scientific) knowledge should form the basis on which further action is taken.

This thesis can add to the understanding of the water balance in the Tana basin, and thus contribute to the EA's goals in the area.

Lastly, UNEP is facilitating the Tana Basin Coordination Mechanism (hosted by WRMA), i.e. a platform for exchanging ideas and information between Tana basin stakeholders. UNEP, Wetlands International (under the flag of the Ecosystem Alliance in Kenya), the Dutch Ministry of Economic Affairs and WRMA are developing a basin-wide mapping and valuation of ecosystems services. This study is called 'TEEB for Tana', with TEEB meaning 'The Economics of Ecosystems and Biodiversity' (TEEB, 2013). This work is part of what is envisaged in Kenya's National Water Master Plan and the Tana Catchment Management Strategy, all contributing to Kenya's Vision 2030.

Kenya's Vision 2030 "aims at transforming Kenya into a newly-industrializing, middle income country providing a high quality of life to all its citizens in a clean and secure environment" (Government of Kenya, 2007, p. viii).

The study also falls under the project "Institutional development and capacity building of the Tana Catchment Area for the rehabilitation of critical water ecosystems" contributing towards the achievement of UNEP's Programme of Work for 2012 – 2013, output #3b2 (Tools and Methodologies for Assessing and Maintaining Freshwater Ecosystems). For the Dutch government this study fits within a program where they link biodiversity to food security through the landscape approach (Dutch Ministry of Economic Affairs, 2013). It is assumed that the results of this thesis can support the mapping and valuation study carried out by UNEP, Wetlands International, the Dutch Ministry of Economic affairs and WRMA (van Weert, pers. comm., 2013).

1.4 Previously conducted studies

There are several studies describing the hydrology of (part of) the Tana basin: Kitheka & Ongwenyi (2002); Maingi & Marsh (2002); Emerton (2005); Kitheka et al. (2005); Hoff et al. (2007); Snoussi et al. (2007); Dickens et al. (2012); Duvail et al. (2012); Knoop et al. (2012); Leauthaud et al. (2013a; 2013b); and Oludhe et al. (2013). In all studies it is concluded that the hydrology of the Tana River is strongly altered by anthropogenic influences. However, mostly due to lacking data, there are considerable uncertainties in the hydrological system, mainly in the upper basin (Dickens et al., 2012). Actual quantitative studies on the hydrology of the Tana basin are few: Maingi & Marsh (2002); Kitheka et al. (2005) (focusing on sediments); Hoff et al. (2007); Duvail et al. (2012); Leauthaud et al. (2013b). Thus far, one quantitative modeling study was done for the upper and middle Tana basin (Hoff et al., 2007), one modeling study was done specifically for the Masinga Reservoir (Oludhe et al., 2013) and one for the Tana delta (Leauthaud et al., 2013b). The conclusions of these quantitative studies are described below.

Maingi & Marsh (2002) investigated the flooding pattern of the Tana River between Garissa and Hola and how this changed after dam construction. They found a reduction in peak discharges and sediment load and an increase in low flows. These alterations adversely affect the riverine forests along the Tana River. In their study they demonstrate that damming in the upper basin not only results in negative environmental effects near the reservoirs, but also downstream. They call for future studies to include these downstream effects as well.

Kitheka et al. (2005) focused on modeling the sediment transport in the Tana basin. They found that the Tana River shows a marked seasonal signal, which differs from patterns in other dammed river

systems. This is attributed to the fact that the reservoirs in the Tana River are relatively small, and a considerable part of the discharge is added to the river downstream of the reservoirs. Furthermore, they found that the majority of the transported sediments are the result of soil erosion due to poor land use activities. The total sediment load has been strongly reduced after construction of the reservoirs, which trap the sediments.

Hoff et al. (2007) used the Water Evaluation and Planning tool (WEAP) to assess the water balance in the upper and middle Tana basin in a scenario-based setup. This study looked at the effects of green water credits on the water balance, mainly siltation of reservoirs and groundwater recharge. "Green water credits is a mechanism to pay rural people for specified land and water management activities that determine all fresh water resources at source" (Hoff et al., 2007, p. 0). Three green water management scenarios were defined: contour strips, mulching, and tied ridges. It was found that especially in dry years the hydrological benefits (e.g. groundwater recharge and soil loss) of these management practices were considerable.

Oludhe et al. (2013) used multi-model climate forecasts to improve water and, hence, energy management in the Masinga Reservoir. The study mainly focused on evaluation of probabilistic streamflow forecasts from single general circulation models and multi-model climate forecasts to improve hydropower generation by the Masinga dam in dryer periods (such as during La Niña). Their conclusion was that multi-model forecasts performed better than single-model forecasts.

For the modeling study in the Tana delta the model TIM (Tana Inundation Model) was created (Leauthaud et al., 2013b). This model was used to quantify the spatial and temporal flooding characteristics – i.e. flood extent, duration, timing and frequency of occurrence – in the Tana delta. According to the authors, this is the first study to have done this. They succeeded in accurately simulating the discharges at Garsen (figure 5). The authors found that the dams, although modifying the volume of routed water, did not affect the flood propagation characteristics.
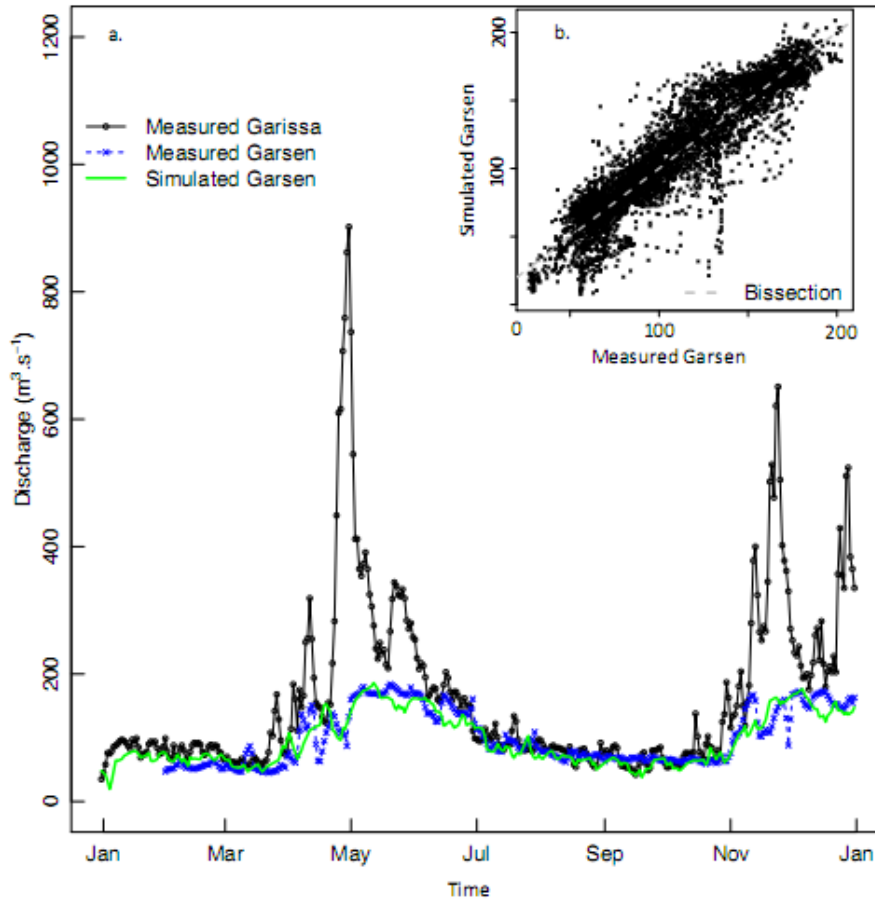
Figure 5: Hydrograph from a modeling study by Leauthaud et al. (2013b, p. 3062). (a) The measured discharges at Garissa and Garsen, with the simulated discharge at Garsen for the year 1988. (b) The simulated versus measured discharge at Garsen for two validation periods, 1963-1986 and 1991-1998.

Above-mentioned studies mainly focus on dams and to a lesser extent on irrigation schemes. Scientific peer-reviewed papers about the Lamu Port and its expected impacts could not be found. Only a feasibility study and an ESIA have been developed for the first three berths of the proposed Lamu Port (JPC & BAC/GKA JV, 2011; Ministry of Transport, 2013). This illustrates the lack in available literature showing the effect on the interventions that are modeled in this study. This study was initiated, because no study has yet been conducted to assess the effects of all the above-mentioned interventions.

1.5 Aim

This study aims to provide improved understanding of the hydrological consequences of anthropogenic interventions on the hydrological system in the Tana basin, with specific focus on water supply to the Tana delta. Since the wetlands in the area are greatly dependent on water supply from the Tana River, with its biannual floods, the (future) water availability in the region is imperative for the health of the ecosystem and its ability to deliver services to sustain people's livelihoods. The knowledge from this study is assumed to contribute to better-informed decision-making about the development of the region.

This aim corresponds with one of the main targets of WRMA, i.e. the provision of a reliable water balance for the Tana (Dickens et al., 2012).

1.6 Research questions

Following the research aim, this master's thesis provides a quantitative analysis of the Kenyan Tana basin water balance under several possible land and water-use scenarios using the global hydrological model PCR-GLOBWB. The main research question that is addressed in this thesis is:

How will the river discharge of the Tana River in the Tana delta be affected by climate change and anthropogenic developments in the region?

This research question is answered with the following sub-questions:

1. *What is the effect of climate change on the river discharge of the Tana River and the related water availability in the Tana delta?*
2. *How will the discharge and the related water availability in the Tana delta be affected by the High Grand Falls Dam?*
3. *How will the discharge and the related water availability in the Tana delta be affected by the expected irrigation schemes in combination with the High Grand Falls Dam?*
4. *How will the discharge and the related water availability in the Tana delta be affected by the expected construction of the Lamu Port and expected additional water demand due to the expansion of the Nairobi area?*
5. *How will the discharge and the related water availability in the Tana delta be affected if all these interventions are combined?*

The remaining part of this thesis is structured as follows: first the research methodology and the details on PCR-GLOBWB are discussed, as well as the set-up of this study (chapter 2). Then, the scenarios are explained in detail (chapter 3), followed by the presentation of the results (chapter 4). The results are discussed next, along with the uncertainties of this study in the discussion chapter (chapter 5). Finally, in the conclusion chapter the research questions are answered (chapter 6), followed by recommendations (chapter 7).

2. Methodology

2.1 Model choice

To answer the research questions a regionally downscaled version of the global hydrological model PCR-GLOBWB 2.0 (hereafter referred to as PCR-GLOBWB) is used (van Beek & Bierkens, 2008; Wada et al., 2014) (figure 6). PCR-GLOBWB is scripted in PCRaster, hence the name <u>PCR</u>aster <u>Gl</u>obal <u>W</u>ater <u>B</u>alance.
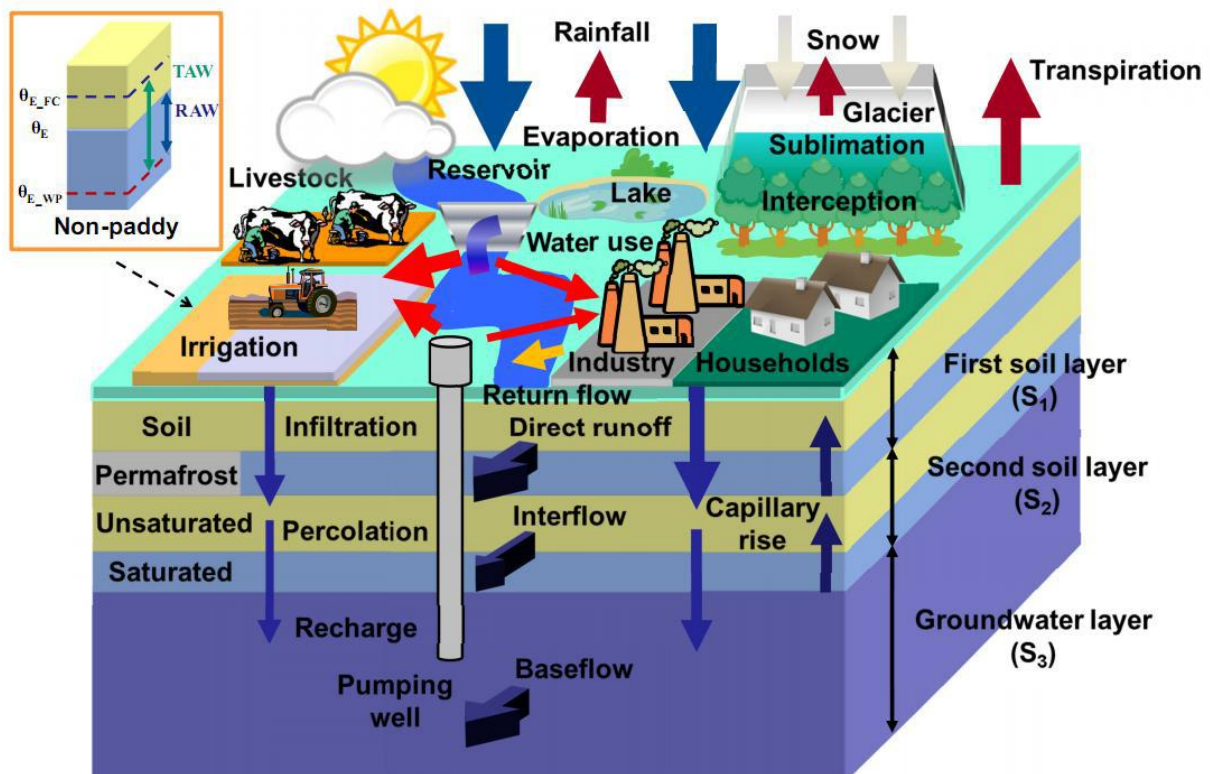
Figure 6: Schematic representation of the integrated modeling framework of PCR-GLOBWB that shows the coupling of the hydrological model with anthropogenic activities (Wada, 2013, p. 253).

Besides PCR-GLOBWB there are similar (recent) global and continental hydrological models, e.g. WBM (Fekete et al., 2002), LaD (Milly & Shmakin, 2002), WGHM (Alcamo et al., 2003) and WASMOD-M (Widén-Nilsson et al., 2007). However, PCR-GLOBWB has been chosen for this study because of the way it includes anthropogenic impacts on the water balance (Wada et al., 2014), and because it readily available and accessible for this study.

Furthermore, this study serves as a test to assess its performance in a relatively small catchment in a semi-arid region in Africa. In previous global studies with PCR-GLOBWB, the model appeared to have a limited performance in arid regions (van Beek et al., 2011) and overestimate monthly and yearly discharges of African rivers (van Beek & Bierkens, 2008). Therefore, the model is validated to assess its performance in the Tana basin.

In this chapter, the overall functioning of PCR-GLOBWB and the required datasets are explained, as well as a number of key equations. In-depth explanations of the model concept and the underlying assumptions and equations in PCR-GLOBWB are found in Wada et al. (2014).

2.2 Model description

2.2.1 Water balance

Water balance calculations in PCR-GLOBW are determined as follows: for each grid cell (5 arc-minutes, i.e. 0.08333° or roughly 86 km^2 for the Tana basin) and time step (daily), the water storage in two vertically stacked soil layers, and in an underlying groundwater layer is simulated. The sub-grid variability is determined by including short and tall vegetation separately, open water (i.e. lakes, reservoirs, floodplains and wetlands), soil types from the FAO Digital Soil Map of the World (FAO, 2003), area fraction of saturated soil, which is calculated with the improved Arno scheme (Todini, 1996; Hagemann & Gates, 2003)) and the frequency distribution of groundwater depth, which is based on the surface elevations of the HYDRO1k dataset (USGS EROS Data Center, sine anno). The groundwater store is represented as a linear reservoir model, and its parameterization is based on the lithology (Dürr et al., 2005) and topography (Wada et al., 2014). Snow storage and canopy interception are modeled as well (Wada, 2013).

The groundwater reservoir is not directly influenced by vegetation, but is fed directly by active recharge, i.e. net precipitation and percolation of irrigation water. Additionally, the fluxes between these layers (infiltration, percolation, and capillary rise) and between the top layer and the atmosphere (rainfall, evapotranspiration, and snow melt) are simulated (Wada et al., 2014). The specific runoff in cells consists of direct (saturation excess) runoff, interflow (lateral drainage from soil), and base flow (groundwater reservoir) (van Beek & Bierkens, 2008; Wada, 2013). See appendix 3 for the hydrological model concept only.

2.2.2 Meteorological forcing

To force PCR-GLOBWB, monthly climate forcing from the Climatic Research Unit (CRU TS 2.1) is used, with a resolution of 0.5° x 0.5°. The CRU dataset is based on monthly climate observations from meteorological stations and covers the global land mass (Mitchel & Jones, 2005; van Beek, 2008; Wada, 2013). The details of forcing PCR-GLOBWB with CRU data are explained in van Beek (2008). The monthly CRU data have been downscaled to daily values using the ERA-Interim reanalysis dataset, with a resolution of 1.5° x 1.5° (Dee et al., 2011). The meteorological forcing is applied uniformly over each grid cell (van Beek & Bierkens, 2008). The ERA-Interim reanalysis dataset is available from the start of the year 1979, meaning that it can only be used to simulate discharges starting from 1979. This is why model validation (see chapter 2.4) has only been done only from 1979 onwards.

2.2.3 Land use

PCR-GLOBWB takes anthropogenic water demand into account, i.e. from agriculture (crops and livestock), industry and households (figure 6). Allocation of the water for each sector is not prioritized, but is proportional to the amount of water demands per sector. The way PCR-GLOBWB determines the industrial and household water demand (Wada et al., 2014) is not explicitly included in the scenarios. This is especially the case for scenario 3, which deals with the industrial and household water demand for Nairobi and the Lamu Port. Duo to lacking socioeconomic data for the future, the industrial and household water demand is calculated differently in this scenario. The way this is done is clarified in chapter 3.4. Further information on how the water demand per sector is estimated can be found in Wada et al. (2014).

To determine the vegetation cover fraction, the Global Land Cover Characteristics (GLCC) version 2.0 dataset, with a resolution of 30 arc-seconds (roughly 1 km^2) is used (USGS EROS Data Center, 2002). The vegetation cover is divided into tall natural vegetation (forest), short natural vegetation (grassland), rainfed staple crops, irrigated paddy crops (rice), and irrigated non-paddy crops. The GLCC 2.0 dataset is used to determine the Leaf Area Index (LAI) of the natural vegetation, which in turn, is converted into the crop factor for each respective GLCC cover type (Allen et al., 1998; van Beek & Bierkens, 2008).

Irrigation is modeled in PCR-GLOBWB by separate parameterization of paddy (i.e. rice) and non-paddy crops. It is dynamically linked with the surface and soil water balance, because the feedbacks between irrigation and the changes in the surface and soil water balance (i.e. return flow) are considered. This has an effect on the soil moisture, and hence, irrigation water requirements of the crop fields in the following days (Wada et al., 2014). In order to correctly represent the water use of agricultural crops the MIRCA2000 dataset is used (Portmann et al., 2010). MIRCA2000 is a dynamic dataset, in the sense that it uses a crop calendar to assess crops over their development stages, i.e. initial period, mid-season, and end of season. Each part of the growing period has a different crop factor (see figure 7) (Siebert & Döll, 2010). The crop factors are dynamic during a year, but are constant on a year-to-year basis. The MIRCA2000 dataset has a spatial resolution of 5 arc-minutes and contains monthly irrigated and rainfed crop areas around the year 2000 (1998-2002). In total, the MICRA2000 dataset contains 26 crop classes (see appendix 4 for a detailed overview of the parameters per crop class), which have been divided into paddy and non-paddy crops. For the parameterization of these crop classes, the crop-specific parameters have been aggregated by the weighted area of the individual crop classes (Wada et al., 2014).

The crop factors (k_c) are used to calculate the daily (potential) crop evapotranspiration with (Allen et al., 1998; Wada et al., 2014):

$$ET_c = k_c \cdot ET_0 \qquad (2.1)$$

with ET_c [m/day] being the daily (potential) crop evapotranspiration, and ET_0 [m/day] the reference (potential) evapotranspiration. ET_0 is calculated with the Penman-Monteith equation as recommended by the FAO (Allen et al., 1998). The required irrigation demand for paddy and non-paddy crops is determined by ensuring optimal growth (Wada et al., 2014).
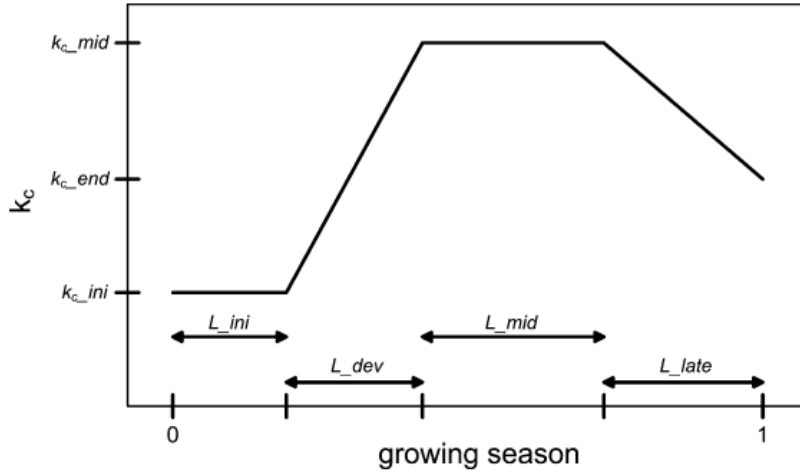
Figure 7: Parameters as they are included in the crop calendar of the Mirca2000 dataset. L represents the lengths of the crop development stages and k_c represents crop factors (Siebert & Döll, 2010, p. 201). For the specific parameters of each crop class see appendix 4.

2.2.4 Routing

By routing the simulated direct runoff, interflow, and baseflow along the local drainage direction (LDD[2]) (based on Vörösmarty et al., 2000) the river discharge is determined. The routing is based on the characteristic distances, R_{cd}, along the LDD-network (Wada et al., 2014):

$$R_{cd} = \frac{bz}{b+2z}^{2/3} \cdot \frac{G^{0.5}}{n}$$

(2.2)

with b and z being the channel width and depth, respectively [m], G the gradient that was derived from the LDD and elevation, and n Manning's roughness coefficient (Wada et al., 2014).

The existing dams and reservoirs are based on the Global Reservoir and Dams dataset (GRanD) (see table 1) (Lehner et al., 2011). The reservoirs are superimposed over the LDD-map. Reservoir release is modeled to satisfy local and downstream water demands that can be met within approximately 600 km (i.e. the distance that is reached with an average discharge velocity of 1 m/s for seven days). If the situation arises that there is no water demand, the reservoir release, R_r [m³/day], is based on the minimum, S_{min} [m], maximum, S_{max} [m] (i.e. 10% and 75% of storage capacity, respectively), as well as the actual reservoir storage, S_r [m], and average inflow, I_{avg} [m³/day] (Wada et al., 2014):

$$R_r = \frac{S_r - S_{min}}{S_{max} - S_{min}} \cdot I_{avg}$$

(2.3)

$$S_{r,t} = min(S_{max}, S_{r,t-1} + I + P_{local} - R_r - EW_r)$$

(2.4)

with I [m³] being the inflow into the reservoir, P_{local} [m³] the precipitation over the reservoir surface, and EW_r [m³] the open water evaporation from the reservoir surface. Whenever the reservoir storage equals 100% of the storage capacity, spills occur (Wada et al., 2014).

---

[2] An LDD-network designates the direction of flow for each cell in eight cardinal directions over 360°, i.e. N, NE, E, SE, S, SW, W, and NW).

Table 1: Reservoir parameters as they are included from the GRanD dataset.

Name	Area [km^2]	Capacity [MCM]	Year
Kiambere	11.4	585.0	1987[3]
Gitaru	2.5	20.0	1978
Kamburu	8.7	150.0[4]	1974
Kindaruma	2.1	16.0	1968
Masinga	69.7	1,560.0[4]	1980[3]

2.2.5 Water allocation

In this study, it is assumed that the water demand is only satisfied by allocating surface water (including reservoirs). So groundwater is not used to satisfy water demand. This assumption is underpinned by a recent study by Altchenko & Villholth (2014). They concluded that groundwater irrigation is hardly used for irrigation purposes in Africa, which is also the case in the Tana basin (Nippon Koei, 2013c). In order to prevent water balance errors in the model, the water is extracted from within a superimposed segment of 1° resolution, where preference is given to the grid cell containing the most water.

2.3 Time slices

For each scenario, the following three periods are used to estimate the effects on the river discharge: 2010-2030, 2025-2045, and 2045-2065, representing the discharges around 2020, 2035, and 2055, respectively. The year 2020 represents the near future. The years after 2020 are set increasingly further apart, due to the increasing uncertainties that arise when looking further into the future. The year 2035 has been chosen because all interventions that are included in this study are assumed to be implemented in 2035, while 2055 represents the long term, where climate change is the only changing factor. In this thesis the period 2010-2030 is referred to as the near future, 2025-2045 as the mid future, and 2045-2065 as the far future.

Due to time constraints several simplifications have been made with respect to modeling climate change and its effect on Tana basin hydrology. Instead of using all Representative Concentration Pathways (RCPs), i.e. CO_2-emission scenarios, from the Fifth Assessment Report of the Intergovernmental Panel on Climate Change (IPCC) (IPCC, 2013) this study uses only RCP6.0[5]. For RCP6.0 the CO_2-equivalent concentrations are roughly 850 ppm by the year 2100 (Moss et al., 2010). RCP6.0 was chosen because it is at the high end of the intermediate stabilization pathways (IPCC, 2013). Since the RCPs, and hence the future projections, start in 2006 (Taylor et al., 2009), the model is run for the period 2006-2065. Climate change is modeled using four general circulation models (GCMs), also known as global climate models, from the Coordinated Modeling Intercomparison Project Phase 5 (CMIP5) (IPCC, 2013) (table 2). The GCMs are all bias-corrected against the CRU data with the Inter-Sectoral Impact Model Intercomparison Project (ISI-MIP) dataset (Hempel et al., 2013). Figure 8 illustrates the variability between the GCMs.

---

[3] The years in which these dams were installed differ slightly from those reported in Nippon Koei (2013b), i.e. 1988 and 1981 for Kiambere and Masinga, respectively.

[4] These reservoir capacities are higher than those reported in Nippon Koei (2013a), i.e. 110 MCM and 1,402 MCM for Kamburu and Masinga, respectively.

[5] So called because of the target radiative forcing for the year 2100, i.e. 6.0 W/m^2 (IPCC, 2013).

Table 2: The four GCMs that are included in this study. The last column shows the mean monthly discharges at Garissa over the period 2006-2065 as calculated with PCR-GLOBWB forced with the respective GCM. For comparison: the mean discharge at Garissa over the period 1979-2009 as calculated with PCR-GLOBWB forced with CRU/Era-Interim data is 157.10 m³/s

GCM	Organization	Mean monthly discharge [m^3/s]
IPSL-CM5A-LR	Institute Piere-Simon Laplace (Hourdin et al., 2013)	195.74
MIROC-ESM-CHEM	JAMSTEC, NIES, AORI (The University of Tokyo) (Watanabe et al., 2011)	229.44
GFDL-ESM2M	NOAA Geophysical Fluid Dynamics Laboratory (Dunne et al., 2012)	146.77
NorESM1-M	Norwegian Climate Centre (Bentsen et al., 2012)	139.76
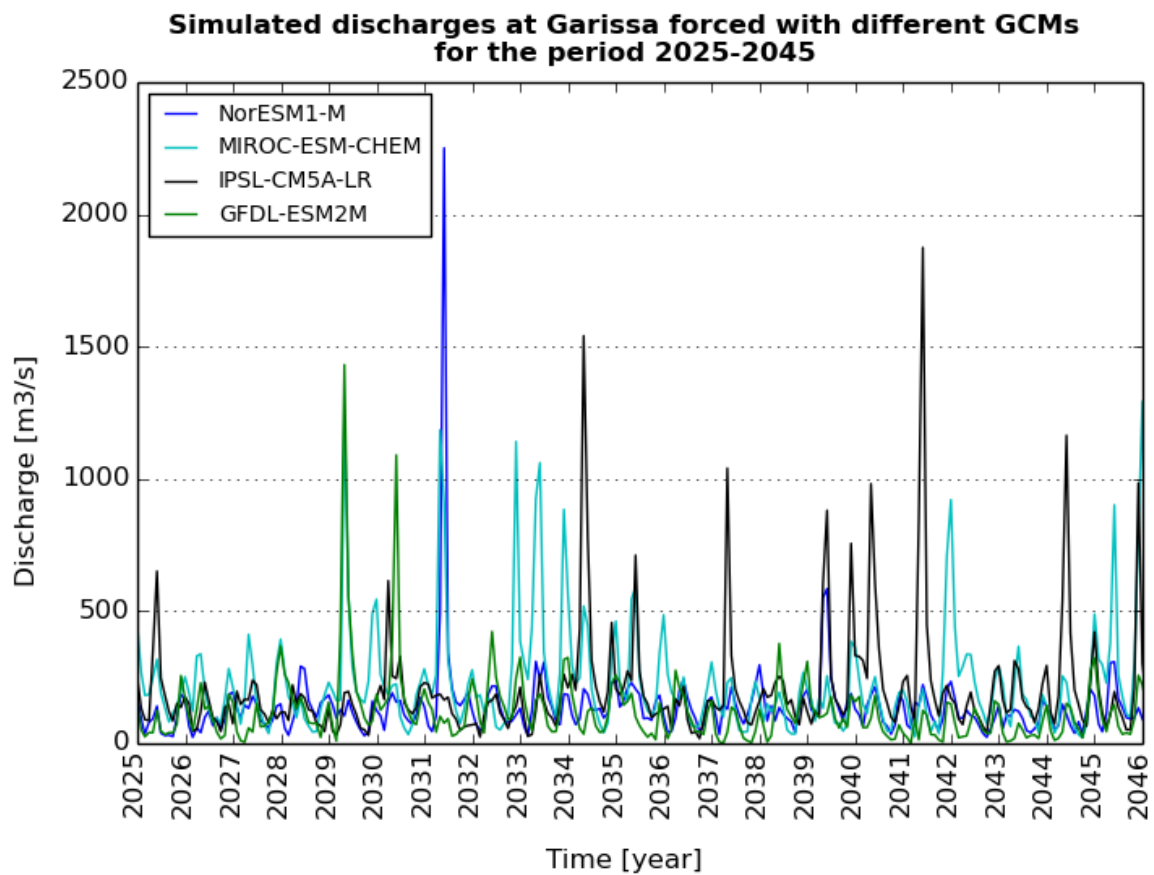
Figure 8: Hydrographs at Garissa for the period 2025-2045 as calculated with PCR-GLOBWB forced with the respective GCMs.

2.4 Model calibration and validation

The fit between observed and modeled discharges was assessed using the logarithmic Nash-Sutcliffe efficiency method (LNSE) (Nash & Sutcliffe, 1970), Pearson's coefficient of determination (R^2), and the root mean square error (RMSE). A disadvantage of the normal Nash-Sutcliffe efficiency is that the difference between the observed and modeled discharges is squared. This means that that model performance is biased towards reproducing peak flows, and giving little weight to low flows. This is preferable for flood forecasting but not if the interest is on water availability, as is the case here. To reduce this problem, the natural logarithm (ln) of the observed and modeled discharges is taken. By doing this, the peaks are smoothed out, while the low flows remain relatively unchanged. This

increases the sensitivity to systematic model over- or underpredictions (Krause et al., 2005). The LNSE is calculated as:

$$\text{LNSE} = 1 - \frac{\sum_{i=1}^{n}\left(\ln Q_i^{obs} - \ln Q_i^{mod}\right)^2}{\sum_{i=1}^{n}\left(\ln Q_i^{obs} - \overline{\ln Q^{obs}}\right)^2} \qquad (2.5)$$

with Q_i^{obs} being the ith observed discharge, Q_i^{mod} being the ith modeled discharge, $\bar{Q}$ being the mean discharge, and n being the total number of observations (Krause et al., 2005). The values of LNSE range between -∞ and 1. The closer the value is to 1 the better the model performs. Negative LNSE-values indicate that the mean of the observed discharges is a better predictor than the modeled discharges (Moriasi et al., 2007).

R^2 is calculated with:

$$R^2 = \left(\frac{\sum_{i=1}^{n}\left(Q_i^{obs} - \overline{Q^{obs}}\right)\left(Q_i^{mod} - \overline{Q^{mod}}\right)}{\sqrt{\sum_{i=1}^{n}\left(Q_i^{obs} - \overline{Q^{obs}}\right)^2}\sqrt{\sum_{i=1}^{n}\left(Q_i^{mod} - \overline{Q^{mod}}\right)^2}}\right)^2 \qquad (2.6)$$

It describes how much of the observed dispersion is explained by the model. The values of R^2 range between 0 and 1. An R^2 of 0 means there is no correlation, while a value of 1 means there is a perfect linear relationship (Krause et al., 2005; Moriasi et al., 2007). The R^2 is very sensitive to the seasonal timing in the discharge. With a correct seasonal timing it can still be high even if a model systematically over- or underestimates the discharge (Sutanudjaja, pers comm., 2014).

The model was validated using observed monthly discharges at Grand Falls, Garissa, Hola, and Garsen, respectively (see figure 1, for their respective locations). However, complete time series could not be found and some gaps exist in the records. Garissa has the most complete record. Validation[6] was done on the longest (near-)complete consecutive series of years after 1979 for Grand Falls (1979-1996), Garissa (1979-2009), Hola (1979-1988) and Garsen (1979-1993) (see appendix 5).

The model performed poorly without any calibration[7], largely overestimating the peak discharges and underestimating the low flows (see appendix 6 for validation results before calibration). As a first measure to reduce the peak discharges, the wetlands (including the river floodplains) in the Tana basin were modeled as part of the open water fraction. These wetlands were identified with the Global Lakes and Wetland Database 3 (GLWD) (Lehner & Döll, 2004; van Beek et al., 2011). By including the wetlands in the open water fraction, there is more open water to evaporate, thereby reducing the discharge.

To further improve the model performance calibration was done using an ensemble Kalman filter (EnKF)-based calibration routine, which minimizes the RMSE between the modeled and observed discharges:

---

[6] Validation is the process of determining how well the model results fit the observed data (Legates & McCabe Jr., 1999).
[7] "Calibration is the process of estimating model parameters by comparing model predictions (output) for a given set of assumed conditions with observed data for the same conditions" (Moriasi et al., 2007, p. 885).

$$\text{RMSE} = \sqrt{\frac{\sum_{i=1}^{n}\left(Q_i^{mod} - Q_i^{obs}\right)^2}{n}} \qquad (2.7)$$

with Q_i^{mod} being the modeled ensemble mean discharge, Q_i^{obs} the observed discharge, and *n* the total number of observations (Wanders et al., 2014). The calibration is based on observed mean monthly discharges of Grand Falls, Garissa, Hola and Garsen (appendix 5) over a period of 18 years (1979-1997). Details about the used calibration routine can be found in Evensen (2003) and Wanders et al. (2014).

The following parameters were calibrated: minimum soil water storage capacity (W_{min}[8] [m]), recession constant for linear groundwater reservoir (i.e. residence time, *J* [days]), saturated hydraulic conductivity for both soil layers (K_{sat} [m/day]), Manning's roughness coefficient (*n* [-]), crop factor of open water (*cropKC* [-]), and precipitation (*P* [m/day]). This timeframe (18 years) was chosen for practical reasons, i.e. runtime and because the observed discharges at both Grand Falls and Garsen form almost complete time series until 1997, with hardly any missing values (see appendix 5). The calibration (using the EnKF) was conducted several times, with different parameters and parameter limits using between 60 and 396 ensemble members, depending on available computing resources. While this improved the model results, it was still not enough to yield useful results.

Therefore, in addition to the EnKF-based calibration routine, manual calibration was done to improve model results. First, the model results were improved by reducing the precipitation with a factor of 0.75 over the entire catchment. This significantly reduced the peaks, but the low flows (i.e. baseflow) were still underestimated. The baseflow in PCR-GLOBWB is calculated by the groundwater flux into the river channel. However, varying the recession constant did not produce significant improvements on the baseflow. Hence, the problem is probably (partly) determined by vertical recharge of the groundwater storage. The saturated hydraulic conductivity of the soil layers determines how quickly water flows through the soil. The low flows were improved up to certain point by increasing K_{sat} with a factor 500. The K_{sat} values of the soil layers determine how quickly water flows through the soil. By increasing K_{sat}, more water is able to infiltrate into the groundwater storage, which increases the baseflow. The other parameter changes were an increase of W_{min}, *J* and *cropKC* by roughly 100%, and a slight reduction of *n*. These resulted in the best model performance that could be gained within the limited timeframe for this study. See chapter 4.1 for validation results.

Because after calibration the model performance was still not acceptable, a normalized correction method is applied after calibration to remove the model bias, i.e. the systematic over- and underestimation of discharges. This is done only for the results at Garsen, because it is used as a proxy for the Tana delta and thus the most important location for this study. This normalized correction method is explained next.

First, both the observed and simulated discharges for the period 1979-1998 are log-transformed with the natural logarithm to reduce the standard deviations. Next, the ratios between the modeled and observed means and standard deviations of these log-transformed discharges is taken. Only the simulated monthly discharges for which there are corresponding observations have been included.

---

[8] W_{min} determines the amount of runoff versus infiltration. If W_{min} = 0, there is always direct runoff after rain events. If W_{min} > 0, there is only direct runoff if the total soil water storage exceeds W_{min} (Sutanudjaja et al., 2014).

These ratios are then used as scaling factors, which are applied on all future modeled discharges at Garsen.

From the simulated discharges of each period the *z*-scores are calculated to normalize the errors:

$$Z = \frac{X_i - \mu}{\sigma} \tag{2.8}$$

with X_i being the *i*th modeled discharge, μ the modeled mean and σ the standard deviation of the modeled discharges. The *z*-score basically shows the number of standard deviations a certain discharge is away from the mean (Wonnacott & Wonnacott, 1990).

The modeled mean and standard deviation are then multiplied with their respective scaling factors. After they have been scaled, the *z*-scores are removed again, by first multiplying with the scaled standard deviation followed by the addition of the scaled mean. The resulting discharges are then back-transformed again (taking the exponential) which results in the final model bias-corrected discharges. In other words, the corrected FDCs (for 1979-1998) are scaled such that the mean and standard deviation are roughly equal to the observed FDC. See chapter 4.1 for the results. This correction is applied to the results of all scenarios, using the same scaling factors as for the model validation.

2.5 Analysis of results

To assess the impacts of the scenarios on the river discharge, flow-duration curves (FDCs) are used. FDCs represent the frequency that a given discharge is exceeded. As stated before, Garsen is the focus of this study, so all analyses are done only with respect to Garsen. FDCs are created for each assessed period, i.e. near, mid- and far future. The mean FDC is calculated by taking the mean discharge of all GCMs per percentile, as well as the spread (i.e. the minima and maxima) between the GCMs.

In chapter 4 only the FDCs for the period 2025-2045 are shown, because this is between the near and far future. This is done to improve the readability of the text. The FDCs of the other periods can be found in the appendix 7. The FDCs are shown for discharges over the entire year, as well as for the rainy and dry seasons separately. This highlights the seasonal variations of the interventions.

The FDCs of the status quo (see chapter 3.1) is compared with the observed discharges, to get an understanding of the effect of climate change on the river discharge. The FDCs of each future scenario (see chapters 3.2-3.5) are compared to the FDCs of the status quo for the same period and season to determine the relative changes in discharge. Additionally, the changes in minimum, mean, and maximum Q10 and Q90 – i.e. discharges with an exceedence probability of 10 and 90%, respectively – with respect to the status quo scenario are given in a table to get a quick overview.

By assessing the inter-scenario changes in Q10 and Q90 the changes in peak flows (Q10) and low flows (Q90) can be compared. Q10 and Q90 are determined by linearly interpolating between the nearest percentiles and their respective discharges. An overview of the minimum, mean, and maximum Q10 and Q90 discharges per period is given in a table per scenario. Because the focus of this study is on the relative changes (i.e. the effects of the scenarios compared to the status quo), the tables with the absolute discharges are shown in appendix 7.

In the next chapter the scenarios are introduced in detail and the way they are modeled in PCR-GLOBWB is described.

3. Scenarios

For each intervention a scenario is developed. First, the hydrological effects of the interventions are modeled individually. Lastly, a scenario is created in which all proposed interventions are accumulated. The scenarios have been checked with stakeholders during two sessions. The first session was a consultation meeting for the 'TEEB for Tana' study (March 2014), during which government representatives at county level were also present (presented by H. de Moel and M. Eiselin). The second session was during the AFRIDELTA conference in May 2014, where mainly academic researchers focusing on wetlands research were present (presented by J. Mulonga).

3.1 Status Quo

The status quo is modeled by leaving out any planned future interventions, meaning that the current situation is projected into the future. Thus, the land use will stay constant throughout the entire model run. The only changing factor is climate change (the way climate change is included is explained in chapter 2.3).

The land use is modeled using the global datasets GLCC 2.0 and MIRCA2000, and the five major existing dams in operation. However, the Gitaru and Kindaruma reservoirs are aggregated as a single reservoir, because they are located in the same grid cell (Wada et al., 2014). The result is a reservoir with an area that is the sum of both separate reservoirs. The dams that supply water to Nairobi (Sasumua and Thika dams (Nippon Koei, 2013a)) are not included in the model. The water demand for Nairobi is modeled instead by extracting 181 MCM/year, i.e. 495,890 m^3/day, which is the currently installed transport capacity (Nippon Koei, 2013a). The location of the water extraction for Nairobi is the same as for scenario 3 (see chapter 3.4.2)

All other scenarios use the status quo as starting point. As such, the unaltered land use and used GCMs is the same in all scenarios. From this starting point the other interventions are added (table 3). As such, the status quo will serve as a baseline scenario, with which the other scenarios are compared.

Table 3: Scenarios and corresponding interventions as they are included in this study.

Scenarios	Current situation	HGFD	Proposed irrigation Schemes	Lamu Port & Nairobi expansion
Status quo	✓			
Scenario 1	✓	✓		
Scenario 2	✓	✓	✓	
Scenario 3	✓			✓
Scenario 4	✓	✓	✓	✓

3.2 Scenario 1

This scenario is designed to assess the impact of the HGFD on the water balance. The only change with respect to the status quo is incorporation of the HGFD itself. In total, a number of 11 dams is expected to be built in the Tana basin. This will result in a total effective storage volume of 5,729 MCM (Nippon Koei, 2013a). However, because of time constraints and lack of information, only the HGFD dam is included in this study. The HGFD will have by far the largest storage capacity (5,000 MCM) of all proposed dams (Nippon Koei, 2013a), and is thus most important to include. The HGFD

project is a flagship project for the Kenyan government (Nippon Koei, 2013a). The High Grand Falls Irrigation Project (HGFIP) is not incorporated in this scenario. These irrigation schemes are included in scenario 2 in which the planned large-scale irrigation schemes are modeled (see chapter 3.3).

The HGFD will be built in two stages. Construction of the dam will soon commence, and the first stage is expected to be finished in 2018. In this stage the HGFD will have a hydropower capacity of 500 MW, which will be increased with an additional 200 MW in stage two (after 2027) (Republic of Kenya, 2011a; Nippon Koei, 2013d). This upgrade in capacity from 500 to 700 MW will be realized by installing an extra turbine (Mbui, pers. comm., 2014). However, since this version of PCR-GLOBWB (2.0) does not explicitly include hydropower generation these stages are not modeled separately. Instead, the dam is included in the model as a single stage in 2018.

The height of the HGFD will be 115 m and will be built such that the crest is at an elevation of 555 m above sea level (Republic of Kenya, 2011a). This information is used to calculate the size of the reservoir that will form. A water surface at an elevation of 555 m above sea level was calculated, which will be the reservoir surface. When the reservoir is completely filled (100%) the model assumes a resulting storage of 6,187 MCM, which is more than the 5,000 MCM that is reported in Nippon Koei (2013a). Figure 9 illustrates the size of the expected HGFD reservoir in relation to the existing ones. The Tana and Athi River Development Authority (TARDA) estimates the reservoir to fill up over the course of a maximum of three years (Mbui, pers. comm., 2014). In the model the reservoir starts to fill up in the year 2018, when it is first included, and, depending on the GCM, it takes roughly three to six years before the reservoir storage reaches 80% of its maximum capacity.

3.2.1 HGFD Operations

As described in chapter 1.2.1, the HGFD will be used for flood management, power generation and supply of irrigation, drinking and industrial water. Except for power generation, these facets are included in PCR-GLOBWB (Wada et al., 2014).

Flood regulation is one of the most important aspects of the HGFD and has priority over the other purposes. The HGFD ensures a perennial flow with a discharge of 10 m^3/s during the rainy season and 30 m^3/s during the dry season to provide to improve livelihoods. It should be noted, however, that nowhere it is specified where these amounts are based on. The release of 10 m^3/s is modeled in the period April-May-June and November-December, while the other months give a release of 30 m^3/s. Additionally, the HGFD will provide two artificial floods per year in early June and early December to simulate the 'natural' floods. Each flood will have a volume of 400 MCM, representing a discharge of 660 m^3/s for one week (Republic of Kenya, 2011a). These artificial floods are modeled in the first week of June and December, respectively.

The HGFD will provide firm and peak power. Firm power is the amount that will always be provided year round, even in dry years. Construction of the HGFD will triple the currently generated firm power in the Tana basin (from 2 GWh/day to 6 GWh/day). Peak power, i.e. 500 MW in stage 1 and 700 MW in stage 2, is mainly required from 19.00 to 22.00 hr (Republic of Kenya, 2011a). However, as mentioned before, these stages will not be modeled separately. Since PCR-GLOBWB does not take hydropower generation directly into account, reservoir release is only based on downstream water demand (see chapter 2.2.4).

Irrigation water supply by the HGFD has the lowest priority, but is important nevertheless, because it can reduce reliance on large-scale pumping by facilitating gravity supply due to a more constant river discharge. As such, it can make irrigation schemes economically more attractive. Dependence on pumping has resulted in the failures of the Bura and Hola irrigation schemes in the past (Adams, 1990; Republic of Kenya, 2011a). The irrigation development of the HGFIP will be implemented in three stages (see chapter 3.3.1). The most important aspect of drinking and industrial water supply by the HGFD project is the proposed supply to the Lamu Port (see chapter 3.4.1). From the Nanigi Barrage a conveyance canal will transport the water via Ijara to the Lamu Port (Republic of Kenya, 2011a).
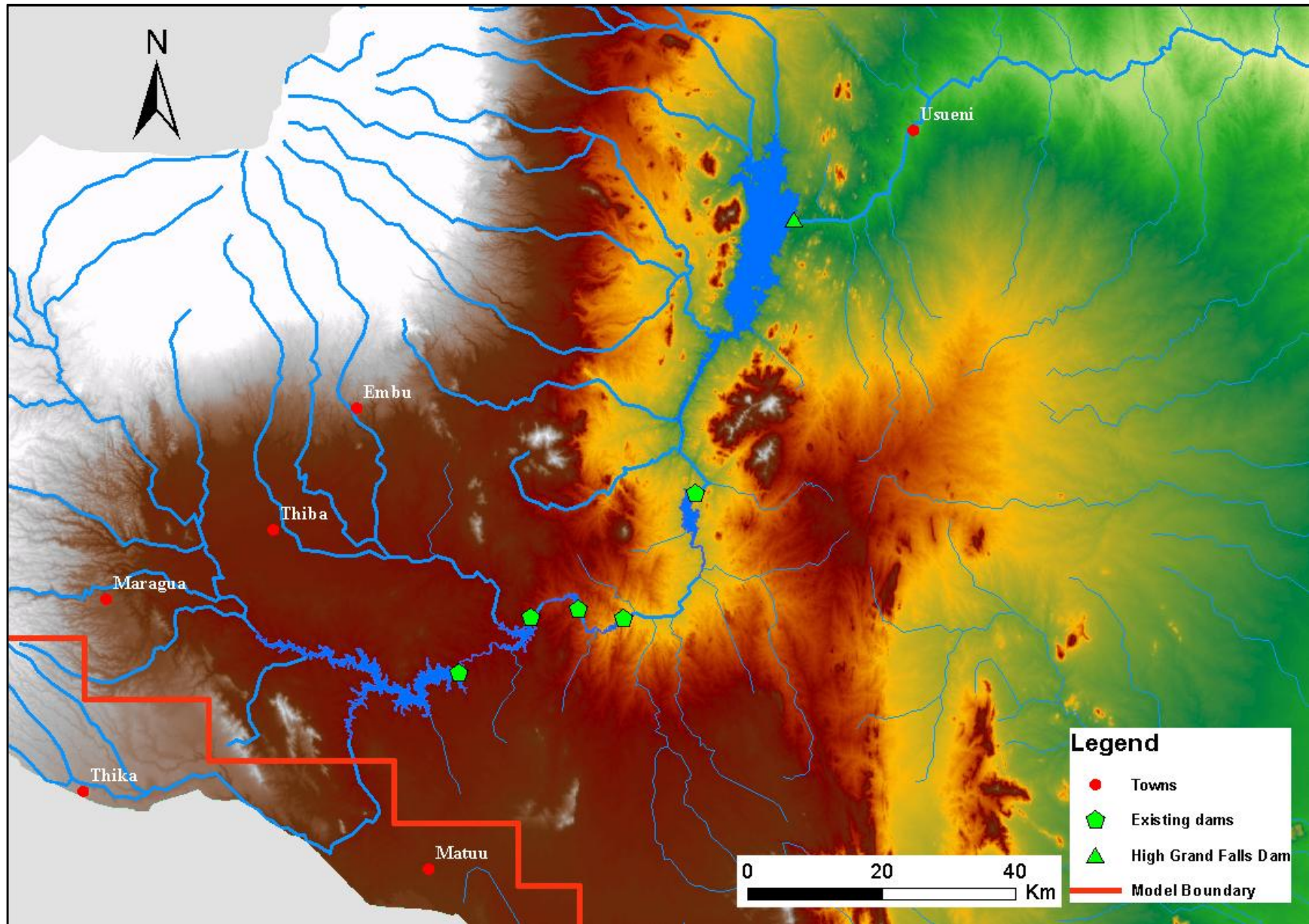
Figure 9: Digital Elevation Map (DEM 90m) showing the locations of the existing dams and their respective reservoirs as well as the expected High Grand Falls Dam and reservoir. The used GIS maps were downloaded from WRI (2007).

3.3 Scenario 2

This scenario determines the effect of planned large-scale irrigation schemes on the water balance. At first, it was designed to only include the irrigation schemes. However, since the majority is dependent on the HGFD (as part of the HGFIP), it was decided to include the HGFD to increase the veracity of this scenario. The HGFD operations are identical to those specified for scenario 1.

In 2010, a total of 64,425 ha was classified as irrigation area. This total consisted of 17% large-scale irrigation schemes (i.e. each having an area larger than 500 ha), 23% small-scale and 60% private schemes (Nippon Koei, 2013a). In this study only proposed large-scale irrigation schemes are included (added to the already existing land use in the MIRCA2000 dataset). Table 4 shows the expected maximum irrigation development in 2030. It can be observed that by far the biggest increase in area will be due to large-scale irrigation schemes, i.e., 1,314%. The main reason for this is the HGFIP, which will cover an area of 106,000 ha (Nippon Koei, 2013a). The HGFIP is an overarching project consisting of several irrigation schemes.

Table 4: Proposed irrigation areas in 2030 (after Nippon Koei, 2013a).

Category	Existing Irrigation Area in 2010 [ha]	Total Irrigation Area in 2030 [ha]	Percentage increase [%]
Large-scale	11,200	147,161	1,314
Small-scale	14,823	30,607	239
Private	38,402	48,456	126
Total	64,425	226,224	351

3.3.1 Irrigation expansion stages

The proposed irrigation schemes that are part of the HFGIP are represented in three stages. The first stage (2011-2019) includes small-scale irrigation in the floodplains, the Bura (Republic of Kenya, 2011b) and Hola schemes, and the Tana Delta Irrigation Projects (sugar and rice) (Republic of Kenya, 2011a; Nippon Koei, 2013c). The small-scale irrigation projects in the floodplains are not included in this study, only the irrigated area that is incorporated in the MIRCA2000-dataset is included.

In the second stage (2019-2027), the irrigation potential will be increased by the construction of a barrage at Nanigi and canals to divert the water to both banks (figure 10). Construction of the Nanigi barrage is financially attractive because it will facilitate gravity supply, thereby reducing currently high pumping costs (Republic of Kenya, 2011a). The Masalani irrigation scheme is assumed to be constructed during this stage (Republic of Kenya, 2011b).

For the third stage (2027-2035), a new regulating reservoir is planned at Usueni to extend the irrigated area by up to 25,000 to 75,000 ha or more (Republic of Kenya, 2011b). No specifics on this area could be found, yet completely disregarding this amount of irrigated area would reduce the veracity. Due to a lack of information and the uncertainty of the plans, an area of 66,000 ha (see table 5) is included as the modeled irrigation area. Instead of the planned reservoir at Usueni, the water supply is regulated by the HGFD for modeling purposes.

For some of the proposed irrigation schemes, conveyor systems and canals are planned to provide them with enough irrigation water (Republic of Kenya, 2011a). There are several proposed transfer schemes, but it is unclear which of those will be realized. However, these transfers are not included

in the model, because the used LDD-map (local drain direction) remains fixed for this study. Instead, only the expected increase in irrigated area due to these transfer systems is modeled.
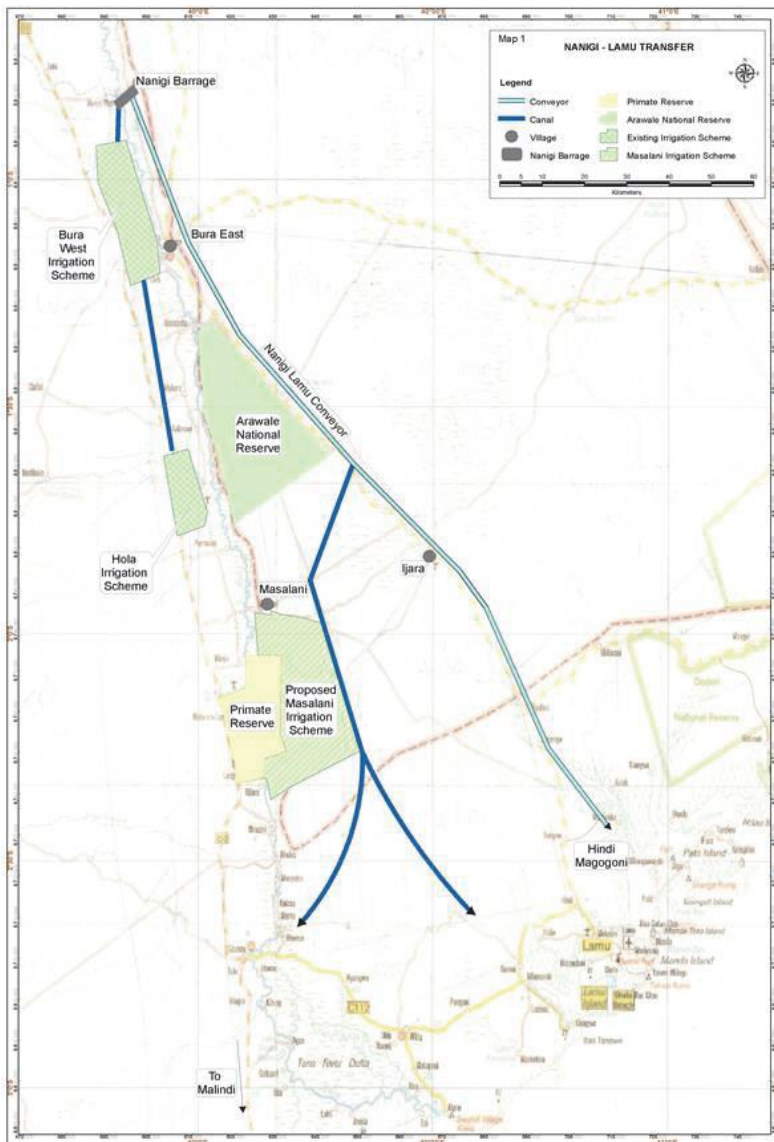
Figure 10: Proposed Nanigi transfer schemes (Republic of Kenya, 2011b, p. D-22).

3.3.2 Specifics on included irrigation schemes

There is a division in the way that large-scale irrigation schemes are modeled. Some irrigation schemes are described in detail in the literature, while others are not. First, these detailed schemes are described in a downstream order, after which the schemes about which no detailed information is available are explained. When summing all irrigated areas that are included in this study a total of 146,000 (table 5) ha is obtained. This roughly corresponds to the expected total irrigation area in 2030 (table 4).

Mwea irrigation scheme

The Mwea irrigation scheme is located in the upper Tana basin. This irrigation scheme is currently the biggest in Kenya with respect to rice cultivation, contributing to roughly 80% of the national rice production. It covers an area of 9,000 ha, with possible expansion of another 4,000 ha (Ndiiri et al., 2013), although in Nippon Koei (2013e, table 1.1, p. DB 1-1) it is stated that it will increase to a maximum of 10,000 ha. The rice is grown by continuously flooding the paddy fields (Ndiiri et al.,

2013). In this study an area of 10,000 ha is used for the Mwea irrigation scheme, which is modeled over the period 2013-2017 (see table 5).

Bura and Hola irrigation schemes

Bura and Hola are both existing irrigation schemes that were used for cotton production. In the mid 1980s they accounted for 39% of the national cotton production (Ikiara & Ndirangu, 2002; Duvail et al., 2012). However, these projects have been deemed failures (Adams, 1990; Duvail et al., 2012). This is mainly due to the poor performance of the pump station at Nanigi, resulting from poor maintenance, poor availability of spare parts, fuel supply, and lack of trained operators and mechanics (Adams, 1990). Yet, as part of the HGFIP they are to be rehabilitated and expanded, this time by supplying the water by gravity, whereby reducing the reliability on pumps. The Bura scheme will, again, consist of cotton (Republic of Kenya, 2011b). It is unclear whether this is also the case for the Hola scheme. However, since in the past, before they failed, both schemes consisted of cotton, for this study it is assumed that both the Bura and Hola schemes will consist of cotton. The location of both irrigation schemes is shown in figure 10. In this scenario, the Bura irrigation scheme is divided into Bura East and Bura West, both of which cover an area of 3,250 ha, respectively. They are modeled by linearly expanding them from 2011 to 2017 (Republic of Kenya, 2011a) until they reach the expected area (see table 5).

Masalani irrigation scheme

The Masalani irrigation scheme is a component of the HGFIP consisting of an area of approximately 30,000 ha (Republic of Kenya, 2011b). It is part of the Nanigi left bank transfer system. Since it is described in quite some detail, it has been taken as a separate irrigation scheme for modeling purposes. The proposed location is shown in figure 10. Various crops will be grown in Masalani. The fractions of land that will be planted with the various crops as used in this study are shown in table 6. Even though this table is only for an area of 20,000 ha, in this study this is the assumed cropping pattern for the entire 30,000 ha.

Since the MIRCA2000 parameterization is used to model agricultural land cover, not all crops from table 6 are modeled individually. Beans and green grams, along with sesame and vegetables are included in the crop class 'other annuals', while mango is included in the crop class 'other perennials'. The development of the Masalani scheme is modeled by linearly expanding the irrigated area from 2019 to 2027 (stage 2) until an area of 30,000 ha is reached (see table 5).

Table 5: Large-scale irrigation schemes that are included in this study (after Republic of Kenya, 2011a; 2011b; Nippon Koei, 2013a; 2013e). First the irrigation schemes with detailed information, e.g. location and crop type, are shown. Secondly, irrigation schemes are shown for which only the general location is known. For the Kora-Baricho and Rahole transfer systems no years could be found. Therefore they are assumed to have the same time span as the Nanigi transfers. Rehab. and Ext. are rehabilitation and extension of existing irrigation schemes, respectively.

Irrigation schemes *with* specific information available	Irrigation area [ha]	Project type	Expected crops	Years[9]
High Grand Falls Irrigation Project	40,000 (sum)	New		
- Bura West & East	6,500	Rehab. + Ext.	Cotton	2011 - 2017
- Hola	3,500	Rehab. + Ext.	Cotton	2011 - 2017
- Masalani	30,000	New	Various	2019 - 2027
Tana Delta Irrigated Sugar Project	20,000	New	Sugar cane	2015 - 2035[10]
Tana Delta Irrigation Project (Rice)	10,000	Rehab. + Ext.	Rice	2015 - 2035[9]
Mwea Extension	10,000	Ext.	Rice	2013 - 2017[11]
Irrigation schemes *without* specific information available	Irrigation area [ha]	Project type	Expected crops	Years[9]
High Grand Falls Irrigation Project	66,000 (sum)	New		
- Nanigi left bank transfer system (excl. Masalani irrigation scheme)	30,000	New	Unknown	2019 - 2030
- Nanigi barrage-Sabaki River transfer system	14,000	New	Unknown	2019 - 2030
- Kora-Baricho transfer system	14,000	New	Unknown	2019 - 2030
- Rahole transfer system	8,000	New	Unknown	2019 - 2030

Table 6: Fractions of crops that will be grown in the Masalani irrigation scheme (Republic of Kenya, 2011b, p. D49) as they are included in the model. The used fractions are the percentages in the 'short rains' column.

CROPPING PATTERN AND GROSS WATER REQUIREMENTS													
PROJECT:	MASALANI AREA					COMMAND AREA:		20 000 HA					
NOTE: NO VALUES TO BE CHANGED IN THIS SHEET						CROPPING PATTERN:		Cpfinal_commercial_average					
Crop	irrigation	percentage area		cropped area (ha)		efficiencies			water requirements				
	method	short rains	long rains	short rains	long rains	field	distribut	project	m3/crop ha		MCM/period		
									short	long	short	long	year
MAIZE (food&seed)	PIVOT	25%	25%	5 000	5 000	75%	90%	68%	10 482	10 662	52,4	53,3	105,7
SORGHUM	IMPROVED GRAVITY	0%	0%	0	0	65%	90%	59%	0	0	0,0	0,0	0,0
BEANS & GREENGRAMS & SIMS	GRAVITY SURFACE	5%	3%	1 000	600	55%	90%	50%	7 341	10 095	7,3	6,1	13,4
SESAME	IMPROVED GRAVITY	1%	3%	200	600	65%	90%	59%	6 629	10 238	1,3	6,1	7,5
SOYBEANS	IMPROVED GRAVITY	15%	15%	3 000	3 000	65%	90%	59%	9 610	8 121	28,8	24,4	53,2
GROUNDNUTS	CP	15%	15%	3 000	3 000	75%	90%	68%	7 569	9 998	22,7	30,0	52,7
VEGETABLES	IMPROVED GRAVITY	10%	10%	2 000	2 000	65%	90%	59%	15 408	15 788	30,8	31,6	62,4
ONION	GRAVITY SURFACE	0%	0%	0	0	55%	90%	50%	0	0	0,0	0,0	0,0
TOMATO	DRIP	0%	0%	0	0	90%	90%	81%	0	0	0,0	0,0	0,0
MANGO	DRIP	4%	4%	800	800	90%	90%	81%	10 797	10 911	8,6	8,7	17,4
BANANA	DRIP	0%	0%	0	0	90%	90%	81%	0	0	0,0	0,0	0,0
COTTON	GRAVITY SURFACE	0%	0%	0	0	55%	90%	50%	0	0	0,0	0,0	0,0
SUGAR CANE	CENTRE PIVOT	0%	0%	0	0	75%	90%	68%	0	0	0,0	0,0	0,0
PASTURE/FODDER	CP AND GRAVITY	25%	25%	5 000	5 000	65%	90%	59%	14 953	17 699	74,8	88,5	163,3
total/average		100%	100%	20 000	20 000				11 342	12 433	227	249	476
peak demand		18,78											
peak demand		0,94											

---

[9] Where possible, Republic of Kenya (2011a, Table I 2, p. 58; Figure I 4, p. 59) is used. However, this list is not entirely complete. If a scheme is not included in this table, it is still used to estimate a time span for that scheme.

[10] Given the lack of information, the Tana Delta Irrigation Projects are estimated to be built over the course of all three stages, starting in 2015.

[11] Nippon Koei (2013e) Table 1.2, p. DB 1-3.

Tana Delta Irrigation Project and Tana Delta Irrigated Sugar Project

In the Tana delta two large-scale irrigation schemes are planned: Tana Delta Irrigation Project (TDIP) and Tana Delta Irrigated Sugar Project (TDISP) (Temper, 2010; Duvail et al., 2012; Nippon Koei, 2013e). In total 20,000 ha is to be converted to irrigated sugar cane plantations (TDISP), and 10,000 ha will be used to grow rice (TDIP) (Nippon Koei, 2013e). The location and sizes of the irrigation schemes are illustrated in figure 11. This information has been used to model the irrigation schemes in the delta. It should be noted, however, that the Jatropha areas in figure 11 are not included, because of bankruptcy of Bedford Biofuels Ltd (Barnes, 2013). They are also not included in the National Water Master Plan 2030. Thus, for this study, only the sugar cane and rice schemes are included in the Tana delta over a time span of 2015-2035.
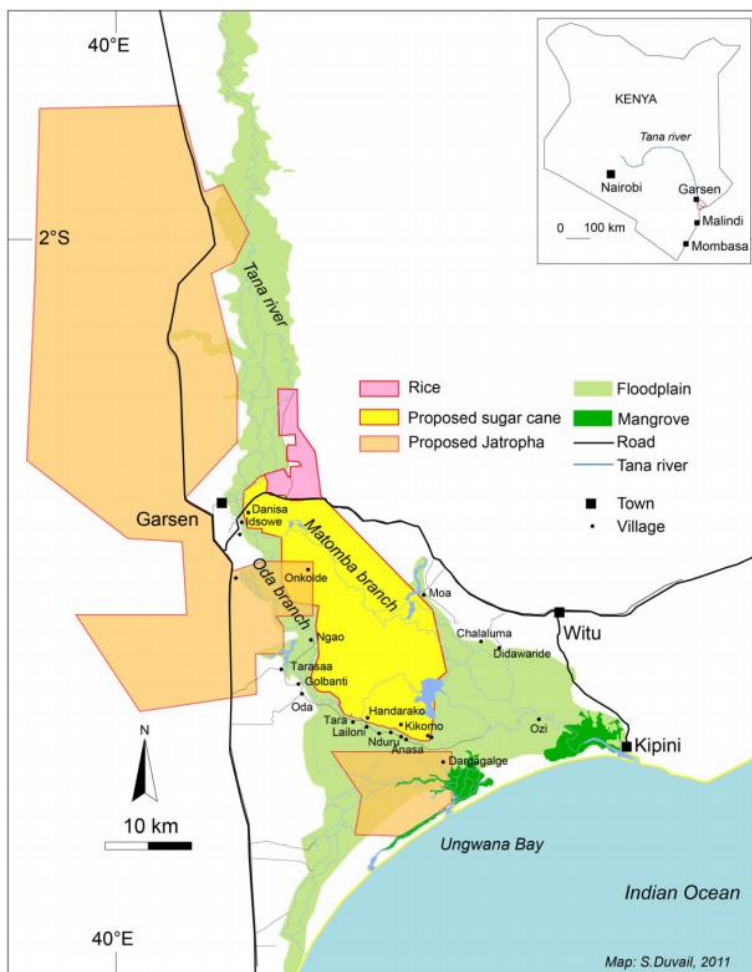
Figure 11: Proposed irrigation schemes in the Tana delta on land that has been acquired or sub-leased by private companies (Duvail et al., 2012, p. 325).

There is only little information available about some proposed irrigation schemes, including schemes that are part of the encompassing HGFIP. Often, there is information available about the expected sizes of schemes, but nothing about their exact location, years of construction or intended crops, which is ideally required in order to include them in the model. This is especially true for irrigation schemes that are planned after 2020. At first, it was proposed to leave out large-scale irrigation schemes for which the required information could not be obtained. However, this would have reduced the veracity of this scenario, since a significant amount of irrigated land would be neglected. Therefore, it has been decided to include them as well (table 5).

These irrigated areas, with no known specifics (e.g. size, location, crop), are implemented in PCR-GLOBWB by expanding the currently irrigated area along the Tana River downstream of the HGFD until the irrigated area has increased with 66,000 ha, of which 44,000 ha for the Nanigi schemes, and 22,000 ha for the Kora-Baricho and Rahole schemes (table 5). The Nanigi transfer schemes are included around the 'Bura-Hola-Masalani-Garsen'-area, while the Kora-Baricho and Rahole transfers are modeled by expanding the irrigated area from roughly the area of Rahole National Reserve, to a point approximately in the middle between of Garissa and Bura. Because the crops that will be grown in these areas are unknown, the existing crop fractions – and corresponding crop factors – of the expanded areas are used. The locations of all included irrigation schemes as included in the model are shown in figure 12.

Modeling the expansion of the irrigated area is done at the cost of rainfed crops and the natural vegetation. When expanding the irrigated areas no preference is given to either rainfed crops, forest or grassland, meaning that the overall ratios between the rainfed crops and natural vegetation types do not change[12].

Specifics of the expected time span were difficult to be found. In fact, only for the Nanigi left bank schemes it is specified that they will be developed from 2019 to 2035, when they will have a total area of 23,600 ha. It is assumed that the development of 30,000 ha (which is used in this study for the Naniga left bank schemes) will take until 2040. However, because the total irrigated area is expected to be roughly 146,000 ha in 2030, it is modeled over the period 2019-2030. In this way, also some schemes that are not explicitly included in this model are represented. The other schemes in table 5 without known specifics are assumed to have the same time-span (2019-2030). The expansion of irrigation schemes over time is modeled with linear yearly increments.

With respect to the specific large-scale irrigation schemes (table 5), often a time span is given to illustrate the stage of the HGFIP in which these are planned to be constructed (stage 1: 2011-2019, stage 2: 2019-2027, and stage 3: 2027-2035) (Republic of Kenya, 2011a). However, this only applies to schemes that are part of the HGFIP. It has been difficult to find specific years for the irrigation schemes in the Tana Delta due to contradicting, or lacking information. Some sources (Republic of Kenya, 2011a) state that the TDIP (as part of the HGFIP) will be constructed from 2015-2035. However, in Nippon Koei (2013e) the irrigation projects in the Tana Delta are explicitly not part of the HGFIP. As information is lacking in this regard, it is assumed that they will be completed over the period 2015-2035.

It is important to note that these are not the only planned large-scale irrigation schemes. Yet, because of lack of, and contradiction between, information in the literature, as well as time constraints no other schemes are explicitly included. Some schemes have been left out, because of cancelled plans. This is the case with plans for Kora (25,000 ha), Masinga (10,000 ha) and Kiambere (10,000 ha) irrigation. These plans were part of the National Water Master Plan 2030 (Nippon Koei, 2013c; 2013e), but have been cancelled due to lack of funding (Nippon Koei, 2013d; Mbui, pers. comm., 2014). The total area of the irrigation schemes that have been included in this scenario corresponds to the target irrigated area in 2030 (table 4).

---

[12] For example: if the rainfed:forest:grassland ratio was 1:23:75 before expansion of irrigated area, this ratio will be the same after expansion.
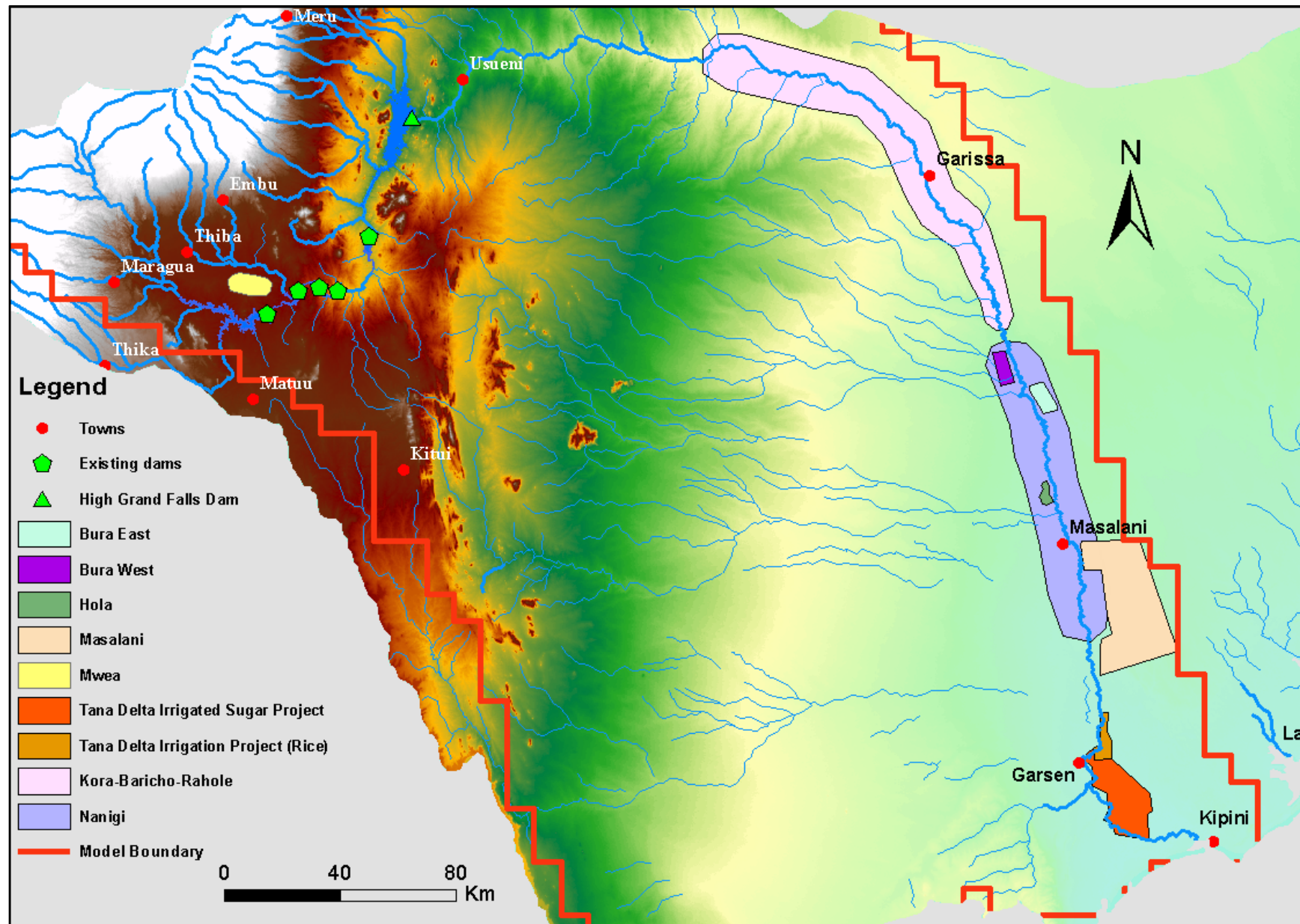
Figure 12: Digital Elevation Map (DEM 90m) showing the locations and sizes of all irrigation schemes and dams as they are included in scenario 2. The used GIS maps were downloaded from WRI (2007).

3.4 Scenario 3

This scenario looks at the urban expansion of the Lamu Port and Kenya's capital city Nairobi. These expansions are expected to have a large impact on the water balance in the Tana basin due to population growth and industrial expansion (UN-Habitat, 2006; JPC & BAC/GKA JV, 2011).

3.4.1 Lamu

Currently, Lamu town has a water demand of approximately 3,000 m^3/day. In the future, with the construction of the Lamu Port as part of the LAPSSET project, this is expected to increase to 181,550 m^3/day in 2030 and 296,750 m^3/day in 2050 (JPC & BAC/GKA JV, 2011). Nippon Koei (2013a) estimates this amount a little lower at 108,750 m^3/day in 2030. In this study, the water demand that is estimated in JPC & BAC/GKA JV (2011) is used, because this information can be used to extrapolate a trend. The water demand for the Lamu Port is included in the model from 2010 onward, as is illustrated in figure 13. The water is required for domestic and industrial purposes (e.g. planned oil refineries (JPC & BAC/GKA JV, 2011), which have a high water demand (Wu et al., 2009)) and is assumed to be supplied by transporting water from the Nanigi Barrage with a conveyance canal. Several other options for the water supply to Lamu are currently being looked into. Yet, because this option seems the most cost-effective (JPC & BAC/GKA JV, 2011; Republic of Kenya, 2011a; Nippon Koei, 2013c) it is included in this study. The Lamu area is situated outside of the modeled area. Nevertheless, its water supply is included in PCR-GLOBWB by increasing the water demand from the grid cell that represents the Nanigi Barrage. In order to model the expected increase in water withdrawal for Lamu, the expected water demand is imposed on a single grid cell (grid cell with pink square in figure 14). This is done by subtracting the water demand from the channel storage, i.e. the amount of water in the channel. As explained in chapter 2.2.5, the water is extracted from surface water within a superimposed segment of 1°, where preference is given to the grid cell containing the most water.

The expected water demand for Lamu is modeled by polynomial extrapolation between the three known amounts in 2010, 2030 and 2050, respectively (figure 13). This form of extrapolation is used, because it represents a more realistic trend than, e.g., linear or logarithmic extrapolation.
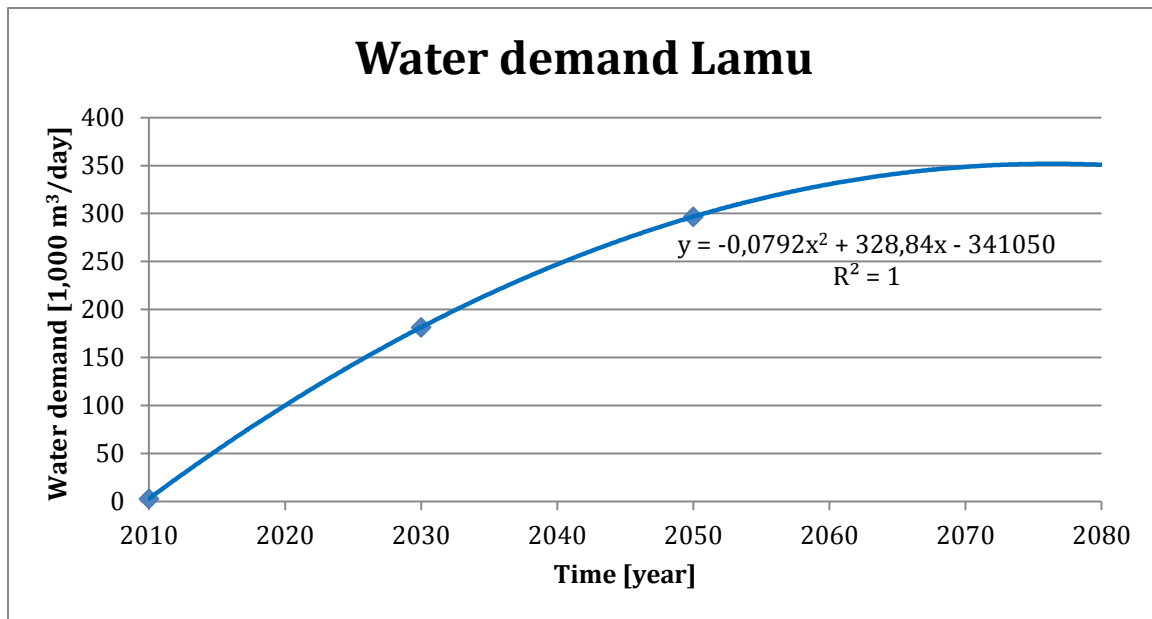
Figure 13: Expected future water demand in Lamu. The marked data points represent the information on which the rest of the graph is based (JPC & BAC/GKA JV, 2011).

3.4.2 Nairobi

Nairobi is situated in the neighboring Athi basin, but to be able to keep up with its water demand, part of it is supplied from the Sasumua and the Thika dams in the upper Tana basin (Nippon Koei, 2013c). However, population growth will increase Nairobi's water demand. Annual growth rates for Nairobi are projected to be 3.5% for 2015-2020 and 3.0% for 2020-2035. The expected water demand is assumed to increase on average with a factor of roughly 1.23 every five years (AWSB, 2011). For this reason, five additional dams are proposed in the upper Tana basin: Ndiara, Maragua, Maragua 8, Karimenu 2, and Chania-B (Nippon Koei, 2013c) (figure 14). It is not specified what proportions of Nairobi's water demand will be extracted from, respectively, the Tana and Athi basins. Therefore, Nippon Koei (2013a) is used to determine the expected water transfer. Currently, roughly 181 MCM/year, or 495,890 m^3/day is transported to Nairobi (as is included in the status quo). In the future, the inter-basin water transfer from the Tana basin to Nairobi is estimated to have an additional capacity of approximately 168 MCM/year or, 460,275 m^3/day (Nippon Koei, 2013a). There is no mention about the time span or in what year this will be realized. In this study it is assumed that in 2030 (corresponding to the Vision 2030) there is an increase of water transport to Nairobi of 460,275 m^3/day. The result is a constant water extraction from 2030 onwards of 956,165 m^3/day. These figures describe the maximum capacity of the system, but it does not necessarily mean that this capacity is actually used all year. Nevertheless, it is used for calculation purposes. It is furthermore assumed that any other additional future water demand of Nairobi will not be met from the Tana basin.

In order to model the expected increase in water withdrawal for Nairobi, the expected water demand is satisfied similar to the water demand for Lamu. In this case the grid cell with the purple square in figure 14 is assumed to represent the location of water diversion. As can be observed in figure 14, the Ndiara, Karimenu 2 and Chania-B dams are situated outside of the modeled area.
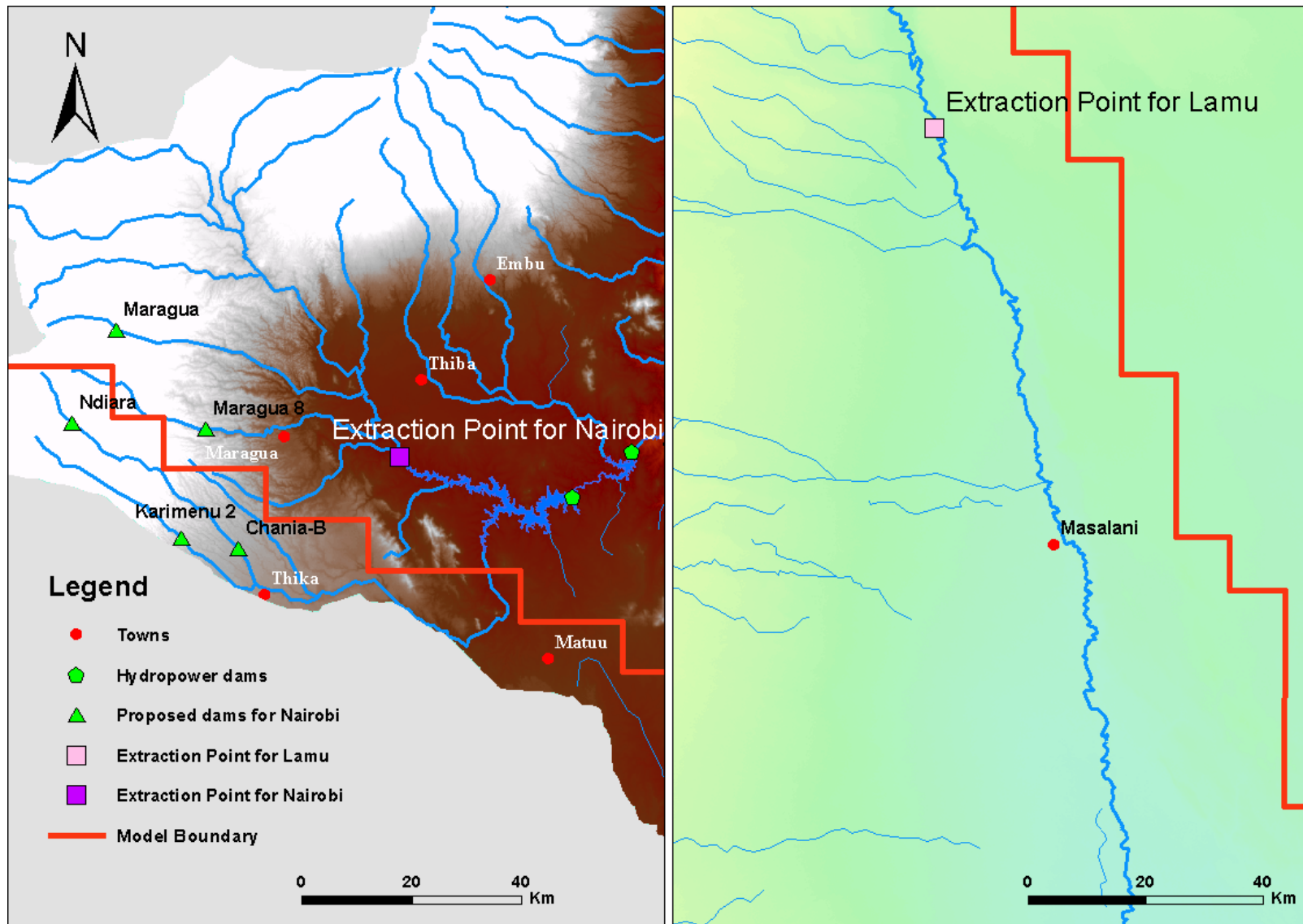
Figure 14: Digital Elevation Map (DEM 90m) showing the locations of the future dams (green triangles) that will supply water to Nairobi (after Nippon Koei, 2013c). The existing dams to supply water to Nairobi are not shown here, because they are not included in the model. The purple square (left) indicates in which grid cell in the model the water for Nairobi is extracted. The pink square (right) illustrates the location of the planned Nanigi Barrage, where the water will be extracted for the Lamu Port. The red line indicates the boundary of the area as it is included in PCR-GLOBWB. The used GIS maps were downloaded from WRI (2007).

3.5 Scenario 4

This scenario includes all proposed interventions that are included in the other scenarios. As such, the HGFD, the proposed large-scale irrigation schemes, as well as the water demand for Nairobi and the Lamu Port are all combined. The interventions are modeled as described in the previous chapters. All interventions in this scenario are incorporated in the National Water Master Plan 2030 (Nippon Koei, 2013a-2013e).

4. Results

4.1 Model validation

The model performance significantly improved after calibration, mainly by largely reducing the peaks but also by increasing the low flows. The model results before calibration are shown in appendix 6. Comparing table 7 with appendix 6a and figure 15 with appendix 6b illustrates the improvements of the hydrographs due to calibration. The regression plots after calibration for each location are shown in figure 16. However, while the calibration improved the model performance it did not lead to good validation results (see table 7). Performance is better in the upstream region, with Garissa having the only positive LNSE (0.15). This means that in the other locations the mean of observed discharges is a better predictor than the model (Moriasi et al., 2007). While calibration improved the LNSE, the R^2 remained roughly unchanged. The fact that R^2 is relatively high means the seasonal timing is fairly represented. Additionally, the RMSE has been significantly improved, yet remaining quite large. It is lowest at Grand Falls, and highest at Garsen. The increase of the RMSE between Hola and Garsen is due to a fairly unchanged modeled discharge, while in reality the discharge is strongly reduced. It can be observed in figure 15 and figure 16 that the discharge in low flow conditions is often underestimated, most of all at Grand Falls. In the downstream region the peak flow is largely overestimated, most significant at Garsen.

The validation results are least good at Garsen. However, since Garsen is the focus of this study, the normalized correction method is applied here. The results of this correction are shown in table 7, figure 17 and figure 18. From table 7 it can be seen that the biggest improvement is in the RMSE. The LNSE has improved but remains (slightly) negative, while the R^2 is slightly reduced. Since in this study, the changes in the FDCs are assessed, the timing of the peaks is less relevant. Therefore, the change in RMSE is more important than the change in LNSE and R^2. Figure 17 illustrates the reduction in peak flows resulting from the correction method.

From figure 18 it can be observed that this correction method significantly improves the FDCs for all seasons. The biggest gain is found in the extremes, i.e. very high and very low exceedence probabilities. Especially in the rainy season the improvement is significant, due to the fact that PCR-GLOBWB has problems with the reduction of the peak flow. Before the normalized correction method, the average Q10 in the rainy season was overestimated with approximately 300 m^3/s. After the correction, the average Q10 is roughly equal to the observed Q10. As such, the model bias for the peak flows has been removed. Since in this study, the changes in Q10 and Q90 are assessed, this correction significantly improves the results.

Table 7: Final model validation results after calibration (upper). For Garsen, the validation results after the correction are also shown (lower).

	LNSE	R^2	RMSE [m^3/s]
Grand Falls	-0.25	0.46	83.01
Garissa	0.15	0.58	92.00
Hola	-0.38	0.49	89.92
Garsen	-2.96	0.45	123.85
After correction			
Garsen	-0.10	0.41	34.14
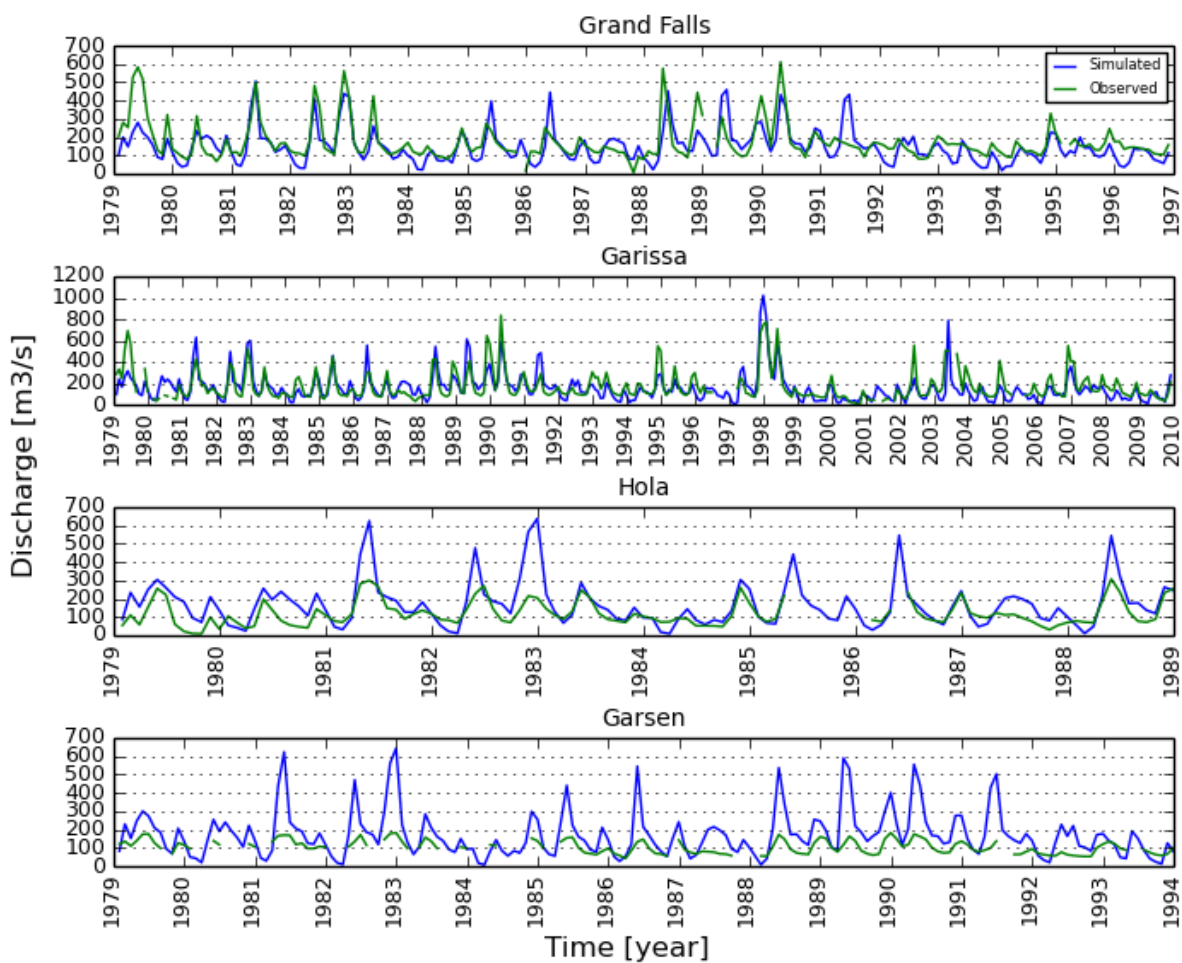
Figure 15: Hydrographs of the simulated and observed mean monthly discharges for each location after calibration. Note the differences in x-axes for each location, which depends on the number of available observations.
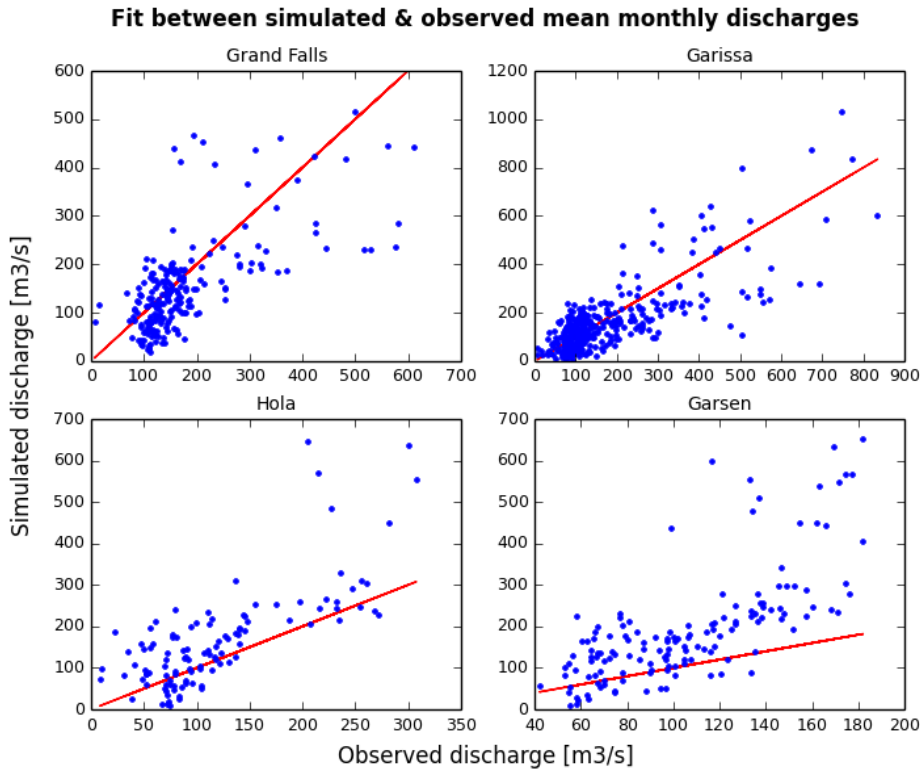
Figure 16: Fit between the simulated and observed mean monthly discharges for each location after calibration. The red line represents the 1:1 slope between the smallest and largest observed discharges.
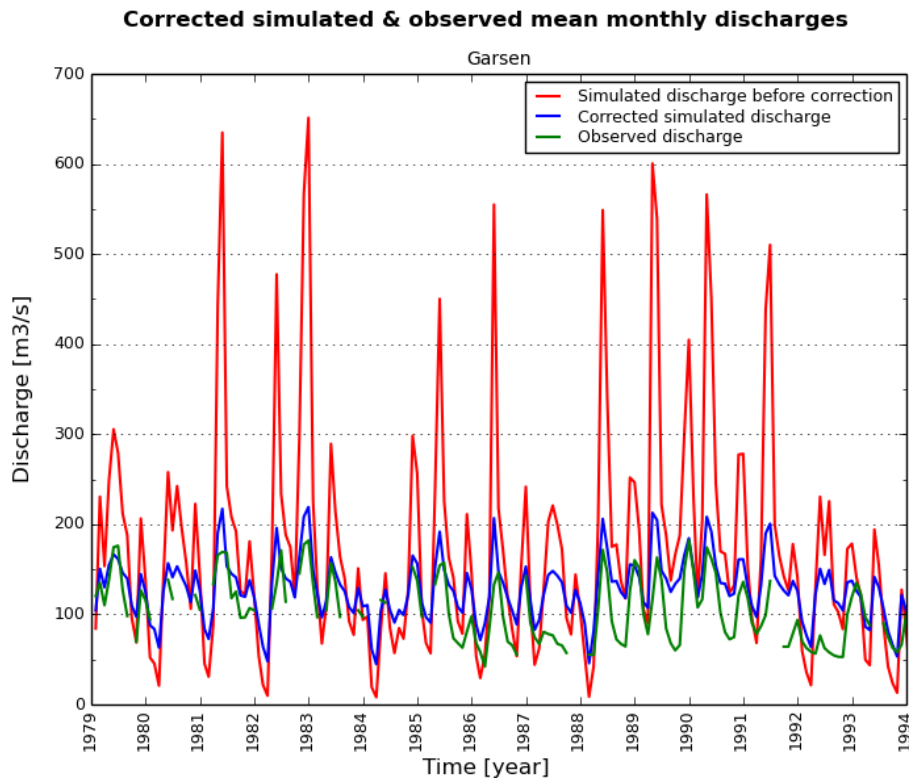
Figure 17: Hydrograph showing the effect of the applied normalized correction at Garsen.
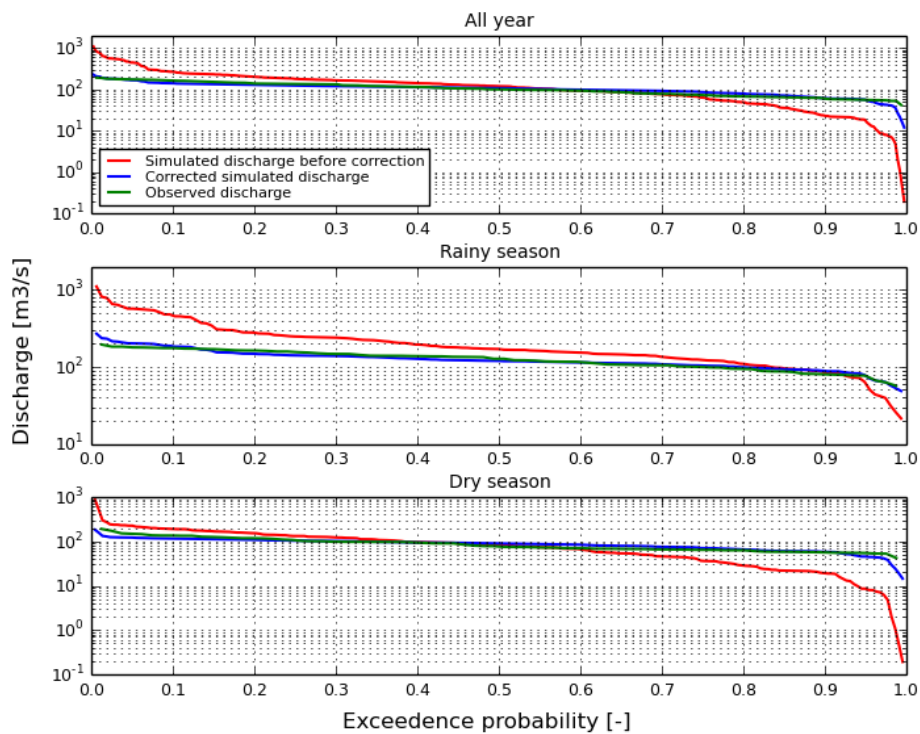
Figure 18: FDCs showing the effect of the applied normalized correction at Garsen. Note that the y-axes are given on a log-scale and the ranges differ per season to better illustrate the effect.

4.2 Status quo

For all scenarios, first the effect on the all-year FDC is assessed, followed by the rainy and dry season, respectively. As explained in chapter 3.1, the status quo represents an unchanging land use and water demand, with the only changing factor being the climate. The status quo forms a baseline with which the other scenarios are compared. For comparison table 8 shows the Q10 and Q90 values of the observations. These are used to compare the results of the status quo with.

Table 8: The Q10 and Q90 for the observations at Garsen over the period 1979-1998 per season. The discharges are in m^3/s.

	Q10	Q90
1979-1998		
- All year	163.48	60.09
- Rainy season	174.52	79.73
- Dry season	135.04	57.03

From figure 19 and appendix 7a it can be observed that the mean modeled discharge for the all-year FDC crosses the FDC of the observed discharges three times for the near and mid future. Discharges with a very low exceedence probability (roughly less than 3%) increase compared to the observations, while discharges with an exceedence probability between roughly 3% and 35% decrease. Discharges with exceedence probabilities between roughly 40% and 97% are above the observations, and only the low flows with an exceedence probability above roughly 97% are lower than the observations. For the far future, the shape of the FDC remains similar. However, the observed discharges are exceeded for all percentiles, except discharges with an exceedence probability above roughly 98%.

For the rainy season there is a distinct difference between mean modeled discharge and the observed discharges. Here, the observed discharges are below (near future) or correspond with (mid and far future) the minimum GCM discharges. This can be attributed to the very large peaks that can also be observed in figure 8 (in chapter 2.3). Hence the results show that the uncertainty between the GCMs is largest for the rainy season[13], but the effect of climate change on the mean discharge is also most pronounced in the rainy season. This is illustrated in table 9 as well, which shows that climate change will lead to increasing discharges in the rainy season. Especially the discharges with a very long return period (Q5 and higher) are projected to strongly increase in the rainy season. This can also be observed in the all-year FDC (figure 19). In the dry season a decrease in the minimum and mean Q10 and Q90 is expected. Only in the far future there is an increase in mean Q90 (3.77%) (table 9). In the near future there is a clear difference for discharges that are exceeded half of the time, which are below the observations. In the far future this effect is much less clear, with the FDCs being roughly equal, besides the peak flows). Overall, climate change leads to increasing discharges with time.
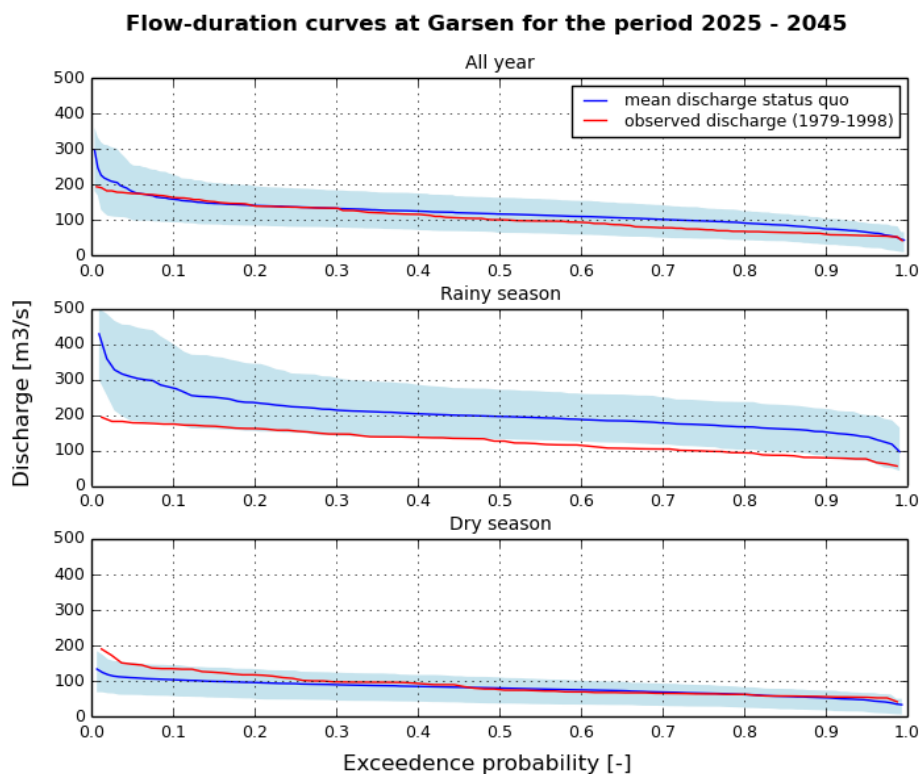
Figure 19: The flow duration curves of the status quo at Garsen for the entire year and both seasons for the period 2025-2045. The mean discharge is calculated from all GCMs (blue line), and the spread shows the variability between predictions of the GCMs (light blue). The observed discharge (for the period 1979-1998) is shown for comparison (red line).

---

[13] The rainy season having the largest range between minimum and maximum discharges is the case in all scenarios.

Table 9: An overview of the changes [%] of the status quo in minimum, mean and maximum Q10 and Q90 of all GCMs combined with respect to the observed discharges per season for the three assessed periods. Note that the changes in minimum, mean and maximum Q10 and Q90 are assessed with respect to the actual Q10 and Q90 from the observations (table 8).

	Min Q10	Mean Q10	Max Q10	Min Q90	Mean Q90	Max Q90
2010-2030 [%]						
- All year	-29.41	-12.96	+1.87	-9.99	+21.71	+48.17
- Rainy season	+5.30	+28.36	+53.74	+17.00	+64.77	+112.40
- Dry season	-40.65	-26.96	-14.00	-33.18	-8.93	+19.35
2025-2045 [%]						
- All year	-42.94	-3.01	+39.27	-48.63	+24.80	+72.02
- Rainy season	+0.87	+58.26	+129.31	+4.29	+90.86	+172.59
- Dry season	-57.21	-22.84	+7.41	-69.05	-6.82	+28.82
2045-2065 [%]						
- All year	-26.23	+14.18	+91.63	-16.79	+42.70	+120.86
- Rainy season	+8.61	+74.12	+198.39	+11.42	+99.39	+213.79
- Dry season	-37.23	-12.10	+38.28	-37.52	+3.77	+54.00

4.3 Scenario 1

Scenario 1 assesses the impact of the HGFD on the discharge in the Tana delta. Besides inclusion of the HGFD, everything is the same as for the status quo. From figure 20 (and appendix 7b) it appears that the construction of the HGFD results in increasing discharges. Similar to the status quo, the spread between the minimum and maximum discharges is largest in the rainy season and increases with time. The mean Q10 in the rainy season seems to increase in the near future respective to the status quo, but decrease in the mid and far future (table 10). With respect to the low flows, the mean Q90 in the rainy season appears to increase with roughly 9%. In the dry season the mean Q10 seems to increase with roughly 23 to 31% (depending on the period), while the mean Q90 in the dry season shows a larger increase, i.e. roughly 53 to 33%. The effect of the HGFD is most pronounced in the dry season, particularly for the minimum Q10 and Q90 the period 2025-2045. This apparent increase in discharge is, however, a result of the applied correction (see discussion: chapter 5.2.2). Therefore, the results have to be interpreted with care.

Flow-duration curves at Garsen for the period 2025 - 2045
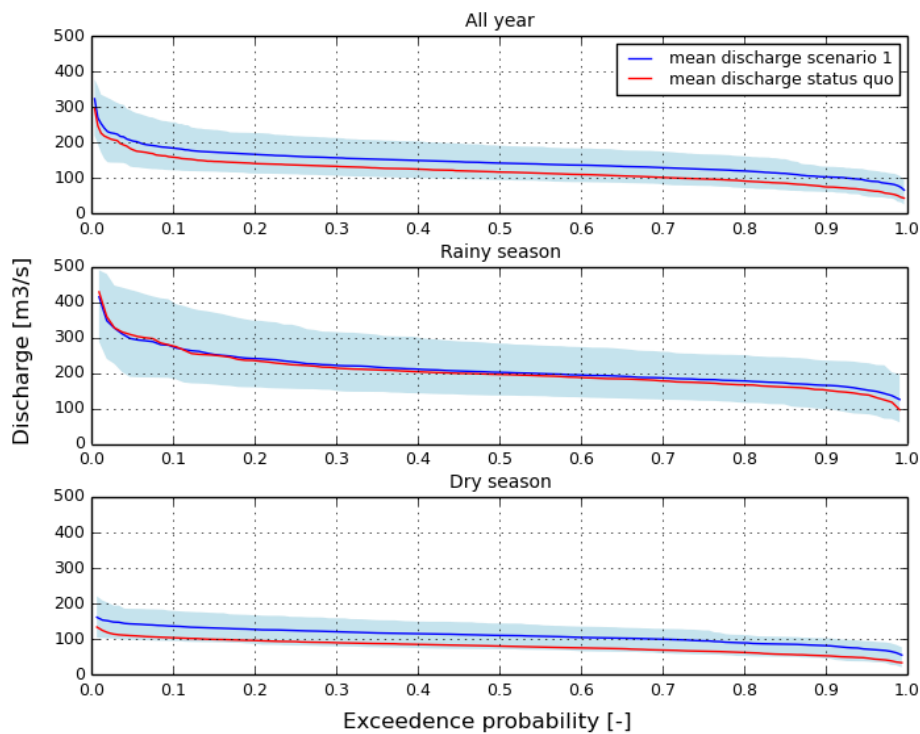
Figure 20: The flow duration curves for scenario 1 at Garsen for the entire year and both seasons for the period 2025-2045. The mean discharge is calculated from all GCMs (blue line), and the spread shows the variability between predictions of the GCMs (light blue). The mean discharge from the status quo is included for comparison (red line).

Table 10: An overview of the changes [%] in scenario 1 in minimum, mean and maximum Q10 and Q90 of all GCMs combined with respect to the status quo per season for the three assessed periods.

	Min Q10	Mean Q10	Max Q10	Min Q90	Mean Q90	Max Q90
2010-2030 [%]						
- All year	+14.48	+15.53	+15.20	+56.61	+34.64	+26.56
- Rainy season	-2.43	+3.51	+1.42	+22.87	+9.34	+5.60
- Dry season	+25.23	+25.67	+21.92	+79.58	+53.24	+36.19
2025-2045 [%]						
- All year	+30.58	+16.14	+12.78	+97.44	+37.63	+27.70
- Rainy season	+4.50	-0.87	-0.26	+18.45	+8.66	+8.16
- Dry season	+64.47	+31.08	+23.86	+156.93	+53.74	+39.47
2045-2065 [%]						
- All year	+18.13	+8.85	+4.26	+55.29	+24.56	+19.64
- Rainy season	+1.90	-1.39	-1.83	+26.55	+8.62	+8.35
- Dry season	+28.85	+22.53	+17.42	+68.44	+33.64	+27.80

4.4 Scenario 2

This scenario expands on scenario 1 by including the proposed large-scale irrigation schemes. The difference with the status quo is the inclusion of the HGFD with the planned irrigation schemes. Similar to scenario 1, the applied correction distorts the effect of the HGFD (see discussion: chapter 5.2.2). Therefore, also for this scenario, the results have to be interpreted with care. From figure 21 it can be seen that the all-year FDC shows a decrease in peak flow and an increase in low flows compared to the status quo[14]. This is also visible in the near future, but becomes clearer with time (appendix 7c). The reason why the effect is less visible in the near future is because the dam is not included until 2018 and the irrigation schemes are not completely finished before 2035.

The discharge in the rainy season shows the largest decrease (for all percentiles) (figure 21). The relative decrease is approximately the same for the mean Q10 and Q90, i.e. roughly 13 to 35% (depending on the period) and 13 to 32%, respectively. The mean Q10 and Q90 increase with roughly 10 to 21% and 30 to 36% in the dry season, respectively. The largest change is found for the minimum Q90 in the dry season (table 11).
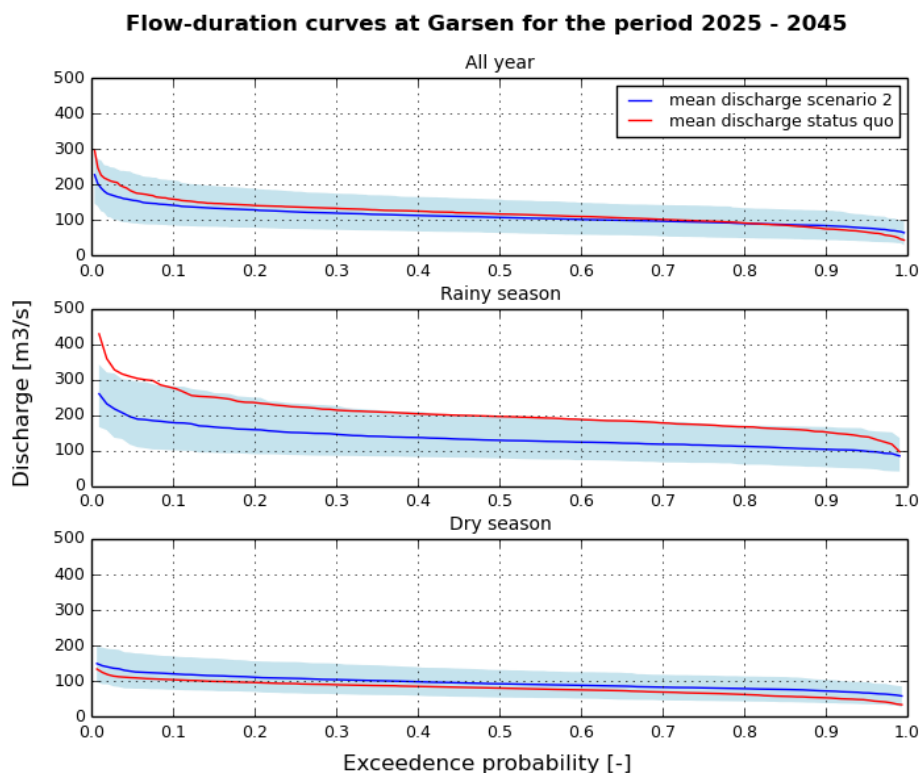
Figure 21: The flow duration curves for scenario 2 at Garsen for the entire year and both seasons for the period 2025-2045. The mean discharge is calculated from all GCMs (blue line), and the spread shows the variability between predictions of the GCMs (light blue). The mean discharge from the status quo is included for comparison (red line).

---

[14] This is the effect one would expect to see also in scenario 1, as a result of the HGFD (Dingman, 2008).

Table 11: An overview of the changes [%] in scenario 2 in minimum, mean and maximum Q10 and Q90 of all GCMs combined with respect to the status quo per season for the three assessed periods.

	Min Q10	Mean Q10	Max Q10	Min Q90	Mean Q90	Max Q90
2010-2030 [%]						
- All year	-5.14	-1.44	-0.18	+23.29	+11.92	+9.02
- Rainy season	-20.89	-13.13	-14.92	-3.95	-13.43	-13.68
- Dry season	+4.72	+10.18	+9.51	+45.83	+30.00	+17.21
2025-2045 [%]						
- All year	-9.18	-10.87	-7.00	+42.15	+12.31	+22.35
- Rainy season	-42.64	-35.25	-29.83	-36.14	-31.94	-23.47
- Dry season	+31.14	+15.53	+17.00	+116.66	+36.49	+40.76
2045-2065 [%]						
- All year	-16.99	-9.55	-4.04	+14.42	+8.65	+21.20
- Rainy season	-39.77	-30.44	-22.83	-21.35	-25.34	-15.65
- Dry season	+5.79	+20.56	+30.29	+42.53	+33.64	+50.02

Comparing the discharges of scenario 2 with scenario 1 illustrates the effect of solely the irrigation water demand (table 12). The minimum, mean and maximum Q10 and Q90 show an overall decrease. However, the maximum Q90 in the mid future dry season and the maximum Q10 and Q90 in the far future dry season show an increase in discharge during the dry season. This can be attributed to the return flows of the applied irrigation water, this being the only factor that can increase the discharge in the dry season.

Table 12: An overview of the changes [%] in scenario 2 in minimum, mean and maximum Q10 and Q90 of all GCMs combined with respect to scenario 1 per season for the three assessed periods. This shows the effects of solely the irrigation schemes on the discharge (without the HGFD).

	Min Q10	Mean Q10	Max Q10	Min Q90	Mean Q90	Max Q90
2010-2030 [%]						
- All year	-17.14	-14.69	-13.35	-21.28	-16.87	-13.86
- Rainy season	-18.92	-16.08	-16.11	-21.83	-20.83	-18.26
- Dry season	-16.38	-12.33	-10.18	-18.79	-15.17	-13.94
2025-2045 [%]						
- All year	-30.45	-23.26	-17.54	-28.00	-18.40	-4.19
- Rainy season	-45.11	-34.68	-29.65	-46.09	-37.36	-29.25
- Dry season	-20.26	-11.87	-5.53	-15.67	-11.22	+0.93
2045-2065 [%]						
- All year	-29.73	-16.91	-7.96	-26.31	-12.77	+1.30
- Rainy season	-40.89	-29.47	-21.39	-37.85	-31.26	-22.15
- Dry season	-17.90	-1.61	+10.95	-15.38	+0.00	+17.38

4.5 Scenario 3

Scenario 3 expands on the status quo by including the future water demands for Nairobi and the Lamu Port. As is shown in figure 22 and table 13 (and appendix 7d), there is an overall decrease in mean discharges compared to the status quo for the all-year FDC and for both seasons. The relative decrease becomes larger in the future (because the water demand also increases with time). From table 13 it can be observed that the biggest relative decrease in Q10 and Q90 is in the dry season. In the near future, the only factor affecting the discharge is the water demand for the Lamu Port, which is fairly limited in this period. This scenario is the only one that shows solely negative effects on the

discharge. Because the water demand is modeled as being constant over a year, the shapes of the FDCs are unchanged, but lowered.
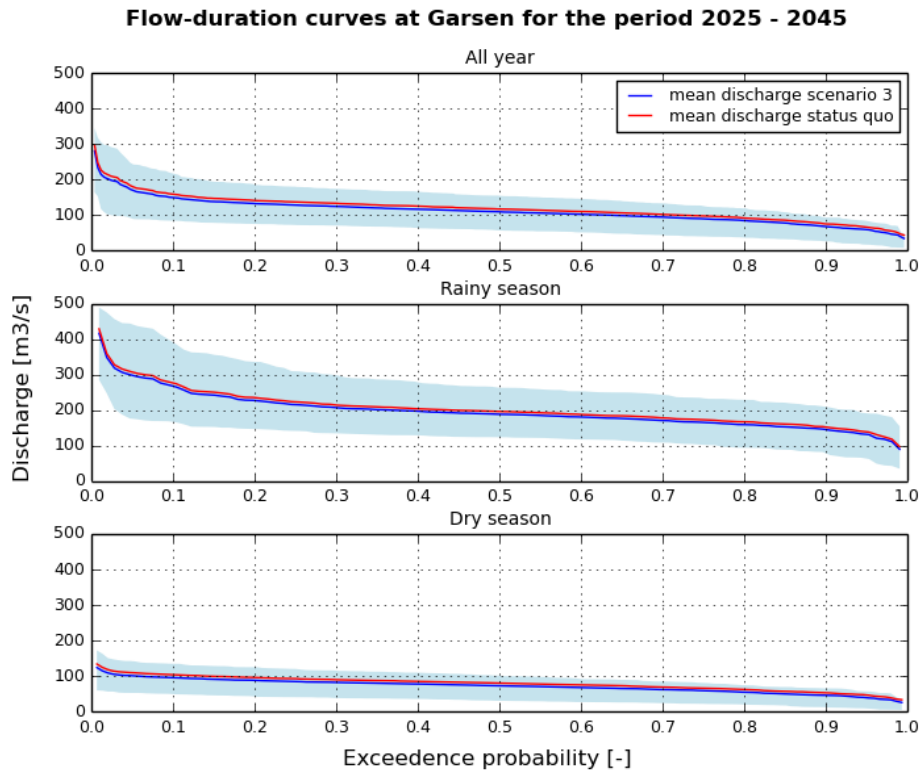
Figure 22: The flow duration curves for scenario 3 at Garsen for the entire year and both seasons for the period 2025-2045. The mean discharge is calculated from all GCMs (blue line), and the spread shows the variability between predictions of the GCMs (light blue). The mean discharge from the status quo is included for comparison (red line).

Table 13: An overview of the changes [%] in scenario 3 in minimum, mean and maximum Q10 and Q90 of all GCMs combined with respect to the status quo per season for the three assessed periods.

	Min Q10	Mean Q10	Max Q10	Min Q90	Mean Q90	Max Q90
2010-2030 [%]						
- All year	-1.58	-1.43	-1.24	-2.68	-2.44	-1.44
- Rainy season	-0.88	-0.78	-0.57	-0.68	-0.93	-0.86
- Dry season	-2.34	-1.81	-1.30	-3.41	-3.09	-1.54
2025-2045 [%]						
- All year	-9.80	-5.90	-4.77	-15.72	-10.06	-10.03
- Rainy season	-5.33	-3.20	-2.33	-5.66	-4.62	-3.80
- Dry season	-14.35	-8.19	-6.93	-28.45	-13.01	-10.75
2045-2065 [%]						
- All year	-11.85	-7.65	-5.39	-20.98	-13.42	-10.03
- Rainy season	-7.18	-4.13	-2.63	-13.17	-6.95	-4.60
- Dry season	-15.11	-10.62	-7.71	-30.04	-18.48	-14.45

4.6 Scenario 4

Scenario 4 is a combination of all other scenarios. As such, it includes the HGFD, the proposed irrigation schemes and the future water demand for Nairobi and the Lamu Port. Also in this scenario the effect of the HGFD is distorted by the applied correction, so the results have to be interpreted with care. From figure 23 and appendix 7e it can be seen that in the near future the effect on the all-year FDC is limited, except for the very high and very low flows which decrease and increase, respectively, compared to the status quo. For the mid and far future, the difference is more clear, with a decrease in peak flows and a small increase in low flows. The biggest effect is seen in the rainy season, which can be attributed to the effect of the irrigation schemes. The mean status quo discharge roughly equals the maximum discharge in the rainy season in the near and mid future, with the exception of the very high and very low flows. In the far future, the range between minimum and maximum discharge increases. In this period the mean status quo discharge in the rainy season is roughly in between the mean and maximum discharge (appendix 7e-1). There is a positive effect on the discharge in the dry season, except for the minimum Q10 in the far future (table 14).
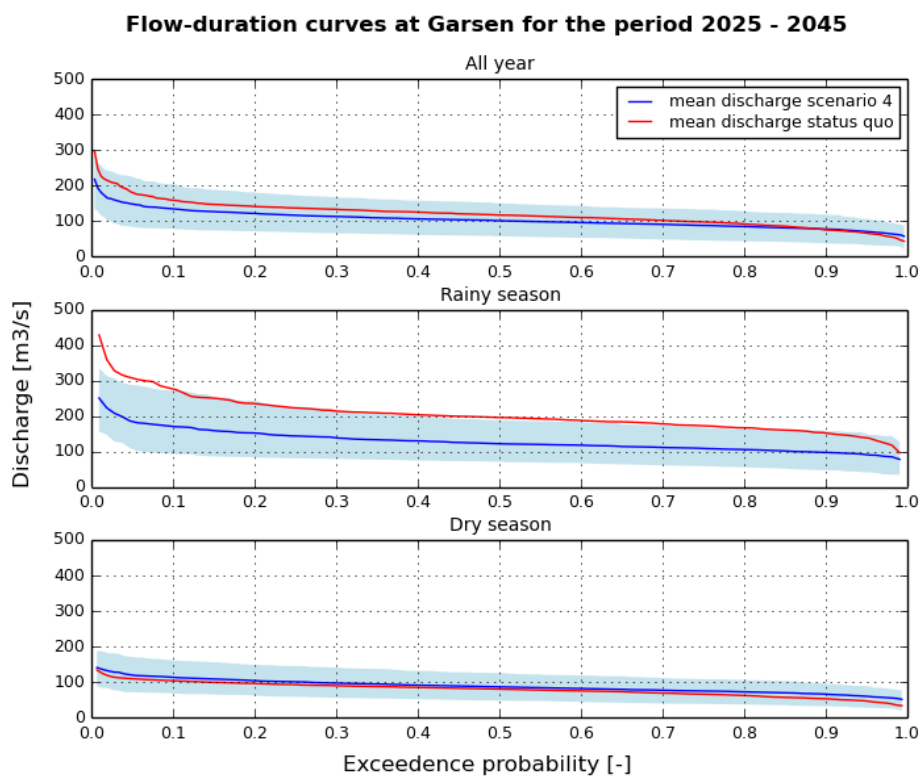
Figure 23: The flow duration curves for scenario 4 at Garsen for the entire year and both seasons for the period 2025-2045. The mean discharge is calculated from all GCMs (blue line), and the spread shows the variability between predictions of the GCMs (light blue). The mean discharge from the status quo is included for comparison (red line).

Table 14: An overview of the changes [%] in scenario 4 in minimum, mean and maximum Q10 and Q90 of all GCMs combined with respect to the status quo per season for the three assessed periods.

	Min Q10	Mean Q10	Max Q10	Min Q90	Mean Q90	Max Q90
2010-2030 [%]						
- All year	-6.44	-2.60	-1.07	+20.34	+10.07	+7.64
- Rainy season	-21.80	-13.84	-15.41	-5.61	-14.59	-14.49
- Dry season	+3.07	+8.86	+8.20	+42.87	+27.63	+15.52
2025-2045 [%]						
- All year	-16.50	-15.16	-10.61	+20.73	+3.38	+14.38
- Rainy season	-47.28	-38.17	-32.01	-42.61	-35.89	-27.18
- Dry season	+18.17	+8.80	+11.33	+82.65	+24.94	+30.88
2045-2065 [%]						
- All year	-26.30	-15.65	-8.11	+0.23	-2.85	+11.88
- Rainy season	-45.21	-34.22	-25.22	-30.20	-31.46	-19.88
- Dry season	-7.34	+11.68	+23.88	+19.91	+16.42	+35.77

5. Discussion

5.1 Model performance

It was found that for this study, PCR-GLOBWB was not able to correctly reproduce the discharges, mainly in the downstream areas (Hola and Garsen). Where in reality, the Tana River loses water through evaporation in the lower basin, in the model this did not happen. This overestimation of discharges by PCR-GLOBWB in African rivers is also reported in other studies (van Beek et al., 2011; Wada, 2013). Van Beek et al. (2011) attributed this weak model performance to the meteorological forcing, resulting from sparse observations in Africa (Conway et al., 2009; Dee et al., 2011). Besides the sparse meteorological observations, also the number of discharge observations is limited, i.e. only four observation points, with gaps in the record varying from months to years. This reduced the effectiveness of calibrating the model using the EnKF (see chapter 2.4).

While the calibration improved the model performance, it impaired the physical basis of the model. This can be seen in the way PCR-GLOBWB calculates baseflow and groundwater recharge. The used high K_{sat} values may lead to a poor reproduction of the actual soil moisture, but improve the discharge reproduction (Sutanudjaja et al., 2014). These high K_{sat} values are unrealistic in (semi-)arid regions like the Tana basin. However, the use of high K_{sat} values can be supported by the lack of preferential flow in the PCR-GLOBWB model structure (Sutanudjaja, pers comm., 2014). Preferential flow can have large impacts on groundwater recharge (Scanlon et al., 2006). Especially in dryer periods the clay-rich soils in the Tana River floodplains can develop deep cracks and hold much water (Andrews et al., 1975). As such, these high K_{sat} values can be seen as proxies for preferential flow. However, while the model results were improved after calibration, PCR-GLOBWB was not able to correctly reduce the range between peak flow and low flows. This range strongly decreases downstream of Garissa in the observations, but only slightly in the modeled discharges.

Furthermore, the observed discharges at Garsen seem very low compared to the upstream regions which might lead to doubts about the quality of the observations. However, this low discharge is also found by other studies (Maingi & Marsh, 2002; Knoop et al., 2012; Leauthaud et al., 2013b). Leauthaud et al. (2013b) used data from the same gauging station at Garsen, but from a longer period, 1951-1998. With their model (TIM) they were better able to simulate the discharges for several reasons. First, this model was designed specifically for the lower Tana River. Secondly, they used observed daily precipitation and temperature data from the TDIP and monthly precipitation data for Garissa. Lastly, TIM actively simulates the inundation of the floodplains, while this is not included in this version of PCR-GLOBWB (Sutanudjaja, pers. comm. 2014). Inundation of the floodplains will lead to more evaporation, and thus help in attenuating the peaks. The importance of the floodplains for peak attenuation is also stated in Hamerlynck et al. (2010). Besides improving the simulation of the evaporation through inundation of the floodplains, it will also provide soil- and groundwater recharge, thereby adding to the baseflow.

Additionally, besides using unrealistic values for certain parameters, it might seem strange to calibrate the precipitation (*P*), since it is used as input for the model (and based on observations: CRU data). However, since this version of PCR-GLOBWB did not include a floodplain inundation-module, the attenuation of peaks was partly achieved by reducing the precipitation.

This study was done with a spatial resolution of 0.08333°. For a relatively small catchment, such as the Tana basin, the study results might be improved with a finer resolution (Bormann, 2006). In a similar study by Trambauer et al. (2014) PCR-GLOBWB was used with a resolution of 0.05° for the Limpopo river basin in southern Africa. While incorporation of active floodplain inundation is expected to be more important to produce better model results, downscaling of PCR-GLOBWB could also help to improve the results.

At the TDIP, the recorded overall mean temperature for the period 1998-2009 was 28°C, which suggests high evaporation rates of the flooded areas (Leauthaud et al., 2013b). All of the used GCMs report mean annual temperatures at Garsen between 28-30°C over the period 2006-2065 (with the mean annual temperature increasing over time). This suggests the temperature forcing is quite accurate.

The focus of this study is on the Tana delta, with Garsen serving as proxy for the delta. Therefore the FDCs for Garsen are corrected with the used scaling factors for the mean and standard deviation. However, the fact that this correction is necessary means that PCR-GLOBWB was not capable of accurately modeling the discharges (mostly downstream). The result of this correction method is that, no matter the discharge (either very large or very small), the systematic under- or overestimation is removed. Because of this model bias and applied correction method absolute values found in this study are less useful. However, since the relative changes between the scenarios and the status quo are assessed, the results still provide insight into the expected direction of effects of the scenarios on the discharge. However, the results have to be interpreted with care.

It is assumed that the used scaling factors can be applied to all GCMs. The scaling factors are, however, calculated from the observations and the discharges resulting from the CRU/ERA-Interim forcing. As such, the normalized correction factors are not one-on-one compatible with the GCMs. This can be observed in the FDCs for the rainy season in the status quo scenario where even the minimum discharge is higher than the observations (even in the near future). Ideally the correction factors should be calculated for each GCM separately (using historical GCM runs). However, this is not done in this study because of time limitations.

5.2 Scenario assumptions and uncertainties

First, the overall assumptions and uncertainties are described, followed by the individual scenarios. Scenario 4 is not included in this discussion, because it is a combination of scenarios 1,2 and 3. Therefore, all assumption and uncertainties for scenarios 1,2 and 3 apply to scenario 4 as well.

5.2.1 Overall assumptions and uncertainties

Part of the used data and information is not directly derived from scientific research. This is mainly the case for designing the scenarios, for which policy documents where used. Where possible, scientific literature is used to underpin the decisions made in this study. With respect to future plans, the National Water Master Plan 2030 is predominantly used (Nippon Koei, 2013a-2013e). Compared to other policy documents, this is the most comprehensive document.

In this study the effects of the interventions are assessed for the entire year as well as the dry and rainy season separately. The rainy season is defined as the months April to June and November to December, with the dry season being the other months. However, in reality the start and end of the rainy seasons can vary, but this inter-annual variability is not included in this study. This can result in

overestimation of the peak flows in the dry season, and underestimation of the low flows in the rainy season. But since the FDCs are created for a twenty year period, this is expected to have only a minor effect.

A small part of the Tana basin is not included in this study, i.e. the Chania and Thika rivers (see figure 14). This is, however, only a minor problem since the water demand is satisfied from within a superimposed 1° segment (see chapter 2.2.5). Additionally, the discharge at Garsen is strongly overestimated by PCR-GLOBWB (without the normalized correction method). Even with inclusion of the Chania and Thika rivers, the applied correction method would have reduced the effect. Therefore, the exclusion of these rivers did not seriously affect the outcome of this study.

To model the effects of climate change in this study only one RCP (RCP6.0) and four GCMs are included. Besides RCP6.0 three other RCPs are defined in the fifth IPCC report: RCP2.6, RCP4.5 and RCP 8.5 (IPCC, 2013). Because only one RCP is included in this study, uncertainty about the future climate is underestimated. The same can be said about the used GCMs. As can be observed from figure 8, the discharge greatly differs per used GCM. Additionally, there are no confidence intervals given for the GCM variability, which also reduces the interpretability of the results. However, the results that are presented can still be used to observe a trend for the future. Time limitations governed the choice for just one RCP and four CGMs.

For this study it is assumed that only surface water is used to satisfy the water demand. In reality, part of the water demand is satisfied by allocating groundwater. However, the majority of irrigation demand will be supplied by surface water, while groundwater is only used for small-scale irrigation, which is not explicitly included in this study. Domestic water demand is satisfied with groundwater only when there is not sufficient surface water available. To satisfy industrial water demand, groundwater and surface water are equally used (Nippon Koei, 2013c). This results in a slight overestimation of the surface water demand, because, in reality, because part of the water demand will be satisfied with groundwater.

Additionally, all water is extracted from within a superimposed segment with a 1° resolution, in which preference is given to the grid cell containing the most water. This is done to prevent water balance errors in the model. However, it affects the realism of the model, because in reality preference is given to nearby water sources. Whenever water has to be transported over a distance, preference is given to upstream water, because the water can then be supplied by gravity flow, and hence at lower costs (Republic of Kenya, 2011b). However, if a downstream grid cell within the overlying segment contains the most water, this water is used to satisfy the demand.

The consulted policy documents contain a proliferation of planned interventions. This seems to be mainly caused by the fact that multiple institutions are operating on similar projects, i.e. irrigation schemes, but without apparent close collaboration. Several important Kenyan organizations in this field are TARDA, the National Irrigation Board (NIB) and the Ministry of Water and Irrigation. This fact complicated the design of the scenarios for this study. It has been difficult to determine which interventions are most likely to be realized and hence needed to be included in this study.

It has also been difficult to obtain clear and unambiguous information on planned land use and water allocation interventions in the Tana basin due to contradictions found in the studied documents. The Project on the Development of the National Water Master Plan 2030 (Nippon Koei, 2013a-2013e) is

the most extensive document on planned interventions in the Tana basin. However, there are some contradictions within this Water Master Plan. These contradictions were found for e.g. the location of the HGFD and the proposed dams for water supply to Nairobi, which differed between and within sub-sections, and the location and crop types of certain irrigation schemes. In figure 19.1.14 from Nippon Koei (2013c, p. EX-F-78), the locations of the planned dams to transport water to Nairobi are shown. However, in the same document, in table 7.7.1 (p. EX-T-13), two of the five proposed dams to supply water to Nairobi are different: Maragua 4 and Thika 3A (instead of Maragua and Maragua 8). In this study, the dams shown in figure 19.1.14 were used, because it also showed their locations. This information was used to produce figure 14.

The scenarios have been designed to examine the expected impacts of proposed (realistic) interventions on the water balance. However, it should be noted that some interventions (i.e. scenarios) are in reality interlinked with others. For this reason the HGFD is included in scenario 2. However, this is not the done for scenario 3. In reality, the Lamu Port (scenario 3) requires water from the HGFD project (at the Nanigi barrage which can regulate water availability) (JPC & BAC/GKA JV, 2011). In other words, scenario 3 shows the effect the Lamu Port would have on the water river discharge in case the HGFD project is not completed.

Several interventions that are mentioned in policy plans have not been included in this study. This is the case for the Kora and Usueni dams – the latter of which is part of the HGFD project – and several irrigation schemes. The reason for exclusion is because of cancelled plans or a lack of reliable information available. If they had been included in the model assumptions would have been necessary that could not be based on reliable information. As such, it has been deemed best to exclude them from this study.

5.2.2 Scenario 1 assumptions and uncertainties
The HGFD is included in the model from 2018 onwards. With the first eight years being without the HGFD, the effects of the HGFD are less clear for the near future (2010-2030).

The increase in discharge in the all-year FDC that is seen in figure 20 (and appendix 7b) is a result of the applied normalized correction method. Without this correction there is a slight decrease in peak flows due to the HGFD (appendix 7f). This is further made clear by comparing the regime curves[15] with and without correction (figures 24 and 25). It can be seen in figure 24 (without correction) that during the rainy season (i.e. around April-May and November-December) the discharge is slightly lower with than without the HGFD. During the dry season the HGFD results in an increase in discharge. This is the expected result of the construction of a dam. However, in figure 25 (with correction), this pattern is not visible. Instead the discharges seem to increase as a result of the HGFD, which is also seen in figure 20 (and appendix 7b). As such, the observed pattern with increasing discharges is a direct result of the applied correction. Therefore, the results have to be interpreted with care.

Flood regulation is considered to be the most important aspect of the HGFD (see chapter 3.2.1). However, both in appendix 7f and figure 24 (both are without correction) the peaks are only slightly reduced as a result of the HGFD. The all-year mean Q10 (without correction) decreases only in the far future (appendix 7f-2). In the model, the HGFD reservoir (almost) never drops below 75% of its

---

[15] Regime curves show the seasonality of the discharges.

maximum storage capacity. Instead it varies between 75% (4,640 MCM) and 100% (6,187 MCM). It appears that the HGFD reservoir is too full to effectively buffer the peak flows. Thus, the storage capacity seems to be not enough. Therefore, care has to be taken with the actual HGFD operations to reduce this limited storage.

In fact, the modeled storage capacity of the HGFD reservoir is likely an overestimation. In this study the sedimentation rate in the reservoir is not included, while in reality the storage capacity of reservoirs decreases over time due to increased sediment deposits (Kitheka & Ongwenyi, 2002; Kitheka et al., 2005). Therefore, the effect of the HGFD on the discharge is an 'idealized' effect. Additionally, trapping of sediment has an effect on coastal erosion (Kitheka et al., 2005). These effects of sedimentation, however, are not included in this study.
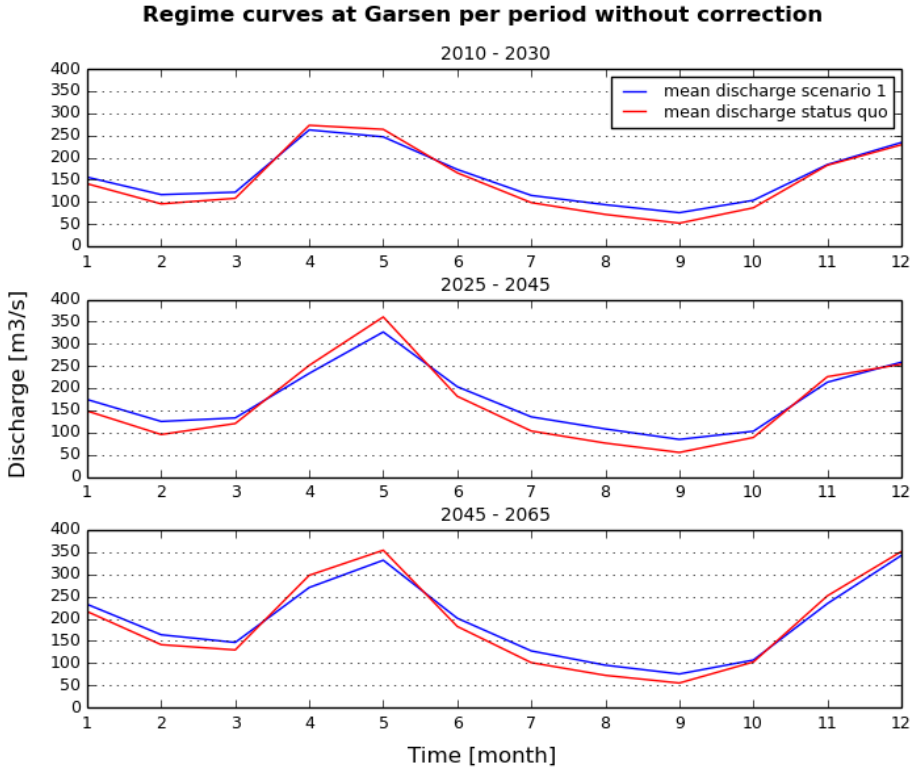
Figure 24: The regime curves (without correction) of mean monthly discharge of all GCMs at Garsen per period showing the effect of the HGFD on the mean monthly discharge per month.
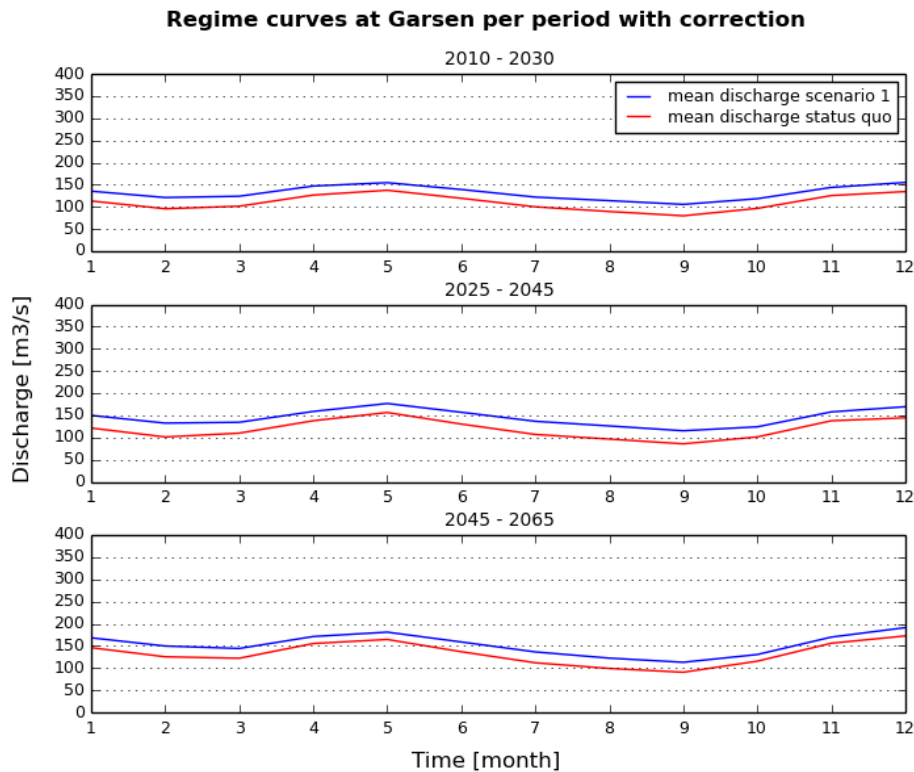
Figure 25: The regime curves (with correction) of mean monthly discharge of all GCMs at Garsen per period showing the effect of the HGFD on the mean monthly discharge per month.

5.2.3 Scenario 2 assumptions and uncertainties

The effect of the applied correction on the HGFD (see chapter 5.2.2) is also present in this scenario. However, by comparing the results from scenario 2 with scenario 1 the effect of the irrigation schemes can be assessed (table 12).

As stated above, various plans for expansion of irrigated agriculture in the Tana basin are incomplete or show contradicting information. For example, for this scenario, one of the above-mentioned contradictions concerns the Hola irrigation scheme. In Republic of Kenya (2011b) it is part of the HGFIP (and included in the 106,000 ha), while in Nippon Koei (2013a; 2013e) it is described as a stand-alone project. However, by including Hola in the HGFIP, the total irrigated area of the HGFIP adds up to 106,000 ha, which is also the total irrigated area of the HGFIP stated in Nippon Koei (2013a; 2013e). Additionally, as stated above, many figures that illustrate plans for the Tana basin are incomplete or show contradicting information. Such discrepancies complicated the process to map out the future schemes.

This difficulty is also encountered when determining the irrigation area of which little is known. For example, it is not entirely clear whether the 66,000 ha (from table 5) is part of the 25,000 to 75,000 ha that is mentioned for the third stage of the HGFIP. However, due to a lack of information and the uncertainty of the plans, this 66,000 ha is included instead of the abovementioned 25,000 to 75,000 ha. Additionally, Nippon Koei (2013a) states that the total irrigated area of the HGFIP is 106,000 ha. When summing all irrigation areas within the HGFIP that are included in this study, the result is an area of 106,000 ha. This indicates that the area sizes of the HGFIP in table 5 (40,000 + 66,000) are correct, which is why they are used in this study.

It should be noted that in reality the total new irrigated area may be larger than the 146,000 ha that is included in this study (see table 5). This is because in this study small-scale and private irrigation schemes are neglected. Only the irrigated area that is included in the MIRCA2000 dataset, i.e. roughly 39,195 ha, is included in the status quo scenario. This means that in 2010 the total irrigated area is underestimated by 25,230 ha (64,425 - 39,195) (see table 4). The new total irrigated area in 2035 (last year in which irrigation schemes are expanded) is 197,697 ha. This means that there is a discrepancy of 28,527 ha (see 226,224 - 197,697) between the modeled area in 2035 and the expected area in 2030 (see table 4). As such, the irrigation water demand is underestimated in this scenario (provided the plans will be realized as planned).

Another simplification applied in the model, is that the proposed specified irrigation schemes consist of a single crop-type (apart from Masalani), though in reality various crops may be cultivated on a single irrigation scheme. This is also the case with the unspecified irrigation schemes, which are modeled as consisting of the crops from the MIRCA2000 dataset that are currently in the area.

5.2.4 Scenario 3 assumptions and uncertainties

The water demand for Nairobi is based on the current and future maximum transport capacity, which is used as proxy for the actual water demand. However, this maximum capacity is not utilized all the time. In reality, the water demand is highest in the dry season, but this inter-seasonal variability is not included in this study (the same is true for the Lamu Port). This simplification results in an overestimation of the water demand in the rainy season and an underestimation in the dry season. Also, the fact that the existing and future reservoirs providing water for Nairobi are not explicitly modeled has an effect on the discharge. In this study the water demand is subtracted directly from the water in the river. Since the existing Sasumua and Thika reservoirs – as well as the planned reservoirs – are relatively small in terms of storage capacity (15.9 MCM and 70 MCM, respectively) (AWSB, 2011; Nippon Koei, 2013a), this is not expected to have a large effect on the discharge. Especially if this scenario is combined with the HGFD and irrigation schemes (scenario 4), it is assumed to have only a minor effect.

Furthermore, residential water demand for recently established apartment blocks in Nairobi is increasingly met by (illegal) groundwater abstractions (Mulonga, pers. comm., 2014). It is unclear how this trend will develop in the future and whether this affects the amount of inter-basin water transfer of surface water from the Tana basin to Nairobi.

Lastly, it is assumed that all water for Lamu is extracted at Nanigi (i.e. within a superimposed segment of 1° resolution, centered on Nanigi), even though in reality this is not the case, since a small part will be supplied locally. However, this is a small fraction of the total water demand, i.e. 530 m^3/day (JPC & BAC/GKA JV, 2011), and will not significantly affect the results.

6. Conclusion

The conclusions from this study are given per scenario (i.e. sub-question), leading up to answering of the main research question. The changes in discharge of the scenarios at Garsen, resulting from included planned land use changes and water allocations, are compared to the discharges of the status quo. Overall, the performance of PCR-GLOBWB was not very good. Therefore a correction method was applied. This reduces the usability of the absolute changes in discharge resulting from the planned interventions. However, the relative changes between the scenarios can still be assessed.

6.1 Status quo

The discharge is expected to change as a result of climate change. However, the further into the future, the larger the uncertainty becomes. In the rainy season a large increase in both peak and low flows is expected in all assessed periods as a result of climate change. In the dry season the peak flows are expected to decrease compared to observations from the period 1979-1998. Even the lowest reported discharges from the GCMs in the rainy season are higher than the observed discharge. This suggests that the discharge in the rainy season will increase, while the peak flows in the dry season will be reduced. This reduction decreases with time. The biggest impact of climate change is predicted for the far future. There is not much change in the mean low flows (Q90) during the dry season. Especially the discharges with a very long return period (Q5 and higher) are projected to increase when assessing the all-year FDCs.

6.2 Scenario 1

Scenario 1 assessed the effect of the HGFD on the discharge of the Tana River. The HGFD is expected to (slightly) reduce the peak flow and increase the low flows. Even though the peaks are expected to be reduced the effect is limited, due to limited storage capacity of the HGFD reservoir. However, this effect is not visible in the FDCs, as a result of the applied correction. Therefore, the changes in Q10 and Q90 cannot be used to draw definite conclusions.

6.3 Scenario 2

Scenario 2 evaluated the effects of the HGFD and planned large-scale irrigation schemes on the discharge of the Tana River. The all-year FDCs show a decrease in peak flows and an increase in low flows with respect to the status quo. For the rainy season the discharge strongly decreases for all exceedence probabilities. Here, the negative effect of the irrigation demand is larger than the seemingly positive effect of the HGFD on the discharge (due to the correction). In the dry season, there is an overall increase in discharge. The biggest effect on Q10 and Q90 is seen in the mid future.

6.4 Scenario 3

Scenario 3 looked at the effects of the future water demand of Nairobi and the Lamu Port on the discharge of the Tana River. The future water demand has an overall negative effect on the discharge at the delta, which is also found for Q10 and Q90, specifically. This decrease in discharge increases with time, which can be attributed to the increasing water demand with time. The strongest effect is seen in the dry season. However, the effects on the discharge are overestimated in the rainy season and underestimated in the dry season.

6.5 Scenario 4

Scenario 4 included all interventions from the other scenarios to assess their combined effect on the discharge of the Tana River in the delta. For the near future, the all-year peak flows are expected to decrease, while the (very) low flows increase. With time, the difference with the status quo increases for the peak flows, while it decreases for the low flows. A decrease in discharge is expected in the rainy season, while the dry season is expected to see a small increase. For the rainy season, the effects on the discharge are largest in the mid future, similar to scenarios 1 and 2. For the dry season, the biggest increase in peak flows is seen in the far future, while for the low flows the biggest increase is seen in the near future.

6.6 Main conclusion

The main research question for this study is:

> *How will the river discharge of the Tana River in the Tana delta be affected by climate change and anthropogenic developments in the region?*

Climate change is expected to lead to an increase in discharge during the rainy season, while a (small) negative effect is expected in the dry season. The High Grand Falls Dam is expected to (slightly) reduce the peak flows and increase the low flows. The water demand for the irrigation schemes, Nairobi and the Lamu Port lead to decreases in river discharge. Overall, the biggest effect on the river discharge at the delta is expected during the rainy season as a result of the irrigation schemes. When all anthropogenic developments are combined, the discharge in the rainy season is strongly reduced, while the discharge in the dry season is slightly increased. In the near, mid- and far future, the all-year mean Q10 decreases by 2.60%, 15.16% and 15.65%, respectively, while the all-year mean Q90 increases by 10.07% and 3.38% and decreases by 2.85%, respectively. This results in a net effect of an overall decrease in river discharge of the Tana River in the Tana delta, except for low flows. Hence, the water availability in the Tana delta is negatively affected by the proposed interventions.

7. Recommendations

7.1 General recommendations

1) In this study, it has been found that the HGFD reservoir is too small to effectively capture the peak discharges. Since flood regulation is its most important feature, it is recommended to use other models to assess whether this conclusion is real or that it is a result of using PCR-GLOBWB. Purely from the results of this study it is recommended to increase its storage capacity. Additionally, the HGFD operations have to be carefully evaluated to reduce this issue of limited storage capacity.

2) In order to do evidence-based policy development and water planning and management, it is key to understand the (changes in the) system. Measuring and monitoring of necessary data (e.g. meteorological data) is important. The more observed data is available the more modeling results can be improved. It is therefore recommended to improve monitoring of precipitation and discharges in the Tana basin, which can help to improve the model results.

3) It is recommended that future hydrological studies in the Tana basin are done using models that have been extensively tested for (semi-)arid regions in Africa, or by creating a model specifically for the Tana basin.

4) In this study only the effects of the interventions on the river discharge are assessed. However, the consequences this has on the ecosystem functioning, and the ecosystem services to provide in the livelihoods of people living in the Tana delta are not explicitly included. Therefore, it is recommended to further research these consequences using this study as a base.

7.2 Recommendations for PCR-GLOBWB

5) The version of PCR-GLOBWB used in this study was not able to accurately reproduce the discharges (mostly downstream). However, PCR-GLOBWB does have an explicit flooding module, that, due to time constraints, was not used in this study. It is recommended that parts of this study are repeated with the extended model (see hereafter), and possibly with a finer resolution. The fact that this was not dynamically simulated in this study could have significant effects on the discharge. This is mainly the case for semi-arid regions like large parts of the Tana basin. By including this dynamic inundation, the role of the floodplains in peak attenuation is better captured and evaporation will play a larger role in case of floods, which will also reduce the peak flows between Garissa and Garsen. Beside improving peak flow simulation it will also improve the baseflow by increasing more infiltration in the floodplains. This can then percolate into the groundwater and provide more baseflow. This could also help to improve the model results in other rivers with similar climates.

6) Preferential flow is not included in the PCR-GLOBWB model structure. Preferential flow can, however, have significant effects on the infiltration and hence the soil water and groundwater. Therefore, it is recommended to include this in PCR-GLOBWB as well.

8. Acknowledgements

First of all, I would like to express my deepest gratitude to my supervisor dr. Rens van Beek for his continued patience and guidance. He was always willing to offer a helping hand in the struggle against my nemesis during this study: Python. He always found the time to help me with programming and resolving errors, even long after office hours.

Furthermore, I want to thank my supervisor Prof. dr. ir. Marc Bierkens for helping me getting started and putting me in touch with Frank van Weert, my supervisor from Wetlands International. Without him, this study would not have been conducted.

I am also greatly indebted to Frank van Weert, who has been a great support throughout this study. He was always willing to brainstorm and provide feedback on my work, which significantly helped to improve this thesis.

Additionally, I would like to thank ir. Niko Wanders for his help with the model calibration, as well as dr. Yoshihide Wada and especially dr. Edwin Sutanudjaja for their patience in answering my questions and helping me getting through the stressful last weeks. I would also like to express my gratitude to all the people who made time for me and helped me with this study: Julie Mulonga, dr. Hans de Moel, Maxime Eiselin and the staff of Wetlands International during my stay there.

Lastly, I want to thank my friends and family, but most of all, my girlfriend Sacha Handgraaf for supporting me all the way and putting up with my frustrations.

9. References

1. Adams, W.M. (1990) *How Beautiful is Small? Scale, Control and Success in Kenyan Irrigation*. World Development 18(10), pp. 1309-1323

2. Alcamo, J., Döll, P., Henrichs, T., Kaspar, F., Lehner, B., Rösch, T. & Siebert, S. (2003) *Development and testing of the WaterGAP 2 global model of water use and availability*. Hydrological Sciences Journal 48(3), pp. 317-337

3. Allen, R.G., Pereira, L.S., Raes, D. & Smith, M. (1998) Crop Evapotranspiration (Guidelines for computing crop water requirements). FAO Irrigation and Drainage Paper No. 56, FAO, Rome, Italy

4. Altchenko, Y. & Villholth, K.G. (2014) *Mapping irrigation potential from renewable groundwater in Africa – a quantitative hydrological approach.* Hydrology and Earth System Sciences Discussions 11, pp. 6065-6097

5. Andrews, P., Groves, C.P. & Horne, J.F.M. (1975) *Ecology of the Lower Tana River Flood Plain (Kenya).* Journal of the East Africa Natural History Society and National Museum 151, pp. 1-31

6. Athi Water Services Boards (AWSB) (2011) *Feasibility Study and Master Plan for Developing New Water Sources for Nairobi and Satellite Towns. Preliminary Review and Update of Scenarios for Water Supply to Nairobi – Working Paper No. 1, Version 02*. Ministry of Water and Irrigation.

7. Barnes, D. (2013) Investors clamour to be heard. Edmonton Journal [Online] http://www2.canada.com/edmontonjournal/news/business/story.html?id=bcf04e67-aca7-40f9-b2d8-de910778652f&p=2 [Cited 26 November 2013]

8. van Beek, L.P.H. (2008) *Forcing PCR-GLOBWB with CRU data.* Report Department of Physical Geography, Utrecht University, Utrecht, the Netherlands. [Online] vanbeek.geo.uu.nl/suppinfo/vanbeek2008.pdf [Cited 13 May 2014]

9. van Beek, L.P.H. & Bierkens, M.F.P. (2008) *The Global Hydrological Model PCR-GLOBWB: Conceptualization, Parameterization and Verification*. Report Department of Physical Geography, Utrecht University, Utrecht, the Netherlands. [Online] http://vanbeek.geo.uu.nl/suppinfo/vanbeekbierkens2009.pdf [Cited 15 November 2013]

10. van Beek, L.P.H., Wada, Y. & Bierkens, M.F.P. (2011) *Global monthly water stress: 1. Water balance and water availability*. Water Resources Research 47(7), pp. 1-25

11. Bentsen, M., Bethke, I., Debernard, J.B., Iversen, T., Kirkevåg, A., Seland, Ø., Drange, H., Roelandt, C., Seierstad, I.A., Hoose, C. & Kristjánsson, J.E. (2012) *The Norwegian Earth System Model, NorESM1-M – Part 1: Description and basic evaluation*. Geoscientific Model Development Discussions 5, pp. 2843-2931

12. Bormann, H. (2006) *Impact of spatial data resolution on simulated catchment water balances and model performance of the multi-scale TOPLATS model.* Hydrology and Earth System Sciences 10, pp. 165-179

13. Conway, D., Persechino, A., Ardoin-Bardin, S., Hamandawana, H., Dieulin, C. & Mahe, G. (2009) *Rainfall and Water Resources Variability in Sub-Saharan Africa during the Twentieth Century.* Journal of Hydrometeorology 10(1), pp. 41-59

14. Dee, D.P., Uppala, S.M., Simmons, A.J., Berrisford, P., Poli, P, Kobayashi, S., Andrae, U., Balmaseda, M.A., Balsamo, G., Bauer, P., Bechtold, P., Beljaars, A.C.M., van de Berg, L., Bidlot, J., Bormann, N., Delsol, C., Dragani, R., Fuentes, M., Geer, A.J., Haimberger, L., Healy,

S.B., Hersbach, H., Hólm, E.V., Isaksen, L., Kållberg, P., Köhler, M., Matricardi, M., McNally, A.P., Monge-Sanze, B.M., Morcrette, J.-J., Park, B.-K., Peubey, C., de Rosnay, P., Tavolato, C., Thépaut, J.-N. & Vitart, F. (2011) *The ERA-Interim reanalysis: configuration and performance of the data assimilation system.* Quarterly Journal of the Royal Meteorological Society 137(656), pp. 553-597

15. Dickens, C., Stassen, R. & Pringle, C. (2012) *A Preliminary Understanding of Environmental Water Requirements for the Tana River, Kenya.* Report to ICRAF and UNEP by the Institute of Natural Resources, Pietermaritzburg, South Africa

16. Dingman, S.L. (2008) *Physical Hydrology – Second edition.* United States of America: Waveland Press, Inc. First edition in 1994. Second edition in 2002, reissued in 2008.

17. Dunne, J.P., John, J.G., Adcroft, A.J., Griffies, S.M., Hallberg, R.W., Shevliakova, E., Stouffer, R.J., Cooke, W., Dunne, K.A., Harrison, M.J., Krasting, J.P., Malyshev, S.L., Milly, P.C.D., Phillipps, P.J., Sentman, L.T., Samuels, B.L., Spelman, M.J., Winton, M., Wittenberg, A.T. & Zadeh, N. (2012) *GFDL's ESM2 Global Coupled Climate-Carbon Earth System Models. Part I: Physical Formulation and Baseline Simulation Characteristics.* Journal of Climate 25, pp. 6646-6665

18. Dürr, H.H., Meybeck, M. & Dürr, S.H. (2005) *Lithological composition of the Earth's continental surfaces derived from a new digital map emphasizing riverine material transfer.* Global Biogeochemical Cycles 19(4), GB4S10

19. Dutch Ministry of Economic Affairs (2013) *Uitvoeringsagenda Natuurlijk Kapitaal.* Den Haag [Online] http://www.rijksoverheid.nl/documenten-en-publicaties/kamerstukken/2013/06/22/kamerbrief-over-uitvoeringsagenda-natuurlijk-kapitaal.html [Cited 23 July 2014]

20. Duvail, S., Médard, C., Hamerlynck, O. & Nyingi, D.W. (2012) *Land and Water Grabbing in an East African Coastal Wetland: The Case of the Tana Delta.* Water Alternatives 5(2), pp. 322-343

21. Emerton, L. (2005) *Values and Rewards: Counting and Capturing Ecosystem Water Services for Sustainable Development.* IUCN Water, Nature and Economics Technical Paper No. 1, IUCN — The World Conservation Union, Ecosystems and Livelihoods Group Asia. [Online] cmsdata.iucn.org/downloads/2005_047.pdf [Cited 14 November 2013]

22. Evensen, G. (2003) *The Ensemble Kalman Filter: theoretical formulation and practical implementation.* Ocean Dynamics 53, pp. 343-367

23. Food and Agricultural Organization of the United Nations (FAO) (2003) *Digital Soil Map of the World, Version 3.6.* [Online] http://www.fao.org/geonetwork/srv/en/metadata.show?id=14116 / ftp://ftp.iist.unu.edu/pub/waterbase/Global_Soil_Data/readme.pdf [Cited 27 May 2014]

24. Fekete, B.M., Vörösmarty, C.J. & Grabs, W. (2002) *High-resolution fields of global runoff combining observed River discharge and simulated water balances.* Global Biogeochemical Cycles 16(3), pp. 1-6

25. Government of Kenya (2007) *Kenya Vision 2030 – A Globally Competitive and Prosperous Kenya* [Online] https://www.opendata.go.ke/api/file_data/IyRGPwVuC0MJhKZnMa1YA3s0vXBJkCVeDWgy_AS5d_0?filename=VISION_2030.pdf [Cited 18 November 2013]

26. Government of Kenya (2013) *Performance Contracting Guidelines on the Vision 2030 Project Indicator FY 2013-2014.* [Online]

http://www.vision2030.go.ke/cms/vds/FINAL_VDS_PC_GUIDELINES_2013_2014(1).pdf
[Cited 26 november 2013]

27. Hagemann, S. & Gates, L.D. (2003) *Improving a subgrid runoff parameterization schemes for climate models by the use of high resolution data derived from satellite observations*. Climate Dynamics 21, pp. 349-359

28. Hamerlynck, O., Nyunja, J., Luke, Q., Nyingi, D., Lebrun, D. & Duvail, S. (2010) *The communal forest, wetland, rangeland and agricultural landscape mosaics of the Lower Tana, Kenya, a socio-ecological entity in peril.* [Online] www.cbd.int/database/attachment/?id=340 [Cited 22 November 2013]

29. Hempel, S., Frieler, K., Warszawski, L., Schewe, J & Piontek, F. (2013) *A trend-preserving bias correction – the ISI-MIP approach.* Earth System Dynamics Discussions 4, pp. 49-92

30. Hoff, H., Noel, S. & Droogers, P. (2007) *Water use and demand in the Tana Basin: Analysis using the Water Evaluation and Planning tool (WEAP)*. Green Water Credits Report 4, ISRIC – World Soil Information, Wageningen. [Online] http://www.futurewater.nl/nl/publicaties/pub2007/ [Cited 14 November 2013]

31. Hourdin, F., Foujols., M.-A., Codron, F., Guemas, V., Dufresne, J.-L., Bony, S., Denvil, S., Guez, L., Lott, F., Ghattas, J., Braconnot, P., Marti, O., Meurdesoif, Y. & Bopp, L. (2013) *Impact of the LMDZ atmospheric grid configuration on the climate and sensitivity of the IPSL-CM5A coupled model.* Climate Dynamics 40, pp. 2167-2192

32. Ikiara, M.M. & Ndirangu, L.K. (2002) *Developing a Revival Strategy for the Kenyan Cotton-Textile Industry: A Value Chain Approach.* Kenya Institute for Public Policy Research and Analysis (KIPPRA). [Online] http://s3.marsgroupkenya.org/media/documents/2011/02/48b43b3e9e98002f40de0ee0ee23baa3.pdf [Cited 8 April 2014]

33. Intergovernmental Panel on Climate Change (IPCC) (2013) *Climate Change 2013: The Physical Science Basis. Contribution of Working Group I to the Fifth Assessment Report of the Intergovernmental Panel on Climate Change* [Stocker, T.F., Qin, D., Plattner, G.-K., Tignor, M., Allen, S.K., Boschung, J., Nauels, A., Xia, Y., Bex, V. & Midgley, P.M. (eds.)]. Cambridge University Press, Cambridge, United Kingdom and New York, NY, USA, 1535 pp.

34. International Union for the Conservation of Nature (IUCN) (2003) *Tana River, Kenya: integrating downstream values into hydropower planning - Case studies in Wetland valuation #6: May 2003.* [Online] http://cmsdata.iucn.org/downloads/casestudy06tana.pdf [Cited 14 November 2013]

35. IUCN NL (2013) *Ecosystem Alliance*. [Online] http://www.iucn.nl/en/themes/green_ic/ecosystem_alliance/ [Cited 15 November 2013]

36. JPC & BAC/GKA JV (2011) *LAPSSET Corridor and New Lamu Port. Feasibility study and master plans report. Volume Three: LAPSSET Corridor master plan and development plan.* Study for LAPSSET Corridor FS & Lamy Port MP & DD. [Online] http://www.coastpropertieskenya.com/lamu-port [Cited 15 November 2013]

37. Kitheka, J.U. & Ongwenyi, G.S. (2002) *The Tana River Basin and the opportunity for research on the land-ocean interaction in the Tana Delta.* In: Arthurton, R.S., Kremer, H.H., Odada, E., Salomons, W. & Marshall Crossland, J.I. (2002) *African Basins – LOICZ Global Change Assessment and Synthesis of River Catchment-Coastal Sea Interaction and Human Dimension.* LOICZ Reports & Studies No. 25, pp. 203-209 [Online]

http://www.loicz.org/imperia/md/content/loicz/print/rsreports/report25.pdf [Cited 2 July 2014]

38. Kitheka, J.U., Obiero, M. & Nthenge, P. (2005) *River discharge, sediment transport and exchange in the Tana Estuary, Kenya*. Estuarine, Coastal and Shelf Science 63, pp. 455-468

39. Knoop L., Sambalino, F., & van Steenbergen, F. (2012) *Securing Water and Land in the Tana Basin: a resource book for water managers and practitioners*. Wageningen, The Netherlands: 3R Water Secretariat

40. Krause, P., Boyle, D.P. & Bäse, F. (2005) *Comparison of different efficiency criteria for hydrological model assessment.* Advances in Geosciences 5, pp. 89-97

41. Leauthaud C., Duvail, S., Hamerlynck, O., Paul, J.-L., Cochet, H., Nyunja, J., Albergel, J. & Grünberger, O. (2013a) *Floods and livelihoods: The impact of changing water resources on wetland agro-ecological production systems in the Tana River Delta, Kenya.* Global Environmental Change 23, pp. 252-263

42. Leauthaud C., Belaud, G., Duvail, S., Moussa, R., Grünberger, O. & Albergel, J (2013b) *Characterizing floods in the poorly gauged wetlands of the Tana River Delta, Kenya, using a water balance model and satellite data*. Hydrology and Earth System Sciences 17, pp. 3059-3075

43. Legates, D.R. & McCabe Jr., G.J. (1999) *Evaluating the use of "goodness-of-fit" measures in hydrologic and hydroclimatic model validation.* Water Resources Research 35(1), pp. 233-241

44. Lehner, B. & Döll, P. (2004) *Development and validation of a global database of lakes, reservoirs and wetlands.* Journal of Hydrology 296, pp. 1-22

45. Lehner, B., Reidy Liermann, C., Revenga, C., Vörösmarty, C.,Fekete, B., Crouzet, P., Döll, P., Endejan, M., Frenken, K., Magome, J., Nilsson, C., Robertson, J.C., Rödel, R., Sindorf, N., & Wisser, D. (2011) *High-resolution mapping of the world's reservoirs and dams for sustainable river-flow management.* Frontiers in Ecology and the Environment 9(9), pp. 494-502

46. Maingi, J.K. & Marsh, S.E. (2002) *Quantifying hydrologic impacts following dam construction along the Tana River, Kenya.* Journal of Arid Environments 50, pp. 53-79

47. Martin, P. (2012) *Conflicts between pastoralists and farmers in Tana River District.* In: Witsenburg, K. & Zaal, F. (2012) *Spaces of insecurity – Human agency in violent conflicts in Kenya*. African Studies Collection 45, African Studies Centre, pp. 167-193 [Online] https://openaccess.leidenuniv.nl/bitstream/handle/1887/20295/asc-075287668-3261-01.pdf?sequence=2#page=177 [Cited 26 November 2013]

48. Milly, P.C.D. & Shmakin, A.B. (2002) *Global Modeling of Land Water and Energy Balances. Part I: The Land Dynamics (LaD) Model.* Journal of Hydrometeorology 3(3), pp. 283-299

49. Ministry of Transport (2013) *Environmental and social impact assessment study report for construction of the first three berths of the proposed Lamu Port and associated infrastructure.* [Online] www.nema.go.ke [Cited 15 November 2013]

50. Mireri, C., Onjala, J. & Oguge, N. (2008) *The Economic Valuation of the Proposed Tana Integrated Sugar Project (TISP), Kenya*. Prepared for Nature Kenya. [Online] http://www.rspb.org.uk/Images/tana_tcm9-188706.pdf [Cited 26 November 2013]

51. Mitchel, T.D. & Jones, P.D. (2005) *An improved method of constructing a database of monthly climate observations and associated high-resolution grids.* International Journal of Climatology 25, pp. 693-712

52. Moriasi, D.N., Arnold, J.G., Van Liew, M.W., Bingner, R.L., Harmel, R.D. & Veith, T.L. (2007) *Model Evaluation Guidelines for Systematic Quantification of Accuracy in Watershed Simulations.* Transactions of the ASABE 50(3), pp. 885-900

53. Moss, R.H., Edmonds, J.A., Hibbard, K.A., Manning, M.R., Rose, S.K., van Vuuren, D.P., Carter, T.R., Emori, S., Kainuma, M., Kram, T., Meehl, G.A., Mitchell, J.F.B., Nakicenovic, N., Riahi, K., Smith, S.J., Stouffer, R.J., Thomson, A.M., Weyant, J.P. & Wilbanks, T.J. (2010) *The next generation of scenarios for climate change research and assessment.* Nature 463 (7282), pp. 747-756

54. Nash, J.E. & Sutcliffe, J.V. (1970) *River flow forecasting through conceptual models part I — A discussion of principles.* Journal of Hydrology 10(3), pp. 282-290

55. Ndiiri, J.A., Mati, B.M., Home, P.G., Odongo, B. & Uphoff, N. (2013) *Adoption, constraints and economic returns of paddy rice under the system of rice intensification in Mwea, Kenya.* Agricultural Water Management 129, pp. 44-55

56. Nippon Koei (2012) *The Project on the Development of the National Water Master Plan 2030 – Progress Report (4)* [Online] http://www.wrma.or.ke/images/presspdf/ProgressReport_4_%20NWMP%202030.pdf [Cited 20 November 2013]

57. Nippon Koei (2013a) *The project on the development of the national water master plan 2030. Final Report. Volume III Part F – Tana Catchment Area.* Republic of Kenya

58. Nippon Koei (2013b) *The project on the development of the national water master plan 2030. Final Report. Volume V Sectoral Report (F) Hydropower*. Republic of Kenya

59. Nippon Koei (2013c) *The project on the development of the national water master plan 2030. Final Report. Volume I Executive Summary.* Republic of Kenya

60. Nippon Koei (2013d) *The project on the development of the national water master plan 2030. Final Report. Volume V Sectoral Report (E) – Agriculture and Irrigation*. Republic of Kenya

61. Nippon Koei (2013e) *The project on the development of the national water master plan 2030. Final Report. Volume VII Data Book.* Republic of Kenya

62. Odhengo, P., Matiku, P., Nyangena, J., Wahome, K., Opaa, B., Munguti, S., Koyier, G., Nelson, P., Mnyamwezi, E., & Misati, P. (2012a) *Tana River Delta Strategic Environmental Assessment Scoping Report.* Published by the Ministry of Lands, Physical Planning Department

63. Odhengo, P., Matiku, P., Waweru, P., Guda, D., Kinara, T., Kathike, S., Mmyamwezi, E., Munguti, S. & Koyier, G. (2012b) *Tana River Delta Land Use Plan Framework 2012.* Published by the Ministry of Lands, Physical Planning Department

64. Oludhe, C., Sankarasubramanian, A., Sinha, T., Devineni, N. & Lall, U. (2013) *The Role of Multimodel Climate Forecasts in Improving Water and Energy Management over the Tana River Basin, Kenya.* Journal of Applied Meteorology and Climatology 52, pp. 2460-2475

65. Portmann, F.T., Siebert, S. & Döll, P. (2010) *MIRCA2000 – Global monthly irrigated and rainfed crop areas around the year 2000: A new high-resolution data set for agricultural and hydrological modeling.* Global Biogeochemical Cycles 24, pp. 1-24

66. Ramsar (2012) *Tana River Delta added to the Ramsar List*. [Online] http://www.ramsar.org/cda/en/ramsar-news-archives-2012-kenya-tana/main/ramsar/1-26-45-520%5E25948_4000_0__ [Cited 19 September 2013]

67. Republic of Kenya (2011a) *High Grand Falls Multipurpose Development Project on River Tana – Feasibility Study*. Ministry of Regional Development Authorities

68. Republic of Kenya (2011b) *High Grand Falls Multipurpose Development Project on River Tana – Feasibility Study. Annex D: Irrigation*. Ministry of Regional Development Authorities

69. Republic of Kenya (2011c) *High Grand Falls Multipurpose Development Project on River Tana – Feasibility Study. Annex A: Climate and Hydrology.* Ministry of Regional Development Authorities

70. Royal Haskoning (1982) *Feasibility study of the Tana Delta irrigation project*. [Online] http://www.tanariverdelta.org/tana/g1/past-plans.html [Cited 14 November 2013]

71. RVI Nairobi Forum (2013) *LAPSSET: Transformative project or pipe dream? - Debating the opportunities and dangers of a transnational megaproject.* Rift Valley Institute Meeting Report Nairobi Forum, 4 October 2013. [Online] www.riftvalley.net/download/file/fid/3092 [Cited 23 November 2013]

72. Samoilys, M., Osuka, K. & Maina, G.W. (2011) *Review and assessment of biodiversity values and conservation priorities along the Tana Delta – Pate Island coast of northern Kenya.*

73. Scanlon, B.R., Keese, K.E., Flint, A.L., Flint, L.E., Gaye, C.B., Edmunds, M. & Simmers, I. (2006) *Global synthesis of groundwater recharge in semiarid and arid regions*. Hydrological Processes 20(15), pp. 3335-3370

74. Siebert, S. & Döll. P. (2010) *Quantifying blue and green virtual water contents in global crop production as well as potential production losses without irrigation.* Journal of Hydrology 384, pp. 198-217

75. Snoussi, M., Kitheka, J., Shaghude, Y., Kane, A., Arthurton, R., Le Tissier, M. & Virji, H. (2007) *Downstream and Coastal Impacts of Damming and Water Abstraction in Africa*. Environmental Management 39, pp. 587-600

76. Sutanudjaja, E.H., van Beek, L.P.H., de Jong, S.M., van Geer, F.C. & Bierkens, M.F.P. (2014) *Calibrating a large-extent high-resolution coupled groundwater-land surface model using soil moisture and discharge data.* Water Resources Research 50(1), pp. 687-705

77. Taylor, K.E., Stouffer, R.J. & Meehl, G.A. (2009) *A Summary of the CMIP5 Experiment Design.* [Online] http://cmip-pcmdi.llnl.gov/cmip5/docs/Taylor_CMIP5_design.pdf [Cited 24 May 2014]

78. Temper, L. (2010) *Let Them Eat Sugar: Life and Livelihood in Kenya's Tana Delta*. Autonomous University of Barcelona, Ecological Economics and Integrated Assessment Unit. [Online] http://www.ceecec.net/wp-content/uploads/2010/02/TANA_DELTA__FINAL.pdf [Cited 15 November 2013]

79. The Economics of Ecosystems and Biodiversity (TEEB) (2013): *Guidance Manual for TEEB Country Studies*. Version 1.0. [Online] http://www.teebweb.org/resources/guidance-manual-for-teeb-country-studies/ [Cited 16 May 2014]

80. Todini, E. (1996) *The ARNO rainfall-runoff model.* Journal of Hydrology 175, pp. 339-382

81. Trambauer, P., Maskey, S., Werner, M., Pappenberger, F., van Beek, L.P.H. & Uhlenbrook, S. (2014) *Identification and simulation of space-time variability of past hydrological drought events in the Limpopo river basin, Southern Africa*. Hydrology and Earth System Sciences 11, pp. 2639-2677

82. United Nations Human Settlements Programme (UN-HABITAT) (2006) *Nairobi – Urban Sector Profile*. [Online] http://asmarterplanet.com/files/2012/09/UN-Habitat-Report-on-Nairobi.pdf [Cited 29 November 2013]

83. USGS EROS Data Center (sine anno) *HYDRO1K* [Online] http://eros.usgs.gov/#/Find_Data/Products_and_Data_Available/HYDRO1K [Cited 27 May 2014]

84. USGS EROS Data Center (2002) *Global Land Cover Characteristics Data Base Version 2.0.* [Online] http://edc2.usgs.gov/glcc/globdoc2_0.php [Cited 13 May 2014]

85. Vörösmarty, C.J., Fekete, B.M., Meybeck, M. & Lammers, R.B. (2000) *Geomorphometric attributes of the global system of rivers at 30-minutes spatial resolution*. Journal of Hydrology 237, pp. 17-39

86. Wada, Y. (2013) *Human and climate impacts on global water resources*. Dissertation. Utrecht studies in earth sciences, Vol 050. Utrecht University, Faculty of Geosciences. [Online] http://dspace.library.uu.nl/handle/1874/286196 [Cited 22 November 2013]

87. Wada, Y., Wisser, D. & Bierkens, M.F.P. (2014) *Global modeling of withdrawal, allocation and consumptive use of surface water and groundwater resources.* Earth System Dynamics 5, pp. 15-40

88. Wanders, N., Bierkens, M.P.F., de Jong, S.M., de Roo, A. & Karssenberg, D. (2014) *The benefits of using remotely sensed soil moisture in parameter identification of large-scale hydrological models*. Water Resources Research, under review

89. Watanabe, S., Hajima, T., Sudo, K., Nagashima, T., Takemura, T., Okajima, H., Nozawa, T., Kawase, H., Abe, M., Yokohata, T., Ise, T., Sato, H., Kato, E., Takata, K., Emori, S. & Kawamiya, M. (2011) *MIROC-ESM: model description and basin results of CMIP5-20c3m experiments*. Geoscientific Model Development Discussions 4, pp. 1063-1128

90. Widén-Nilsson, E., Halldin, S. & Xu, C. (2007) *Global water-balance modelling with WASMOD-M: Parameter estimation and regionalization.* Journal of Hydrology 340, pp. 105-118

91. Wonnacott, T.H. & Wonnacott, R.J. (1990) *Introductory Statistics – Fifth Edition*. United States of America: John Wiley & sons. First edition in 1969.

92. World Resource Institute (WRI) (2007) *Kenya GIS Data*. [Online] http://www.wri.org/resources/data-sets/kenya-gis-data [Cited 17 January 2014].

93. *Wu, M., Mintz, M., Wang, M. & Arora, S. (2009) Water Consumption in the Production of Ethanol and Petroleum Gasoline.* Environmental Management 44, pp. 981-997

Personal communication

- Mbui, G., *Tana Basin Manager at TARDA, Kenya*. pers. comm., 2014. Interviews were conducted by M. Eiselin on 28 April and 13 May, 2014, for the TEEB for Tana study.
- Mulonga, J., *Program manager at Wetlands International Africa, Kenya*. Contact took place via email and skype during the course of this study.
- Sutanudjaja, E.H., dr., *Postdoc at the faculty of Geosciences of Utrecht University*. pers. comm., 2014. Contact took place in meetings during and after the calibration process.
- van Weert, F., *Technical Officer Water and Climate at Wetlands International*. pers. comm., 2013-2014. Contact took place in meetings, on the phone and via email during the course of this study.

10. Appendices

Appendix 1: Ecosystem services in the lower Tana basin

Provisioning services	
Food	recession agriculture, small-scale flood irrigation, mobile livestock keeping, capture fisheries, collection of wild plant and animal food products
Fibre	timber for canoes and construction, beehives, roof thatch and weaving products from palms, wood fuel
Clay	construction of mud houses, brick-baking, pottery, fertilization of soils
Genetic resources	not studied, potentially some traditional crop varieties
Biochemicals, natural medicines and pharmaceuticals	Important role of forests for local medicinal products, honey and palm wine
Fresh water	Surface water for various uses and groundwater recharge (subsurface waters are in general saline)
Regulating services	
Air quality regulation	dynamic forests in different life stages with efficient carbon fixation, barrier to wind erosion
Climate regulation	evapotranspiration by forests, oxbow lakes, etc.
Water regulation	reduction of flood peak between Garissa and Garsen (see Figure 4)
Erosion regulation	Riverine forest slows bank erosion and stabilises meanders
Water purification and waste treatment	absorption of nitrogen, reduction of sediment loads by deposition in the floodplains
Disease regulation	not studied,
Pest regulation	not studied,
Pollination	not studied but most probably important
Natural hazard regulation	Resilient ecosystems continue to provide services during climate extremes
Cultural services	
Cultural diversity	Different livelihood strategies complement each other e.g. fertilisation of fields by livestock, provision of wild foods and milk in exchange for farming produce
Spritual and religious values	Not as strong as in the Mijikenda of the more southern coastal forests but there is a strong emotional affinity with the traditional landscapes
Knowledge systems	Elaborate traditional knowledge under threat (sedentary lifestyle, schools, wage jobs, outmigration to towns)
Educational values	Teaching of bush practice and traditional pharmacopeia
Inspiration	Many locals enjoy transect walks and being in the bush
Aesthetic value	Both traditional and modern
Social relations	Rituals by elders of various communities for access to resources
Sense of place	People who received land at Kipini in compensation have remained attached to their ancestral lands, return of livestock keepers to abandoned TDIP land (Wardei)
Cultural heritage values	The Pokomo claim they brought the Red Colobus with them from Central Africa
Recreation and ecotourism	Good potential but issues with the security situation, access, infrastructure and human capacity (language, training of local guides)
The **Supporting services** : soil formation, photosynthesis, primary production, nutrient cycling and water cycling underlie all the other services and are usually not included to avoid double counting in ecosystem valuation	

Appendix 1: An overview of ecosystem services that are provided in the lower Tana basin, all of which are also applicable to the Tana delta (Hamerlynck et al., 2010, p. 7).

Appendix 2: Components of the LAPSSET Corridor within Kenya
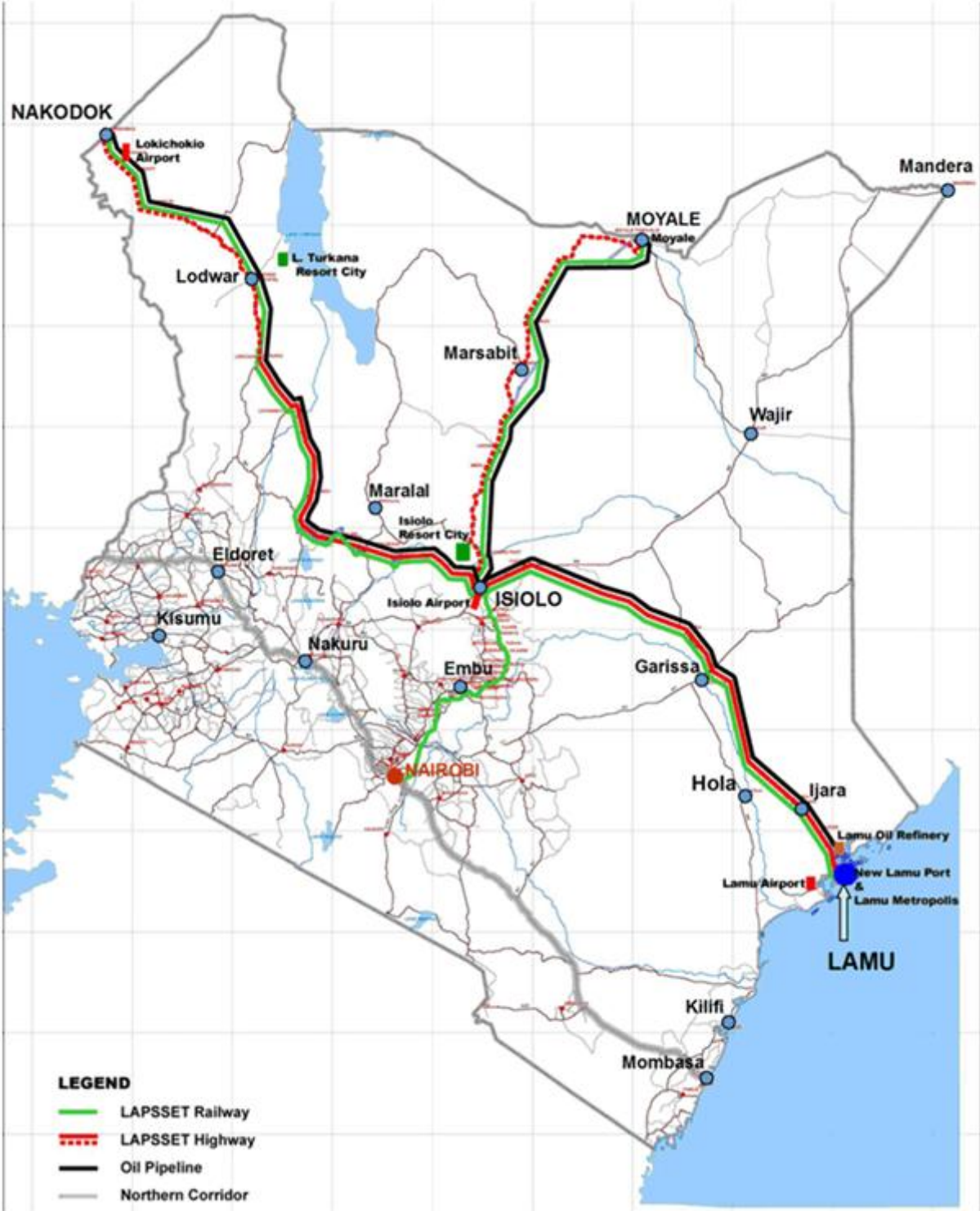
Appendix 2: Overview of the LAPSSET Corridor routes within Kenya as envisaged in the LAPSSET Corridor and New Lamu Port feasibility study and master plans report (JPC & BAC/GKA JV, 2011, p. S3-2).

Appendix 3: Hydrological model concept of PCR-GLOBWB
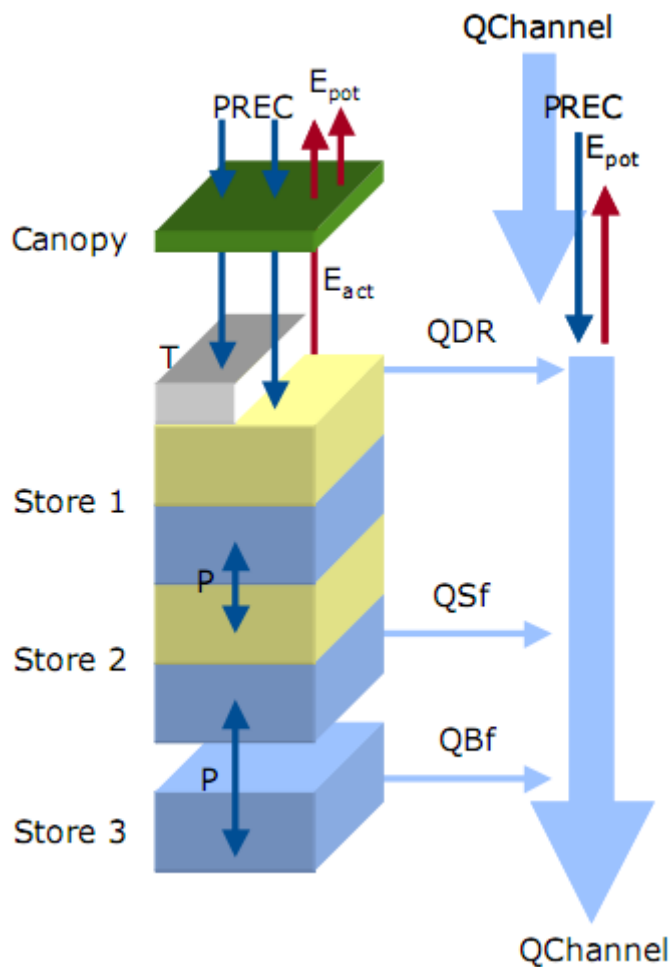
Appendix 3: Hydrological model concept of PCR-GLOBWB (van Beek & Bierkens, 2008). At the left-hand side the hydrological interactions between, and within, the canopy and soil column is represented (stores 1 and 2). Store 3 represents the groundwater reservoir. Precipitation (PREC) falls in the form of rain or snow, depending on the air temperature (T). If the air temperature is higher than 0°C, precipitation falls as rain, otherwise as snow. Snow will accumulate on the surface, until the temperature is high enough that it melts. Potential evapotranspiration (E_{pot}) is divided in canopy transpiration and bare soil evaporation. Based on the soil moisture content of the soil, this is reduced to the actual evapotranspiration (E_{act}). Downward flow into the soil is caused by percolation, while upward flow by capillary rise (P). Movement to the river network is represented by direct overland flow (QDR), interflow (or subsurface stormflow) (Sf), and baseflow (QBf). This movement is directed by the LDD-map, where it accumulates as discharge in the channel (QChannel). Besides being influenced by flows from the soil and groundwater reservoirs, the discharge is directly subject to precipitation and potential evaporation (van Beek et al., 2011).

Appendix 4: Details on the crop classes from the MIRCA2000 dataset

Appendix 4: Lengths of crop development stages as fractions of the whole growing period for initial (L_ini), crop development (L_dev), mid season (L_mid) and late season (L_late); crop coefficients for initial period (kc_ini), mid season (kc_mid) and at the end of season (kc_end); rooting depth (rd), and; standard crop depletion fraction (p_{std}) for the 26 crop classes considered in the MIRCA2000 dataset (Siebert & Döll, 2010, p. 200).

Crop class	Relative length of crop development stage (–)				Crop coefficients (–)			Rooting depth rd (m)		p_{std} (–)
	L_ini	L_dev	L_mid	L_late	kc_ini	kc_mid	kc_end	Irrigated	Rainfed	
Wheat (1)	0.15	0.25	0.40	0.20	0.40	1.15	0.30	1.25	1.60	0.55
Maize (2)	0.17	0.28	0.33	0.22	0.30	1.20	0.40	1.00	1.60	0.55
Rice (3)	0.17	0.18	0.44	0.21	1.05	1.20	0.75	0.50	1.00	0.00
Barley (4)	0.15	0.25	0.40	0.20	0.30	1.15	0.25	1.00	1.50	0.55
Rye (5)	0.10	0.60	0.20	0.10	0.40	1.15	0.30	1.25	1.60	0.55
Millet (6)	0.14	0.22	0.40	0.24	0.30	1.00	0.30	1.00	1.80	0.55
Sorghum (7)	0.15	0.28	0.33	0.24	0.30	1.10	0.55	1.00	1.80	0.55
Soybeans (8)	0.15	0.20	0.45	0.20	0.40	1.15	0.50	0.60	1.30	0.50
Sunflower (9)	0.19	0.27	0.35	0.19	0.35	1.10	0.25	0.80	1.50	0.45
Potatoes (10)	0.20	0.25	0.35	0.20	0.35	1.15	0.50	0.40	0.60	0.35
Cassava (11)	0.10	0.20	0.43	0.27	0.30	0.95	0.40	0.60	0.90	0.35
Sugar cane (12)	0.00	0.00	1.00	0.00	0.00	0.90	0.00	1.20	1.80	0.65
Sugar beets (13)	0.20	0.25	0.35	0.20	0.35	1.20	0.80	0.70	1.20	0.55
Oil palm (14)	0.00	0.00	1.00	0.00	0.00	1.00	0.00	0.70	1.10	0.65
Rapeseed (15)	0.30	0.25	0.30	0.15	0.35	1.10	0.35	1.00	1.50	0.60
Groundnuts (16)	0.22	0.28	0.30	0.20	0.40	1.15	0.60	0.50	1.00	0.50
Pulses (17)	0.18	0.27	0.35	0.20	0.45	1.10	0.60	0.55	0.85	0.45
Citrus (18)	0.16	0.25	0.33	0.26	0.80	0.80	0.80	1.00	1.30	0.50
Date palm (19)	0.00	0.00	1.00	0.00	0.95	0.95	0.95	1.50	2.20	0.50
Grapes (20)	0.30	0.14	0.20	0.36	0.30	0.80	0.30	1.00	1.80	0.40
Cotton (21)	0.17	0.33	0.25	0.25	0.35	1.18	0.60	1.00	1.50	0.65
Cocoa (22)	0.00	0.00	1.00	0.00	1.05	1.05	1.05	0.70	1.00	0.30
Coffee (23)	0.00	0.00	1.00	0.00	1.00	1.00	1.00	0.90	1.50	0.40
Others perennial (24)	0.00	0.00	1.00	0.00	0.00	0.80	0.00	0.80	1.20	0.50
Fodder grasses (25)	0.00	0.00	1.00	0.00	1.00	1.00	1.00	1.00	1.50	0.55
Others annual (26)	0.15	0.25	0.40	0.20	0.40	1.05	0.50	1.00	1.50	0.55

Appendix 5: Observed discharges

Appendix 5a: Grand Falls – mean monthly discharges [m^3/s] – 1979-2009 (Republic of Kenya, 2011c).

YEAR	Jan	Feb	Mar	Apr	May	Jun	Jul	Aug	Sep	Oct	Nov	Dec
1979	202.62	280.17	253.24	528.25	582.24	517.45	304.17	212.83	130.27	107.17	322.16	135.58
1980	114.80	93.59	78.08	114.60	315.59	151.51	105.25	102.96	67.60	103.95	189.63	113.40
1981	119.24	98.25	183.42	296.45	499.69	281.22	209.48	168.07	124.67	165.28	168.77	124.92
1982	113.35	111.70	96.96	174.13	481.19	371.32	142.03	122.76	107.36	350.64	561.82	423.10
1983	166.68	117.28	115.30	185.02	425.23	173.33	139.74	109.67	110.31	123.36	142.92	170.62
1984	121.87	109.30	109.04	151.31	114.34	94.26	93.36	80.93	102.69	149.23	248.79	156.31
1985	119.90	141.08	146.47	275.39	233.70	174.02	146.12	127.30	124.58	118.90		15.93
1986	121.87	121.49	109.67	252.68	212.35	177.18	150.36	123.69	103.46	110.60	199.62	157.50
1987	137.05	119.50	115.72	149.38	138.79	131.97	116.91	117.84	71.90	6.23	89.85	79.61
1988	123.71	107.04	110.19	575.48	357.07	152.98	121.35	111.69	88.16	254.07	443.44	319.53
1989			149.90	310.44	193.65	145.86	113.60	94.49	99.80	157.78	290.70	425.42
1990	299.90	147.32	352.89	610.83	390.87	168.08	140.61	134.49	89.72	179.88	230.23	191.00
1991	164.58	150.30	197.66	177.81	168.83	156.42	148.03	138.77	92.63	143.47	172.72	165.94
1992	155.47	136.14	138.33	192.74	151.75	126.15	116.16	82.40	81.06	88.14	155.00	205.76
1993	185.14	159.74	163.29	161.09	163.39	143.30	131.72	126.83	109.82	93.82	167.93	132.44
1994	112.49	93.98	90.45	178.96	143.52	120.47	126.02	112.53	99.28	144.49	329.35	223.20
1995	168.07		161.30	189.04	153.32	149.83	161.24	130.76	129.96	166.44	246.23	175.51
1996	176.86	134.28	144.14	145.48	141.08	133.97	132.11	110.62	106.20	105.94	157.89	143.31
1997	122.57	104.87	150.99	205.50	144.03	118.78	140.17					
1998												
1999						137.77	148.60	120.63	95.84	92.01		
2000												
2001												
2002												
2003												
2004												
2005	175.94	149.27	125.46	166.15	156.08	142.61	126.62	118.54	112.62	119.27	177.51	164.91
2006	160.14	113.56	81.27	153.37	176.28	139.60	131.05	128.02	160.46	150.97	136.38	167.51
2007	167.76	157.22	149.56	158.3	135.28	142.59	143.93	137.06	138.24	138.85	136.47	155.90

YEAR	Jan	Feb	Mar	Apr
2008				
2009	164.72	107.91	85.63	152.95

Appendix 5b: Garissa – mean monthly discharges [m³/s] – 1979-2009 (Republic of Kenya, 2011c).

YEAR	Jan	Feb	Mar	Apr	May	Jun	Jul	Aug	Sep	Oct	Nov	Dec
1979	287.12	330.38	241.86	516.07	691.52	572.64	254.61	117.84			334.21	119.48
1980		54.95	33.01	58.01		85.75	77.89		58.76	45.92	184.36	105.74
1981	82.08	75.41	147.70	305.96	427.09	297.91	174.27	181.16	104.61	139.34	154.10	109.49
1982	94.39	68.96	67.38	179.23	387.37	333.07	117.78	83.27	73.45	249.9	523.02	406.53
1983	144.06	98.47	80.53	120.45	350.16	175.67	113.96	79.48	74.41	61.47	110.72	104.70
1984	89.13	72.57	70.02	232.54	259.90	184.19	90.25	74.87	75.54	184.32	350.92	169.68
1985	65.72	52.49	114.83	287.42	449.04	233.17	109.46	85.26	87.65	77.27	134.50	145.33
1986	90.67	82.21	78.49	192.37	305.95	296.43	123.49	84.92	78.97	72.06	175.53	316.04
1987	122.35	85.26	97.13	136.78	107.79	117.76	92.81	78.78	49.67	32.15	62.87	72.29
1988	89.83	89.49	83.67	418.16	431.42	204.38	107.50	84.74	75.21	96.71	404.07	342.12
1989	234.75	117.53	101.48	287.90	410.87	211.24	110.46	97.53	83.26	113.27	644.54	573.44
1990	357.54	132.27	261.73	834.38	440.19	252.16	113.75	92.79	88.67	130.46	230.15	306.29
1991	194.84	126.74	123.16	134.04	212.77	288.27	118.98	96.31	88.75	102.60	128.56	166.95
1992	115.48	101.80	94.38	121.34	158.13	105.65	96.63	91.92	89.90	99.39	200.80	304.98
1993	250.25	257.09	146.17	194.84	301.27	195.16	119.01	101.05	89.05	84.64	142.01	202.89
1994	107.04	93.44	89.77	198.73	192.20	128.07	107.53	101.10	99.02	140.32	547.65	505.57
1995	166.13	86.75	118.69	153.88	360.66	206.10	121.83	97.13	87.29	114.59	262.09	298.65
1996	162.29	108.86	172.51	114.02	113.60	114.67						
1997			150.81	251.97	214.97	106.44	98.67	77.00	72.98	135.32	671.85	747.12
1998	773.69	517.32	247.57	377.32	709.12	381.67	173.55	122.22	97.51	69.64	157.11	110.99
1999	94.18	80.87	89.48	81.99	108.95	82.92	78.56	69.18	64.76	80.27	150.43	271.06
2000	122.13	70.02	67.11	80.60	72.44	31.03	17.81	15.60	7.35	5.96	131.47	70.75
2001	44.00	44.14	40.93			33.29	51.62	53.39		37.60	144.50	98.67
2002	68.51	51.41	108.18	215.77	553.64	188.41	81.15	87.29	87.36	96.39	238.90	203.32
2003	129.41	115.31	164.00	505.21	503.06			474.12	291.73	128.50	362.11	276.24
2004	182.86	131.03	110.34	197.74	102.11	102.02	75.38	73.84	75.79	114.77	412.21	261.36
2005	131.42	116.40	92.44					87.60	92.92	101.75	196.62	123.06

2006	90.27	76.59	105.68	232.87	282.49	143.20	101.51	106.46	74.58	75.68	549.73	401.03
2007	405.38	157.50	125.20	197.10	233.94	260.98	140.62	128.08	120.56	133.56	277.83	176.12
2008	163.07	133.48	132.78	244.96	185.41	112.61	97.63	86.93	69.89	116.48	206.11	105.48
2009	99.44	84.44	92.32	138.71	104.38	68.53	56.30	45.26	32.86	91.27	210.41	195.54

Appendix 5c: Hola – mean monthly discharges [m^3/s] – 1979-1991 (Republic of Kenya, 2011c).

YEAR	Jan	Feb	Mar	Apr	May	Jun	Jul	Aug	Sep	Oct	Nov	Dec
1979	54.70	110.64	58.49	155.17	255.89	221.75	60.40	21.8	9.65	8.29	98.93	34.84
1980	104.80	71.18	38.75	49.77	197.47	139.79	79.90	55.85	46.97	41.02	144.00	110.56
1981	78.08	72.16	114.27	281.81	300.15	268.48	147.83	140.56	89.23	116.93	136.52	117.54
1982	86.22	83.04	67.41	138.68	226.68	271.37	145.77	80.31	70.82	136.29	215.31	204.75
1983	144.94	111.23	88.82	130.07	246.64	207.04	119.98	87.42	79.24	70.86	117.92	103.21
1984	93.70	72.71	74.08	94.35	90.26	52.44	52.30	51.55	47.83	106.93	261.38	175.50
1985	102.96	74.27	89.64	216.57								
1986		83.47	74.76	136.12		235.25	129.22	91.42	79.85	71.26	140.45	232.65
1987	121.80	104.42	95.48	122.71	111.36	114.57	94.41	76.67	51.16	30.87	55.51	69.83
1988	78.81	72.33	69.08	187.6	307.97	235.65	127.16	77.23	72.16	88.71	231.69	254.81
1989		118.40	120.00	180.43								
1990	238.20	103.53	165.78	321.30	251.25						212.08	254.05
1991			125.98	144.02	181.35	307.26						

Appendix 5d: Garsen – mean monthly discharges [m^3/s] – 1979-1998 (Republic of Kenya, 2011c).

YEAR	Jan	Feb	Mar	Apr	May	Jun	Jul	Aug	Sep	Oct	Nov	Dec
1979	120.35	135.26	110.09	138.62	174.55	176.25	126.96	98.12		69.75	126.63	115.81
1980	94.60				138.48	117.25					121.50	105.17
1981			133.62	165.87	169.32	168.43	117.95	125.33	96.25	96.71	107.04	104.47
1982				106.57	134.39	171.21	114.18			145.39	177.56	182.07
1983	133.70	96.99		104.72	157.35	136.29	97.23				104.49	97.37
1984				115.94	113.00						152.45	137.53
1985	97.61			133.53	154.32	157.36	100.63	73.51	68.15	63.03	81.01	97.82
1986	68.17	58.19	42.02	85.34	133.05	146.46	97.21	69.81	65.73	55.39		142.19
1987	90.10	74.62	67.21	80.65	78.18	76.80	67.36	65.54	57.28		86.78	
1988		55.29	54.94	106.05	171.70	146.76	92.32	72.27	67.36	64.38	126.67	160.21
1989	151.46	100.73	77.94	116.32	163.20	138.39	84.46	68.11	60.09	65.98	149.08	182.09
1990	148.02	107.73	116.70	174.52	161.94	146.14	101.98	80.33	72.39	74.76	121.12	136.15
1991	117.95	90.24	78.17	86.96	99.21	136.99			64.19	64.18	78.89	93.92
1992	70.04	62.73	58.47	56.42	76.67	62.51	57.91	54.54	52.93	52.73	100.13	119.76
1993	135.19	123.27	96.89	88.00			89.99	74.53	62.95	58.28	66.36	100.71
1994					110.09	93.11						
1995												
1996												
1997			56.17	94.33	134.20	79.73	65.16	57.02			178.19	193.77
1998	190.49	172.89	136.93	139.98	162.22							

Appendix 6: Model validation before calibration

Appendix 6a: Model validation results before calibration.

Location	LNSE	R^2	RMSE [m^3/s]
Grand Falls	-3.17	0.48	161.411
Garissa	-1.39	0.58	203.339
Hola	-1.49	0.47	232.811
Garsen	-8.74	0.44	312.414
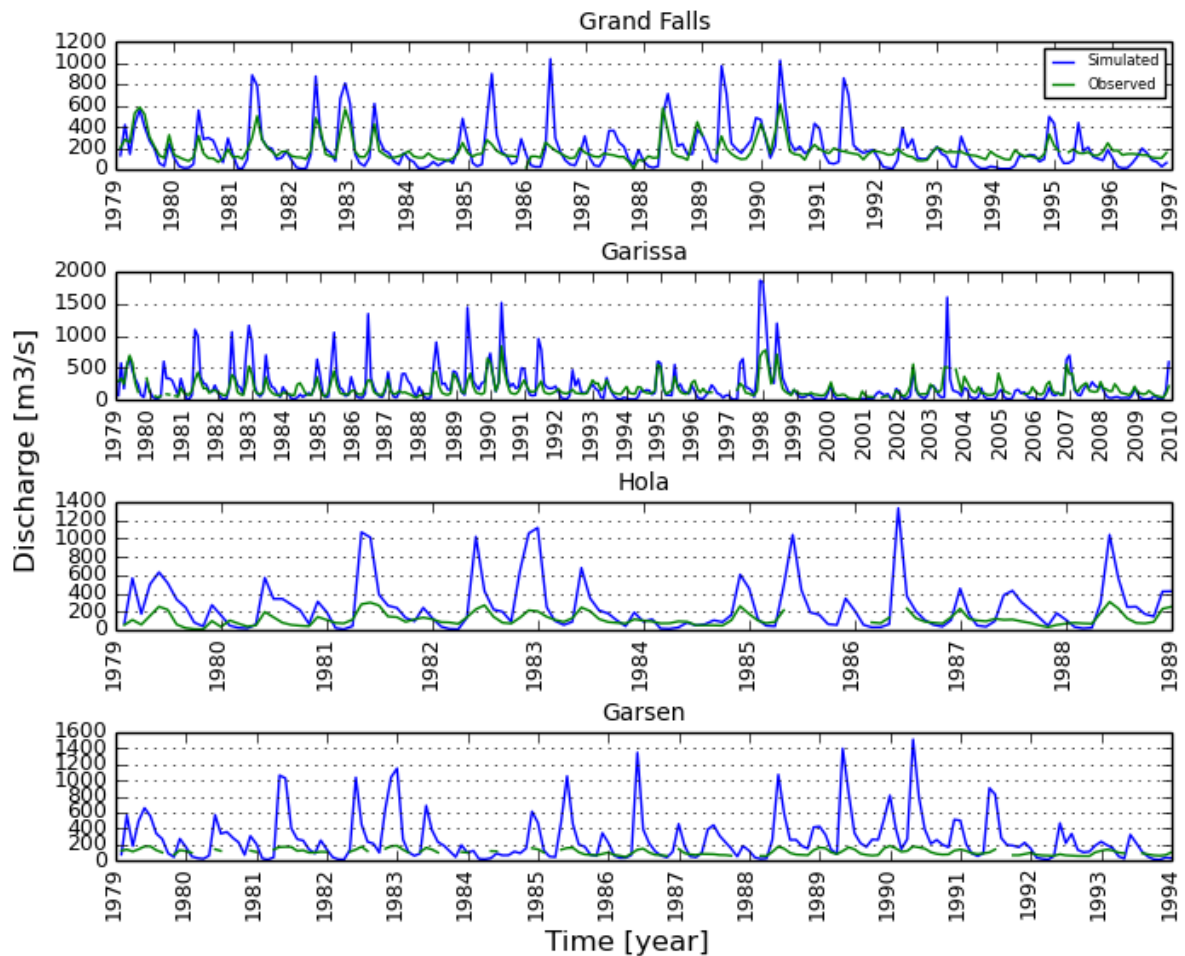
Appendix 6b: Hydrographs of the simulated and observed mean monthly discharges for each location before calibration.

Appendix 7: FDCs for the periods 2010-2030 and 2045-2065

Appendix 7a: Status quo
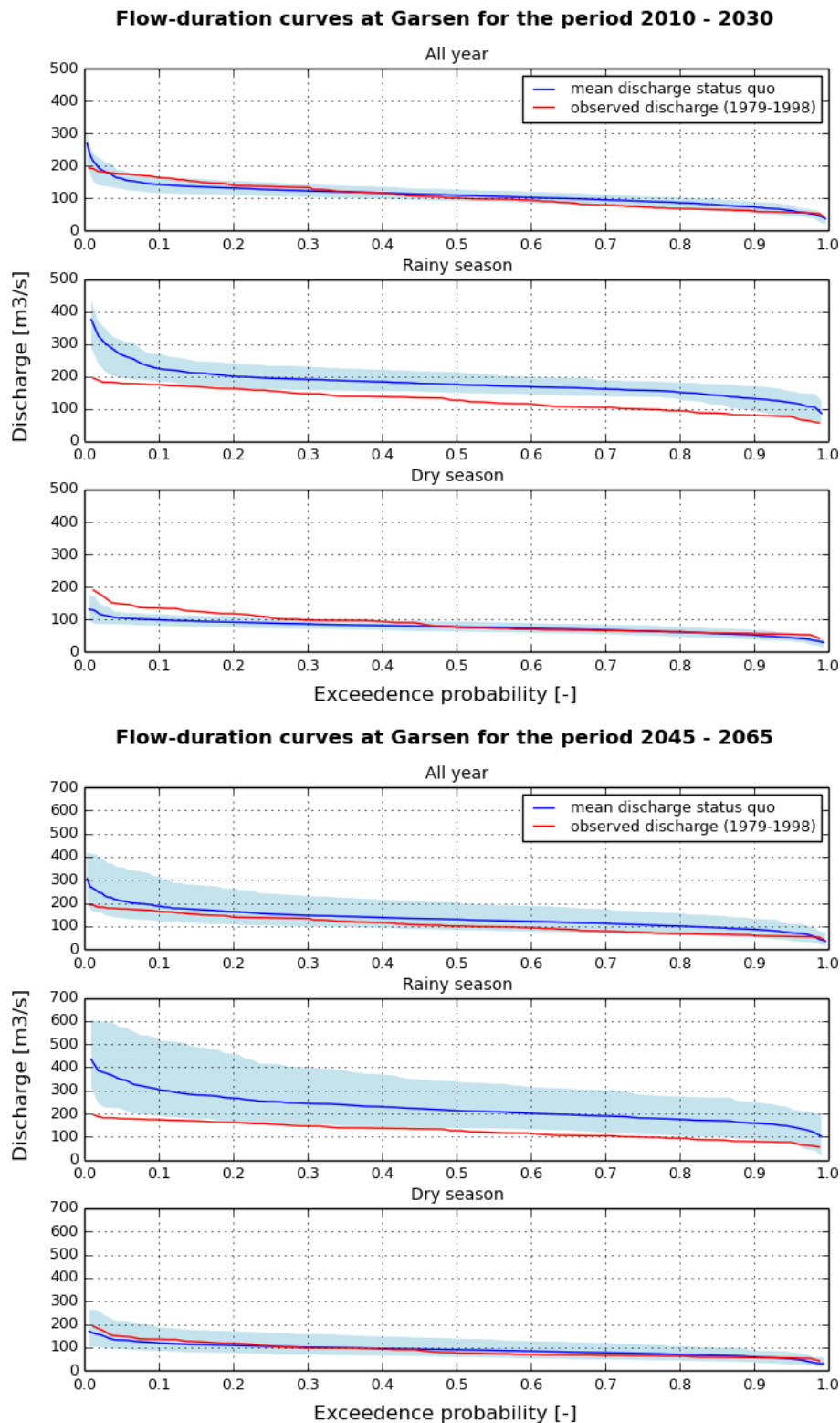
Appendix 7a-1: The FDCs for the status quo at Garsen for the entire year and both seasons separately for the periods 2010-2030 (upper) and 2045-2065 (lower). The mean discharge is calculated from all GCMs (blue line), and the spread shows the variability between predictions of the GCMs (light blue). The observed discharge (for the period 1979-1998) is shown for comparison (red line).

Appendix 7a-2: An overview of the minimum, mean and maximum Q10 and Q90 for the three assessed periods per season of all GCMs combined of the status quo. All discharges are in m³/s.

	Min Q10	Mean Q10	Max Q10	Min Q90	Mean Q90	Max Q90
2010-2030						
- All year	115.41	142.29	166.53	54.09	73.13	89.03
- Rainy season	183.77	224.01	268.31	93.29	131.37	169.34
- Dry season	80.14	98.63	116.13	38.11	51.94	68.07
2025-2045						
- All year	93.29	158.56	227.68	30.87	74.99	103.37
- Rainy season	176.03	276.19	400.20	83.15	152.17	217.34
- Dry season	57.78	104.19	145.04	17.65	53.14	73.47
2045-2065						
- All year	120.59	186.66	313.28	50.00	85.75	132.72
- Rainy season	189.55	303.88	520.74	88.83	158.97	250.19
- Dry season	84.77	118.71	186.73	35.63	59.18	87.83
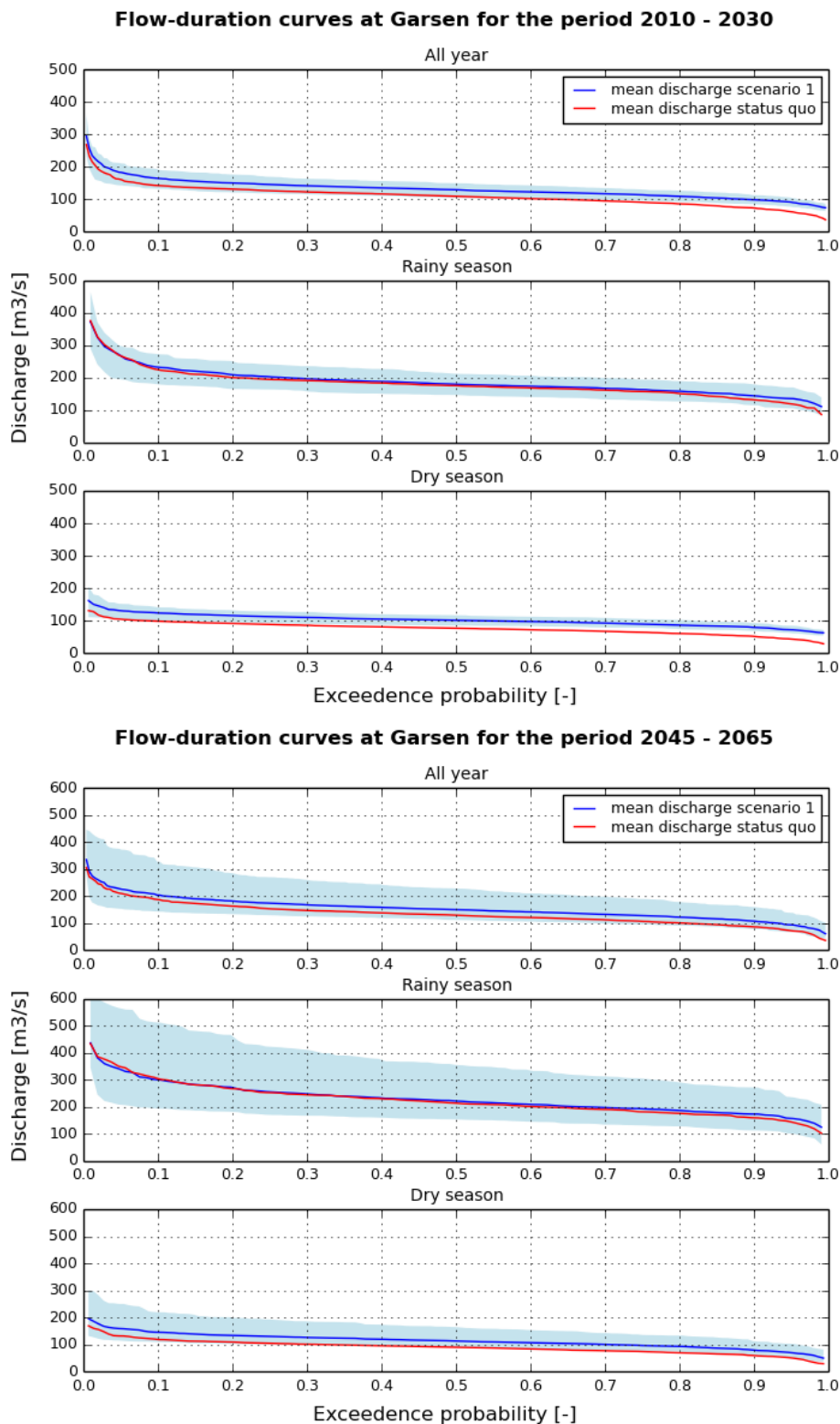
Appendix 7b-1: The flow duration curves for scenario 1 at Garsen for the entire year and both seasons separately for the periods 2010-2030 (upper) and 2045-2065 (lower). The mean discharge is calculated from all GCMs (blue line), and the spread shows the variability between predictions of the GCMs (light blue). The mean discharge from the status quo is included for comparison (red line).

Appendix 7b-2: An overview of the minimum, mean and maximum Q10 and Q90 for the three assessed periods per season of all GCMs combined in scenario 1. All discharges are in m^3/s.

	Min Q10	Mean Q10	Max Q10	Min Q90	Mean Q90	Max Q90
2010-2030						
- All year	132.12	164.39	191.84	84.71	98.47	112.68
- Rainy season	179.30	231.88	272.12	114.62	143.64	178.83
- Dry season	100.36	123.95	141.59	68.44	79.59	92.70
2025-2045						
- All year	121.82	184.16	256.78	60.94	103.21	132.00
- Rainy season	183.94	273.78	399.16	98.50	165.34	235.07
- Dry season	95.03	136.58	179.64	45.35	81.70	102.46
2045-2065						
- All year	142.45	203.18	326.64	77.64	106.81	158.79
- Rainy season	193.15	299.67	511.21	112.42	172.68	271.07
- Dry season	109.22	145.45	219.27	60.02	79.08	112.24

Appendix 7c: Scenario 2

Flow-duration curves at Garsen for the period 2010 - 2030

Flow-duration curves at Garsen for the period 2045 - 2065
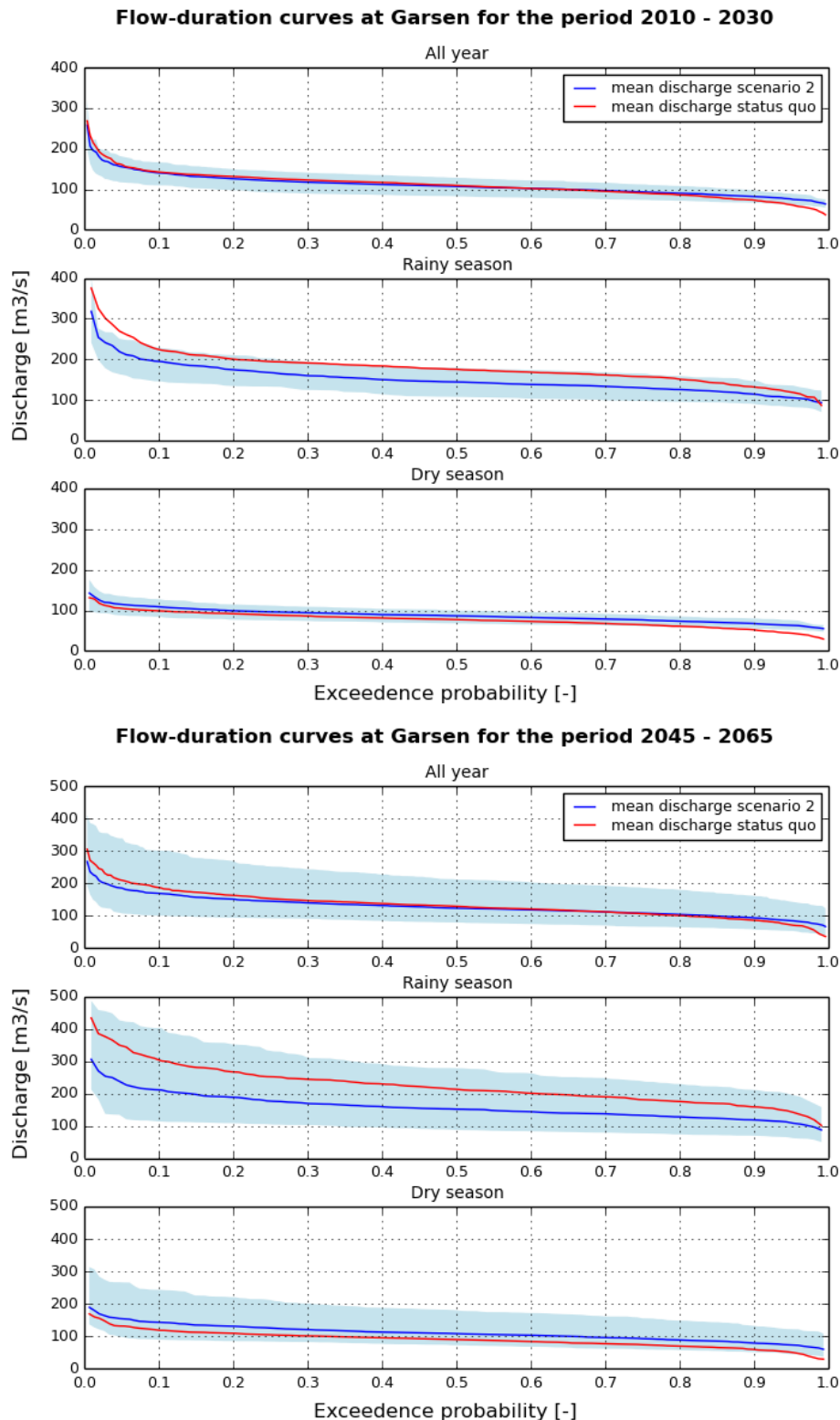
Appendix 7c-1: The flow duration curves for scenario 2 at Garsen for the entire year and both seasons separately for the periods 2010-2030 (upper) and 2045-2065 (lower). The mean discharge is calculated from all GCMs (blue line), and the spread shows the variability between predictions of the GCMs (light blue). The mean discharge from the status quo is included for comparison (red line).

Appendix 7c-2: An overview of the minimum, mean and maximum Q10 and Q90 for the three assessed periods per season of all GCMs combined in scenario 2. All discharges are in m^3/s.

	Min Q10	Mean Q10	Max Q10	Min Q90	Mean Q90	Max Q90
2010-2030						
- All year	109.47	140.24	166.23	66.68	81.85	97.06
- Rainy season	145.37	194.60	228.29	89.60	113.72	146.19
- Dry season	83.93	108.67	127.18	55.58	67.52	79.78
2025-2045						
- All year	84.73	141.32	211.74	43.87	84.22	126.47
- Rainy season	100.97	178.82	280.80	53.10	103.57	166.32
- Dry season	75.78	120.37	169.70	38.24	72.53	103.41
2045-2065						
- All year	100.11	168.83	300.62	57.21	93.17	160.85
- Rainy season	114.17	211.37	401.85	69.87	118.70	211.03
- Dry season	89.67	143.12	243.29	50.79	79.09	131.75
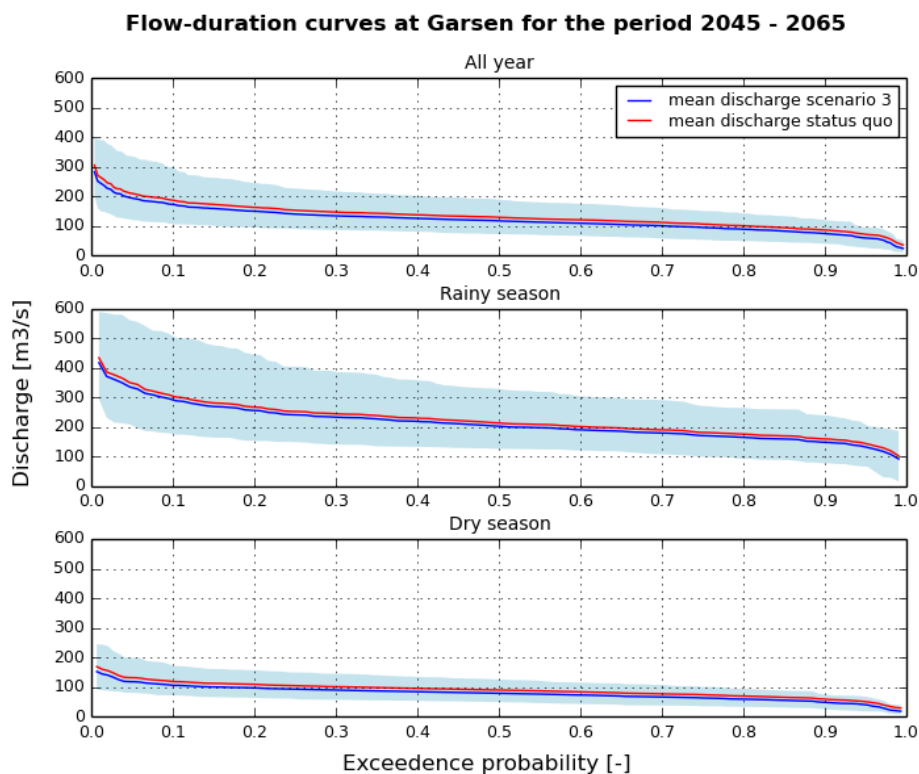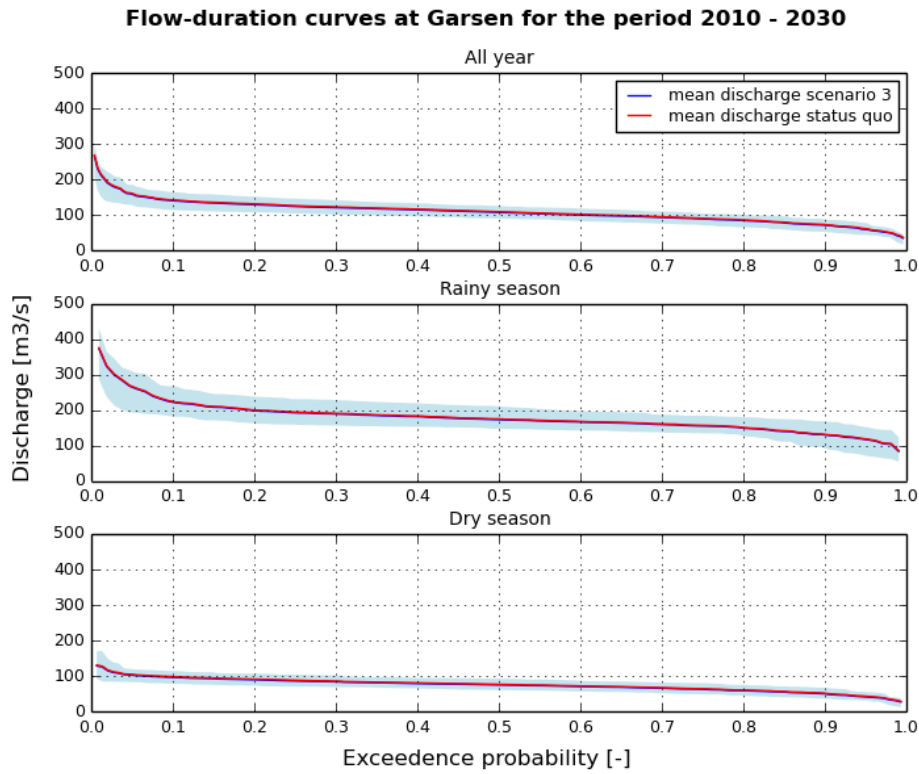
Appendix 7d-1: The flow duration curves for scenario 3 at Garsen for the entire year and both seasons separately for the periods 2010-2030 (upper) and 2045-2065 (lower). The mean discharge is calculated from all GCMs (blue line), and the spread shows the variability between predictions of the GCMs (light blue). The mean discharge from the status quo is included for comparison (red line).

Appendix 7d-2: An overview of the minimum, mean and maximum Q10 and Q90 for the three assessed periods per season of all GCMs combined in scenario 3. All discharges are in m^3/s.

	Min Q10	Mean Q10	Max Q10	Min Q90	Mean Q90	Max Q90
2010-2030						
- All year	112.86	134.77	164.46	38.55	64.79	87.75
- Rainy season	182.16	219.68	266.76	85.37	121.19	167.89
- Dry season	72.47	91.97	114.62	24.12	45.09	67.02
2025-2045						
- All year	84.14	148.90	216.81	26.01	65.33	93.00
- Rainy season	166.64	264.41	390.87	78.45	132.73	209.07
- Dry season	49.49	97.50	134.99	12.63	45.19	65.57
2045-2065						
- All year	106.30	162.27	296.38	39.51	70.26	119.40
- Rainy season	175.94	271.83	507.03	77.13	135.28	238.67
- Dry season	71.96	103.36	172.33	24.93	46.62	75.13
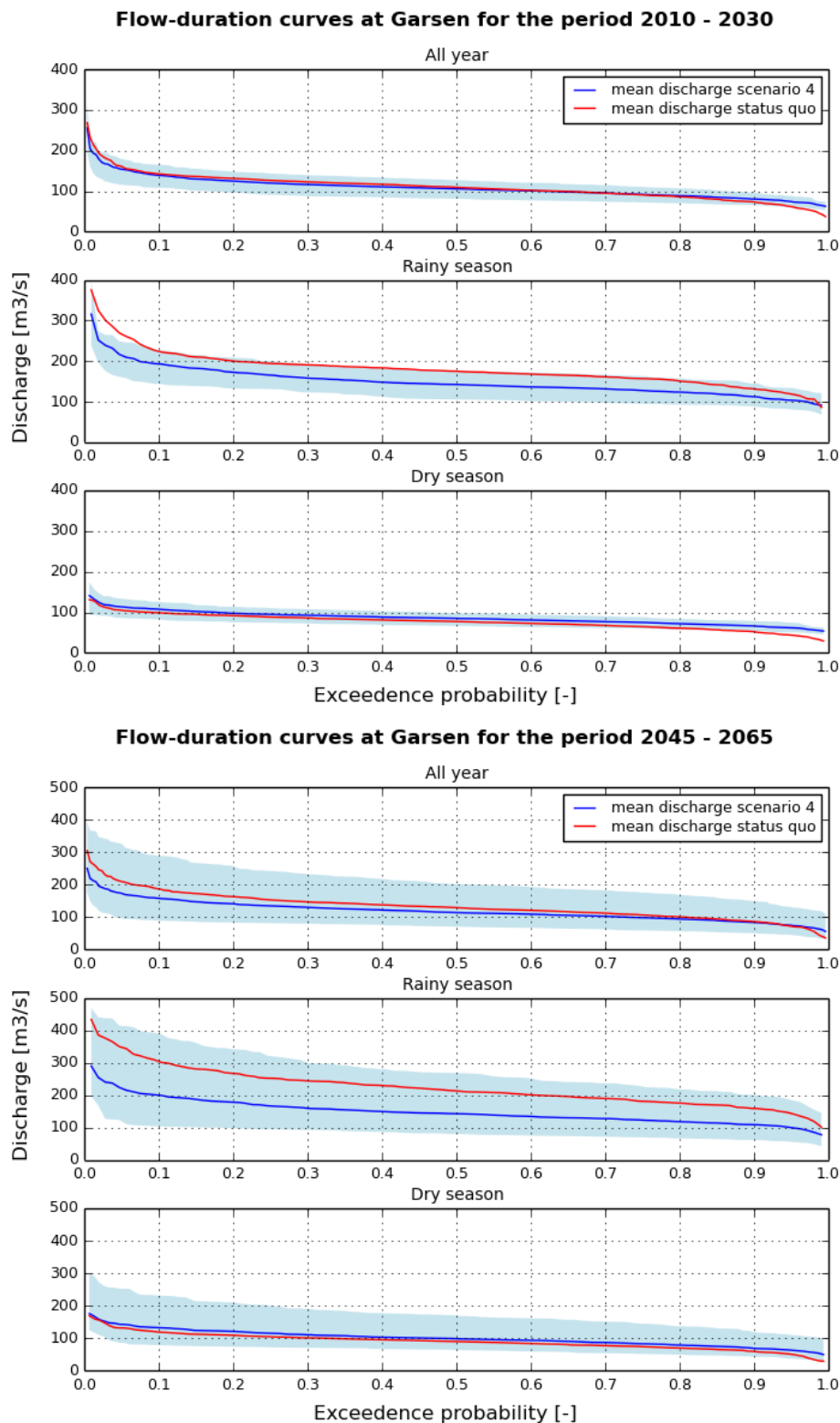
Appendix 7e-1: The flow duration curves for scenario 4 at Garsen for the entire year and both seasons separately for the periods 2010-2030 (upper) and 2045-2065 (lower). The mean discharge is calculated from all GCMs (blue line), and the spread shows the variability between predictions of the GCMs (light blue). The mean discharge from the status quo is included for comparison (red line).

Appendix 7e-2: An overview of the minimum, mean and maximum Q10 and Q90 for the three assessed periods per season of all GCMs combined in scenario 4. All discharges are in m³/s.

	Min Q10	Mean Q10	Max Q10	Min Q90	Mean Q90	Max Q90
2010-2030						
- All year	107.97	138.94	164.74	64.40	77.31	95.84
- Rainy season	143.71	202.66	241.28	88.05	111.43	144.80
- Dry season	82.60	106.30	125.66	47.90	62.61	78.63
2025-2045						
- All year	77.90	143.02	203.52	37.26	77.90	118.23
- Rainy season	92.81	192.77	280.82	47.72	100.09	158.27
- Dry season	68.28	117.83	161.48	32.24	66.03	96.15
2045-2065						
- All year	88.88	155.02	287.88	50.12	80.90	148.49
- Rainy season	103.85	200.69	389.43	62.01	108.39	200.44
- Dry season	78.55	129.38	231.33	42.73	66.73	119.24

Flow-duration curves at Garsen for the period 2010 - 2030
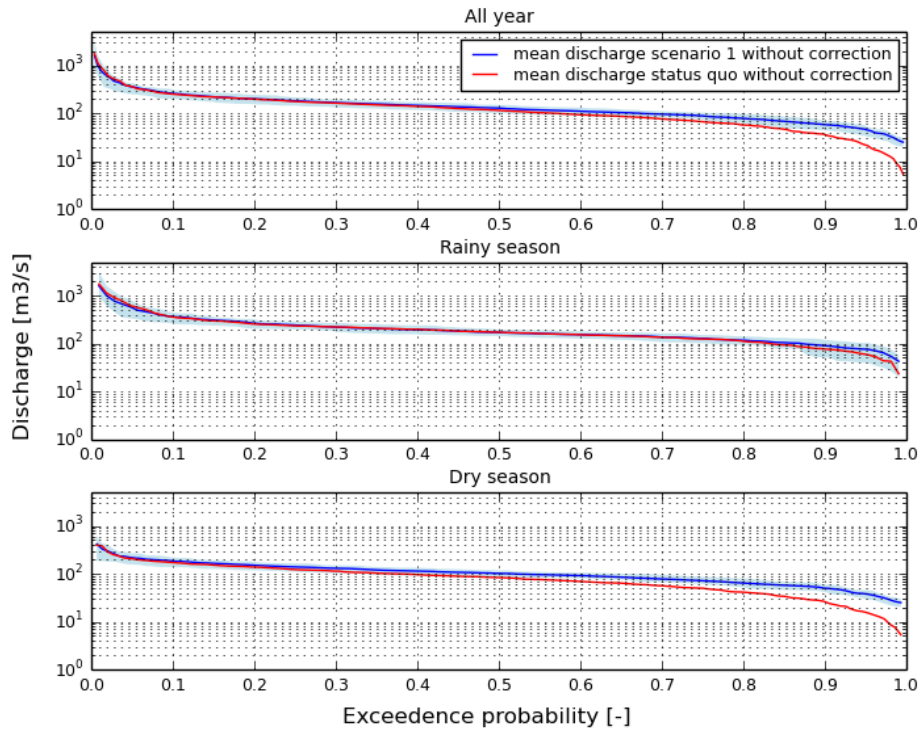
Flow-duration curves at Garsen for the period 2025 - 2045
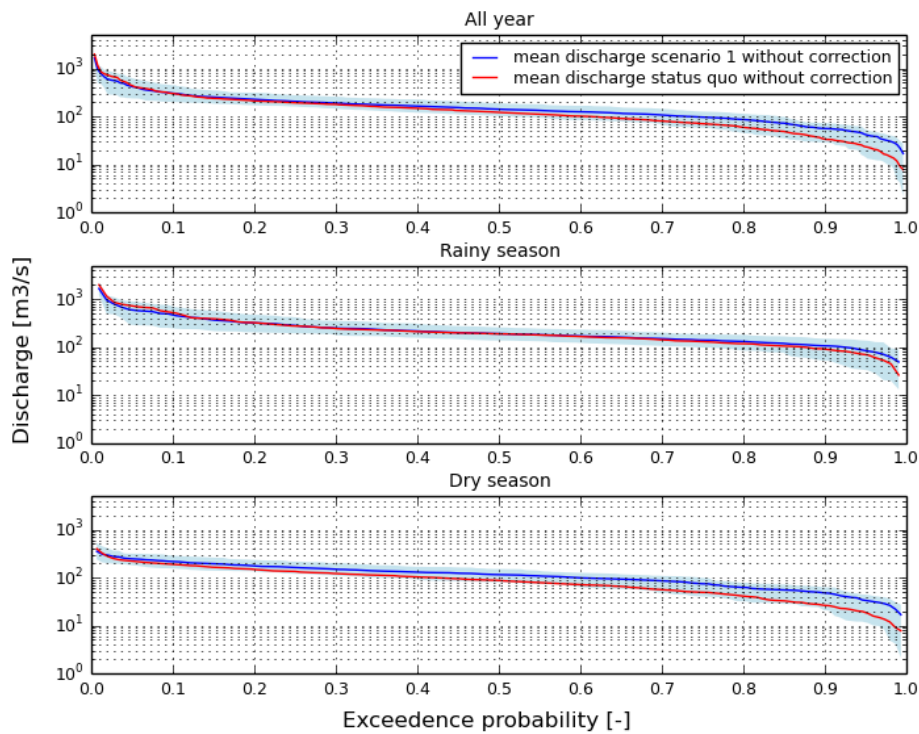
Flow-duration curves at Garsen for the period 2045 - 2065
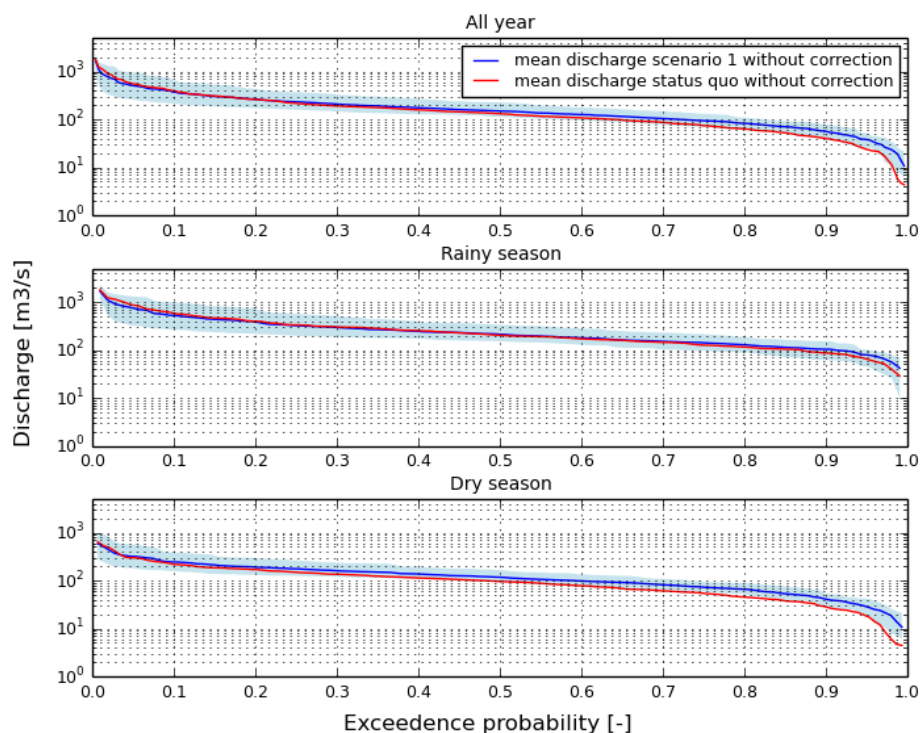
Appendix 7f-1: The flow duration curves for scenario 1 (without the normalized correction method) at Garsen for the entire year and both seasons separately for the periods 2010-2030 (upper), 2025-2045 (middle) and 2045-2065 (lower). The mean discharge is calculated from all GCMs (blue line), and the spread shows the variability between predictions of the GCMs (light blue). The means discharge from the status quo (also without the normalized correction method) is included for comparison (red line). Note that the y-axes are given on a log-scale to better illustrate the effect.

Appendix 7f-2: An overview of the changes [%] in scenario 1 (without correction) in minimum, mean and maximum Q10 and Q90 of all GCMs combined with respect to status quo (without correction) per season for the three assessed periods.

	Min Q10	Mean Q10	Max Q10	Min Q90	Mean Q90	Max Q90
2010-2030 [%]						
- All year	+7.21	+3.58	+4.65	+118.20	+61.62	+44.45
- Rainy season	-4.50	+1.83	+5.81	+53.29	+17.67	+10.94
- Dry season	+8.35	+7.50	+8.17	+159.59	+91.50	+55.56
2025-2045 [%]						
- All year	-0.64	+1.75	+0.69	+224.73	+66.92	+57.13
- Rainy season	-10.68	-10.26	-8.58	+40.63	+17.18	+15.97
- Dry season	+14.59	+13.99	+9.79	+335.60	+81.84	+51.66
2045-2065 [%]						
- All year	-2.33	-5.74	-10.82	+96.57	+40.78	+33.60
- Rainy season	-1.96	-10.31	-10.81	+50.64	+19.67	+19.24
- Dry season	+14.75	+11.70	+11.33	+95.92	+44.31	+42.84